UNIVERSITÉ DE MONTRÉAL

ANALYSIS OF COPPER/FLUOROPOLYMER FILM SYSTEMS FOR MULTILEVEL INTERCONNECTS

Avni ALPTEKIN

DÉPARTEMENT DE GÉNIE PHYSIQUE

ÉCOLE POLYTECHNIQUE DE MONTRÉAL

MÉMOIRE PRÉSENTÉ EN VUE DE L'OBTENTION

DU DIPLÔME DE MAÎTRISE ÈS SCIENCES APPLIQUÉES

(GÉNIE PHYSIQUE)

AVRIL 1998

© Avni ALPTEKIN, 1998

National Library of Canada

Acquisitions and Bibliographic Services

395 Wellington Street
Ottawa ON K1A 0N4
Canada

Bibliothèque nationale du Canada

Acquisitions et services bibliographiques

395, rue Wellington
Ottawa ON K1A 0N4
Canada

Your file Votre référence

Our file Notre référence

The author has granted a non-exclusive licence allowing the National Library of Canada to reproduce, loan, distribute or sell copies of this thesis in microform, paper or electronic formats.

L'auteur a accordé une licence non exclusive permettant à la Bibliothèque nationale du Canada de reproduire, prêter, distribuer ou vendre des copies de cette thèse sous la forme de microfiche/film, de reproduction sur papier ou sur format électronique.

The author retains ownership of the copyright in this thesis. Neither the thesis nor substantial extracts from it may be printed or otherwise reproduced without the author's permission.

L'auteur conserve la propriété du droit d'auteur qui protège cette thèse. Ni la thèse ni des extraits substantiels de celle-ci ne doivent être imprimés ou autrement reproduits sans son autorisation.

0-612-37425-4

Canada

UNIVERSITÉ DE MONTRÉAL

ÉCOLE POLYTECHNIQUE

Ce mémoire intitulé:

ANALYSIS OF COPPER/FLUOROPOLYMER FILM SYSTEMS FOR

MULTILEVEL INTERCONNECTS

Présenté par: ALPTEKIN, Avni

en vue de l'obtention du diplôme de: Maîtrise ès sciences appliquées

a été dûment accepté par le jury d'examen constitué de:

M. WERTHEIMER, Michael, Ph.D., président

M. MARTINU, Ludvik, Ph.D., membre et directeur de recherche

M. SACHER, Edward, Ph.D., membre et codirecteur de recherche

M. MEUNIER, Michel, Ph.D., membre

à mes parents Aydin et Suhran

REMERCIEMENTS

Je veux tout d'abord remercier sincèrement mon directeur et mon codirecteur de recherche, M. L. Martinu et M. E. Sacher. Ils m'ont donné tout le support scientifique et moral nécessaire pour compléter mon projet de recherche.

Je voudrais également remercier M. M. Meunier et M. M. R. Wertheimer d'avoir accepté d'être membres du jury. J'espère qu'ils trouveront la lecture de ce mémoire intéressante.

Je me dois de remercier M. D. Poitras pour m'avoir aidé à corriger le texte de ce mémoire, M. G. Jalbert, Mme. S. Poulin, M. G. Czeremuszkin, M. G. Cerny, Mme. J. Sapieha pour leur aide technique et pour leurs conseils et discussions, et M. M. DiRenzo pour m'avoir appris l'ABC de caractérisation FTIR des couches minces. J'apprécie également toutes les aides morales et scientifiques de mes amis au Laboratoire de Procédés Plasmas.

ABSTRACT

The main objective of this project was to test different copper/fluoropolymer combinations as potential candidates for multilevel interconnects. The low permittivity dielectric films studied involve plasma polymerized fluorocarbons, sputtered fluoropolymers and the commercially available Teflon AF1600. These different fluoropolymer materials are compared according to their fabrication process, dielectric properties over a large frequency range, their thermal stability, and compatibility with the metallization process.

Dielectric properties, namely the permittivity and the dissipation factor, were obtained over a wide frequency range (10^2-10^6 Hz) for metal-insulator-metal (MIM) structures which were temperature-cycled (25°C-250°C) under vacuum. The effect of temperature cycling on the dielectric properties was examined in order to elucidate the thermal stability and to eliminate the effect of components such as low molecular weight species, residual solvent and atmospheric contaminants. After annealing under vacuum at 200 °C, all fluoropolymer films showed a relative permittivity and dissipation factor below 2.0 and 0.001, respectively. The dielectric properties were related to the presence of free radicals and dipoles (C=O) determined by photoacoustic FTIR. The compatibility of fluoropolymers with the metallization process was analyzed by evaluating the adhesion of copper to fluoropolymers exposed to various types of heat treatments. It was found that the adhesion of copper to fluoropolymers was enhanced by preannealing in the atmosphere before copper deposition, and by postannealing in vacuum after copper deposition. The enhancement of adhesion was related to the presence of oxygen-containing groups on the surface, also determined by photoacoustic

FTIR. Diffusion of copper into the polymer was revealed by X-ray photoelectron spectroscopy measurements, and it also helped to increase the copper/fluoropolymer adhesion. Suitability of fluoropolymers for the application in multilevel interconnect structures is discussed.

RÉSUMÉ

Le premier objectif de ce projet a été d'étudier la combinaison du cuivre et des fluoropolymères en tant que candidats potentiels pour les interconnexions multicouches. Les objectifs spécifiques ont été de comparer des fluoropolymères fabriqués selon différents procédés du dépôt (fluorocarbures plasma polymerisés, fluoropolymères pulvérisés et le Téflon AF1600), à leurs propriétés diélectriques sur une large gamme de fréquences, à leur stabilité thermique, et à leur compatibilité avec les procédés de métallisation.

Les propriétés diélectriques, telles que la permittivité et le facteur de perte, ont été obtenues à travers une large gamme de frèquences (10^2-10^6 Hz) pour les structures du type "métal-isolant-métal" (MIM) chauffées (25°C-250°C) sous vide. L'effet du cyclage thermique a été examiné afin de comprendre la stabilité thermique et d'éliminer les effets des fragments à faible masse moléculaire, le solvant résiduel et les contaminants atmosphériques. Nous avons obtenu des couches de fluoropolymères ayant des permittivités moins de 2.0 et facteurs de perte moins de 0.001 après chauffage sous vide à 200 °C. Nous avons aussi évalué les propriétés diélectriques dans la gamme de fréquence jusqu'à 10^{15} Hz. Les propriétés diélectriques sont reliées à la présence des radicaux libres et de dipoles (C=O), mis en évidence par la spectroscopie photoacoustique FTIR. La compatibilité des fluoropolymères avec le processus de métallisation a été examinée en évaluant l'adhérence du cuivre sur les fluoropolymères exposés à différents types de traitements thermiques. L'adhérence du cuivre sur les fluoropolymères a été améliorée par le pré-chauffage (avant le dépôt du cuivre) et le post-chauffage (après le dépôt du cuivre). L'augmentation de l'adhérence a été reliée à

la présence de groupes chimiques de surface contenant de l'oxygène, tel que mis en évidence par la spectroscopie photoacoustique FTIR. La diffusion du cuivre dans les polymères a été observée par l'XPS. Cette diffusion a contribué à l'augmentation de l'adhérence du cuivre sur les fluoropolymères. Nous avons étudié la possibilité de l'utilisation des fluoropolymères dans les interconnexions multicouches.

LONG RÉSUMÉ EN FRANCAIS

L'utilisation prospective de semiconducteurs composés dans les technologies d'integration à très grande échelle (ULSI) et giga-échelle (GSI) requiert une réduction des délais de transmission d'un signal sur les multicouches des dispositifs qui sont faites de couches alternatives de lignes de métal et d'isolant polymérique. Le temps de délai de la transmission est le produit de la résistance des interconnexions métalliques et de la capacitance de l'isolant; il est réduit par une diminution de la résistance des lignes métalliques et de la permittivité de l'isolant polymérique.

Il y a des raisons importantes pour choisir le cuivre comme métal pour les interconnexions et les fluoropolymères comme isolant: le cuivre a une résistivité de 1.67 μΩ-cm, soit seulement de 5% plus élevée que l'argent. Les fluoropolymères ont les plus basses permittivités parmi les polymères, leurs facteur de perte et d'absorptivité de l'eau sont basses, et ils ont une résistance chimique excellente, en plus d'offrir une bonne résistance thermique. Cependant, un problème subsiste: le cuivre n'adhère pas suffisamment aux fluoropolymères. En considérant les hautes températures associées aux étapes de fabrication, ainsi que le chauffage de Joule relié à l'utilisation des dispositifs, les problèmes de l'adhérence deviennent encore plus importants; les contraintes thermiques peuvent résulter en une perte d'adhérence à l'interface si les liaisons chimiques n'y sont pas suffisamment fortes.

Ces problèmes nous ont poussés à étudier l'interphase créée lors du dépôt de cuivre sur différents fluoropolymères. Nous avons déterminé l'adhérence du cuivre déposé et les propriétés diélectriques des fluoropolymères situés entre deux couches de cuivre en fonction du traitement thermique. Nous avons aussi déterminé les types de groupes chimiques sur les surfaces des fluoropolymères par la spectroscopie infrarouge photoacoustique, et nous avons suivi la diffusion du cuivre dans le fluoropolymère par l'XPS.

Nous avons étudié trois types de film fluoropolymère: le Téflon pulvérisé (SP), les fluorocarbones plasma polymerisés (PP) et le Teflon AF1600 déposé par tournette. Les films pulvérisés et plasma polymérisés ont été préparés dans un système de plasma rf (13.56 MHz). Une cible de PTFE conventionnel a été placée sur l'électrode rf et pulvérisée en utilisant un plasma Ar ou CF_4. Les films PP ont été obtenus à partir des monomères C_2F_3H ou C_2F_4. Les substrats utilisés ont été le silicium et le verre, et l'épaisseur des couches était typiquement de 1 µm. La solution Teflon AF1600 6% provenant de DuPont a été diluée avec du solvent Sigma Fluorinert FC-77 et déposée par tournette.

Le cuivre à haute pureté a été déposé soit par évaporation, en utilisant le chauffage résistif, ou par pulvérisation avec un système planaire DC utilisant un magnétron et l'Ar. L'épaisseur du cuivre était d'environ 200 nm, déterminée par profilométrie.

Pour améliorer la stabilité et l'adhérence des films, les échantillons ont été traités thermiquement sous une variété des conditions, soient le préchauffage (avant le

dépôt du cuivre) et le postchauffage (après le dépôt du cuivre). Le préchauffage a été fait sous atmosphère ambiente ou sous vide. Le postchauffage a été fait sous vide seulement, pour éviter l'oxydation du cuivre. Tous les traitements thermiques ont été fait à 200 ^{o}C pendant 30 min.

En plus du traitement thermique, le Téflon AF1600 fait l'objet de traitements de surface par plasma dans certains cas. Ces traitements ont été effectués dans la même chambre de plasma en utilisant le N_2, l'Ar et l'air sur un substrat mis à la masse. Un échantillon non traité de Téflon AF1600 issu de la même gauffre a été conservé pour fins de comparaison. Tous ces échantillons ont été métallisés avec le cuivre par évaporation.

Pour s'assurer que les propriétés diélectriques sont reproductibles et stables, les structures cuivre/fluoropolymère ont subit un cycle thermique sous vide. La capacitance et les pertes diélectriques ont été déterminées à des fréquences entre 10^2 et 10^6 Hz. Nous avons aussi évalué les valeurs de permittivité en haute fréquence par des mesures optiques dans la gamme du visible.

L'adhérence a été mesurée par la technique microrayure et par pelage standard. Pour la microrayure, une pointe hémisphérique a été déplacée sur la surface avec une vitesse constante et une charge augmentant linéairement; la charge critique à laquelle les premiers défauts sont apparus a été déduite par une observation par microscope optique. Le test de pelage a été fait en utilisant un ruban adhésif 3M de type 600. Le ruban a été placé sur l'échantillon et un rouleau de poids de 2 kg a été roulé sur le ruban

deux fois; immédiatement aprés, le ruban a été tiré perpendiculairement de la surface et le pourcentage de cuivre qui a resté sur la surface a été estimé.

Les spectres infrarouges ont été pris en mode de transmission dans un spectromètre équipé avec une cellule infrarouge photoacoustique.

L'analyse XPS a été faite avec la radiation de Mg K_α (1253.6 eV). Des balayages de survol ont été utilisés pour obtenir les concentrations élémentaires pour différents angles de sortie par rapport à la normale (perpendiculaire), qui sont utilisées pour évaluer la diffusion du cuivre dans les films après les traitements thermiques. Les survols de surface par XPS, dans la gamme de 0-1000 eV, ont été obtenus pour les fluoropolymères metallisés, en utilisant les angles de 0° (perpendiculaire) et de 35° pour indiquer les profils de concentration de cuivre. Ces mesures ont été répétées pour plusieurs étapes des chauffages à différentes températures.

L'évolution de la contrainte thermique en fonction de la température a été évaluée pour les fluoropolymères metallisés et non métallisés en utilisant le système commercial sous atmosphère de N_2.

Nous avons mesuré la tension de surface pour les films de fluoropolymère chauffés sous atmosphère ambiente. Ceci a été accompli en utilisant un goniomètre à l'angle de contact et de petites gouttes de 6 différents liquides. La méthode de Kaelble donne les composantes dispersives (γ^d) et polaires (γ^p) de tension de surface.

La permittivité est d'environ 2.5 pour les matériaux tels-que-déposés, et tombe au dessous de 2.0 après un chauffage sous vide à 200 ^{o}C durant 30 min. Cet effet peut être relié à la stabilisation de la microstructure des couches qui initiallement contiennent des radicaux libres (couches déposeés par plasma) et du solvant retenu (Téflon AF1600). Le chauffage est accompagné par l'émission des espèces à faible masse moléculaire.

Après chauffage, le spectre diélectrique ne montrait aucune particularité spécifique dans la gamme de températures utilisées. L'augmentation de tanδ avec la température indique une augmentation de la perte diélectrique. Pour le Téflon AF1600 également, les valeurs de permittivité κ diminuent avec une augmentation de la température. Nous avons corrigé la courbe κ (T) en considérant l'expansion thermique de l'aire et de l'épaisseur du condensateur et en utilisant le coefficient d'expansion thermique donné par le manufacturier. Cependant, cette approche ne change pas l'allure de la courbe considérablement.

Les résultats de microrayure et de pelage indiquent que le préchauffage dans l'atmosphère ambiante peut contribuer de manière significative à l'augmentation de l'adhérence du cuivre sur les fluoropolymères PP et SP. Ceci peut être dû aux réactions avec l'air des radicaux libres, qui sont produits pendant le dépôt par plasma. Les sites qui contiennent l'oxygène sont disponibles pour la réaction avec le cuivre. Cependant, pour le Téflon AF1600, ceci n'est pas le cas: ce polymère n'ayant pas de radicaux libres, l'adhérence du cuivre est faible et ne s'améliore pas par préchauffage atmosphérique. Les résultats montrent aussi que le postchauffage contribue à l'adhérence, dû, probablement à la diffusion du cuivre dans les fluoropolymères (voir

plus loin). En général, le cuivre pulvérisé adhère mieux que le cuivre évaporé, tel qu' indiqué par une charge critique plus élevée. Cet effet est relié aux énergies plus élevées associées à la pulvérisation. Après un postchauffage sous vide, l'adhérence améliore encore plus: aucune couche de cuivre pulvérisée ne montre de perte de l'adhérence après le test de pelage.

L'adhérence du cuivre évaporé sur le Téflon AF1600 s'améliore encore plus par le traitements de surface par plasma. Typiquement, la charge critique augmente de 25%.

Les spectres infrarouges photoacoustiques qui ont leur origine dans la région près de la surface montrent un pic intense à environ 1200 cm^{-1} pour les films PP et SP, dû à un mode de vibration des groupes CF_n. L'autre grand pic à environ 1700 cm^{-1} peut être expliqué par la présence de groupes carbonyles (C=O), qui sont le résultat de réactions des radicaux libres avec l'oxygène atmosphérique. Une absorption à environ 3400 cm^{-1} est due à la présence de groupes –OH qui résultent de la réaction des radicaux libres avec les vapeurs d'eau. Pour le Téflon AF1600, les pics caractéristiques à 1250 cm^{-1}, 1150 cm^{-1} et 980 cm^{-1} sont, respectivement, dûs aux modes de vibrations longitudinales de CF_2, le composant de dioxole fluorine, et aux vibrations de CF_3. Les spectres infrarouges de la surface des fluoropolymères PP et SP sont plus riches en pics des contaminants, particulièrement –OH, en comparaison avec ceux de leur volume, alors que pour Téflon AF1600, les spectres de surface et de volume sont similaires. Ceci confirme la réaction des radicaux libres, créés durant la fabrication avec les composantes de l'air et l'introduction de nouvaux groupes polaires. Nous expliquons la

plus forte adhérence observée sur les fluoropolymères PP et SP comme étant la cause de la formation de liaisons chimiques à l'interphase métal-polymère.

Les changements observés avec l'analyse XPS indiquent que la diffusion du cuivre augmente avec une augmentation de la température. Il est aussi évident que la diffusion de cuivre dans le Téflon AF1600 est plus marquée que dans les fluoropolymères déposés par plasma.

Pour les films de fluoropolymères PP et SP non métallisés, les changements irréversibles de la contrainte thermique ont été observés pendant le premier cycle thermique. Pour les PP(C_2F_4) et le SP Téflon (Ar), la contrainte thermique est initialement très basse (~0 MPa); le PP(C_2F_4) acquiert une contrainte en tension quand la température dépasse 100 ^{o}C et est stable et reproductible pendant les cycles suivants de chauffage et de refroidissement. Le SP Téflon acquiert une contrainte compressive quand il est chauffé. Ces effets peuvent être reliés au processus de dépôt qui utilise les particules aux plus hautes énergies cinétiques, et à la présence d'Ar qui peut être incorporé dans les films. Le Téflon AF1600 subit une contrainte négative (compressive) jusqu'à 200 ^{o}C. Cependant, quand il est chauffé encore plus, à 350 ^{o}C, il se produit des changements substantiels vers des valeurs plus compressives, similaire au comportement de SP Téflon. Après les mesures initiales de contrainte des échantillons fluoropolymères, les échantillons ont été couverts de couches de cuivre évaporé (~200 nm). Nous avons observé que le cuivre contribue à une contrainte en tension qui se stabilise après le chauffage initial.

Les composantes dispersives et polaires des tensions de surface et leur somme ont été tracées en fonction de la charge critique pour les différents fluoropolymères. Evidemment, les deux composantes de la tension de surface augmentent avec une augmentation de la charge critique. Ceci suggére la contribution des deux composantes, polaire et dispersive, à l'adhérence du cuivre sur les fluoropolymères.

Dans ce travail, nous avons étudié le dépôt de cuivre sur des fluoropolymères, en utilisant une approche de caractérisation multitechnique. Nous avons montré que les trois matériaux, les fluorocarbones polymérisés par plasma, le Téflon pulvérisé et le Téflon AF1600 déposé par tournette, possèdent des permittivité sous 2.0 à travers une large gamme de frèquences (10^2 Hz-10^{14} Hz) quand ils sont chauffés à 200 ^{o}C sous vide. Le cuivre adhère bien aux films déposés par plasma, un effet qui est relié à la présence de groupes contenant de l'oxygène près de la surface chimiquement active. L'adhérence sur le Téflon AF1600 et les autres polymères peut être améliorée encore plus par postchauffage, qui à son tour, favorise la diffusion de cuivre dans les polymères.

TABLE OF CONTENTS

PAGE

DÉDICACE....................................iv

REMERCIEMENTS....................................v

ABSTRACT....................................vi

RÉSUMÉ....................................viii

LONG RÉSUMÉ EN FRANÇAIS....................................x

TABLE OF CONTENTS....................................xviii

LIST OF FIGURES....................................xxi

LIST OF TABLES....................................xxxi

PUBLICATIONS....................................xxxii

CHAPTER 1- INTRODUCTION....................................1

CHAPTER 2- CHARACTERISTICS OF FILM MATERIALS CONSIDERED FOR MULTILEVEL INTERCONNECTS....................................9

2.1. STRUCTURE AND DIELECTRIC PROPERTIES OF FLUOROPOLYMER FILMS....................................9

2.1.1 CONVENTIONAL FLUOROPOLYMERS....................................11

2.1.2 PLASMA-DEPOSITED FLUOROPOLYMERS....................................17

PAGE

2.1.3 SHORT COMPARISON BETWEEN THE PLASMA DEPOSITED AND CONVENTIONAL FLUOROPOLYMERS........27

2.2. PROPERTIES OF COPPER FILMS........30

2.3 ADHESION OF METALS TO FLUOROPOLYMERS........35

2.3.1 MECHANISMS OF ADHESION........35

2.3.2 EVALUATION OF ADHESION........38

2.3.3 METAL-FLUOROPOLYMER INTERFACES........44

CHAPTER 3- EXPERIMENTAL METHODOLOGY........51

3.1 FABRICATION OF FLUOROPOLYMER FILMS........51

3.1.1 PLASMA DEPOSITION........51

3.1.2 SPIN COATING........52

3.2 FABRICATION OF COPPER FILMS........53

3.3 CHARACTERIZATION OF FILM MATERIALS........55

3.3.1 DIELECTRIC MEASUREMENTS........55

3.3.2 ADHESION MEASUREMENTS........58

3.3.3 STRESS MEASUREMENTS........61

3.3.4 CHEMICAL CHARACTERIZATION OF THE SURFACES AND INTERFACES........64

3.3.5 THICKNESS MEASUREMENTS........67

PAGE

CHAPTER 4- RESULTS AND DISCUSSION.........68

4.1 DIELECTRIC PROPERTIES OF FLUOROPOLYMER FILMS.........68

4.1.1 THERMAL HISTORY.........68

4.1.2 FREQUENCY DEPENDENCE OF THE DIELECTRIC PROPERTIES.........76

4.2 ADHESION OF COPPER TO FLUOROPOLYMERS.........77

4.2.1 MICROSCRATCH AND PEEL TEST ANALYSIS.........77

4.2.2 XPS PROFILE ANALYSIS.........85

4.2.3 FTIR ANALYSIS.........87

4.2.4 SURFACE TENSION MEASUREMENTS.........89

4.2.5 OBSERVATION OF THE FLUOROPOLYMER SURFACES BY SEM AND AFM.........91

4.2.5 MEASUREMENTS OF STRESS.........93

CHAPTER 5- CONCLUSIONS.........98

REFERENCES.........104

LIST OF FIGURES

PAGE

Figure 1.1: 2

Illustration of a multilevel interconnect scheme.

Figure 2.1: 10

Relationship between tanδ and temperature at constant frequency.

Figure 2.2: 12

Teflon AF: A family of Amorphous Fluoroplastics with T_g ranging from 80°C to 300°C.

Figure 2.3: 13

Chemical structure of Teflon AF 1600 repeat unit.

Figure 2.4: 15

Refractive Index vs. Composition for PDD/TFE Copolymers.

Figure 2.5: 16

Film Thickness vs. Spin Speed for Teflon AF 1600 solutions diluted in Sigma Fluorinert FC-75 and spun onto glass.

PAGE

Figure 2.6:..22

Polymer deposition rate in C_2F_4 and C_3F_8 discharge as a function of ion bombardment energy during film growth. (from Kay E., 1986).

Figure 2.7:..23

A simplified cross section of a sputtering system and the sputtering process.

Figure 2.8:..26

Temperature dependence of $\tan\delta$ before and after thermal treatment in helium (from Nakano T. et al., 1988).

Figure 2.9:..28

Dielectric loss versus temperature at 10^3 Hz for: (a) fully oxidized, unannealed PPTFE film (full line); (b) weakly oxidized, unannealed film (dashed line); (c) fully oxidized film after annealing (dotted line) (from Perrin J. et al., 1985).

PAGE

Figure 2.10:..40

Calculated stress distribution during the scratching procedure (from Hamilton, G. M. and Goodman, L. E., 1966).

Figure 2.11:..41

Illustration of the scratch test.

Figure 2.12:..43

Cross-hatch peel test.

Figure 2.13:..43

Various simple peel tests (from Hardy A., 1963).

Figure 2.14:..45

Illustration of a structured interface region (from Liston, E. M. et al., 1993)

Figure 2.15:..47

XPS C(1s) and O(1s) spectra of Teflon AF (from Shi M. K. et al., 1995).

PAGE

Figure 2.16: 48

XPS C(1s) and F(1s) spectra of PPFC before and after Cu deposition (from Shi M. K. et al., 1995).

Figure 2.17: 50

Effect of treatment gas in microwave plasma on the critical load, L_C, of 200 nm thick evaporated copper films, and on the mean surface roughness (RMS) of as-treated Teflon PFA surfaces (from Klemberg-Sapieha, J. E., 1997).

Figure 3.1: 52

Plasma system used in our laboratory.

Figure 3.2: 57

The experimental set-up and metal-insulator-metal (MIM) sample structure used in our experiments.

Figure 3.3: 60

A summary of possible failure modes observed after the scratching (from Burnett P. J. and Rickerby D. S., 1987).

PAGE

Figure 3.4:..61

SEM picture showing the point at which L_C is typically measured.

Figure 3.5:..63

Schematics of the flexus laser scanning mechanism. (from Courtesy of I. Blech, Flexus Corp., Sunnyvale, CA).

Figure 3.6:..65

Schematic diagram of photoacoustic cell (from R. T. Graf et al., 1987).

Figure 4.1:..72

Effect of cycling on the dielectric constant of Ar-sputtered Teflon.

Figure 4.2:..72

Effect of cycling on the dissipation factor of Ar-sputtered Teflon.

Figure 4.3:..73

Dielectric constant vs temperature for a vacuum annealed Teflon AF1600.

PAGE

Figure 4.4:..73

Dissipation factor vs temperature for a vacuum annealed Teflon AF1600.

Figure 4.5:..74

Dielectric constant vs temperature for a vacuum annealed $PP(C_2F_4)$.

Figure 4.6:..74

Dissipation factor vs temperature for a vacuum annealed $PP(C_2F_4)$.

Figure 4.7:..75

Dielectric constant vs temperature for a vacuum annealed CF_4 sputtered Teflon.

Figure 4.8:..75

Dissipation factor vs temperature for a vacuum annealed CF_4 sputtered Teflon.

Figure 4.9:..76

Dielectric constant as a function of frequency at room temperature for unannealed and annealed fluoropolymers in vacuum.

PAGE

Figure 4.10:.....77

Dissipation factor as a function of frequency at room temperature for annealed fluoropolymers in vacuum (It must be emphasized that near 10^{15} Hz there are two different log f(Hz) values: 14.6 and 15.8 obtained for two frequencies corresponding to a wavelength of 450 and 650 nm).

Figure 4.11:.....79

MST and peel test results for copper deposited on fluoropolymers.

Figure 4.12.....80

The effect of plasma surface treatment on the adhesion of evaporated copper onto Teflon AF1600.

Figure 4.13:.....81

Delaminations of evaporated Cu from the atmosphere preannealed Teflon AF1600. The critical load was around 0.05 N.

Figure 4.14:.....82

Delaminations of evaporated copper from Teflon AF1600 observed with more detail.

PAGE

Figure 4.15:..83

Sequence of pictures seen with the reflection mode of an optical microscope. Bare PP(C_2F_3H) on glass annealed in the atmosphere and analyzed using the scratch tester (Magnification: 550×, tip size:0.8 mm, range of load: 0-3 N, loading rate: 1 N/min, speed of tip: 5 mm/min).

Figure 4.16:..84

Sequence of pictures seen with the transmission mode of an optical microscope. PP(C2F3H) film sputtered with Cu. The sample was not postannealed. (Magnification : 550×, tip size: 0.8 mm, range of load: 0-3 N, loading rate: 1N/min, speed of tip: 5 mm/min).

Figure 4.17:... 86

Atomic concentration of copper as a function of annealing temperature at 0° and 35° take-off angles from normal obtained by XPS.

Figure 4.18:..87

PA signal for fluoropolymers.

PAGE

Figure 4.19: 89

Contamination peaks (CH_n) of two Teflon AF1600 samples. Sample A was kept in laboratory atmosphere for some time whereas sample B (kept in a dessicator) was inserted within seconds into the FTIR spectrometer.

Figure 4.20: 90

Surface Tension as a function of critical load for atmosphere-annealed fluoropolymers (in the order of increasing critical load: Teflon AF1600, PP(C_2F_4), SP Teflon (CF_4), SP Teflon (Ar), PP(C_2F_3H)) .

Figure 4.21: 92

Cauliflower-like surface structure of PP(C_2F_3H) observed under SEM.

Figure 4.22: 92

Cauliflower-like surface structure of PP(C_2F_3H) observed under AFM.

Figure 4.23: 93

The smooth surfaces of PP(C_2F_4) under SEM. We have intentionally focused on a dust particle to make the observed features evident.

PAGE

Figure 4.24:..96

Stress as a function of temperature for bare fluoropolymer films.

Figure 4.25:..96

Stress as a function of temperature for copper evaporated fluoropolymer films.

LIST OF TABLES

PAGE

Table 1.1: 4

Possible candidates for low resistivity metal.

Table 1.2: 6

Candidates for low permittivity dielectric.

Table 2.1: 14

Typical property data for Teflon AF (Grades 1600 and 2400).

Table 2.2: 31

Comparison of electromigration parameters for bulk materials (from Murarka, S. P. and Hymes, S., 1995).

Table 2.3: 32

Properties of possible interlayer metals (from Murarka, S. P. and Hymes, S., 1995).

Table 2.4: 33

Relative adiabatic temperature rise due to Joule heating in various metals and their thermal conductivities (from Murarka, S. P. and Hymes, S., 1995).

PUBLICATIONS

This work has contributed to the following papers and conference presentations:

"Mechanical and Dielectric Properties of Low Permittivity Dielectric Materials", A. ALPTEKIN, G. CZEREMUSZKIN, L. MARTINU, M. MEUNIER, E. SACHER and M. DIRENZO, MRS Symposium Proceedings, Vol. 443 (1997) 79-84.

"Dielectric and Mechanical Properties of Copper/Fluoropolymer Film Structures", A. ALPTEKIN, E. SACHER, G. CZEREMUSZKIN, L. MARTINU and M. DIRENZO, Electrochemical Society Meeting, Abstract, Vol 97(1), 1997.

"The Deposition of Copper onto Teflon AF1600: An XPS Comparison of Vapor Deposition and Sputtering", D. POPOVICI, J. E. KLEMBERG-SAPIEHA, G. CZEREMUSZKIN, A. ALPTEKIN, L. MARTINU, M. MEUNIER, E. SACHER, Metallized Plastics V, 1997, edited by K. Mittal.

"Thermal Stability of Low Permittivity Fluoropolymer Dielectrics", G. CZEREMUSZKIN, L. MARTINU, A. ALPTEKIN, D. POPOVICI, M. MEUNIER and E. SACHER, Electrochemical Society Meeting, Abstract, Vol. 97(1), 1997.

CHAPTER 1

INTRODUCTION

Continuing advances in the fields of VLSI (Very Large Scale Integration) and ULSI (Ultra Large Scale Integration), and the continuing developments of smaller and smaller devices introduced new concerns about the existing metallization schemes for gates, interconnections, ohmic contacts as well as the reliability of the commonly used aluminum conductors. Any metallization scheme used with integrated circuits should satisfy several important requirements, such as (Murarka S. P. et al., 1993):

- Low resistivity
- Easy to form and etch
- Stability in oxidizing environments
- Mechanical stability, good adhesion and low stress
- Surface smoothness
- Stability throughout processing as well as during subsequent operation
- No contamination of devices, wafers and working apparatus
- Good long-term device characteristics
- Low electromigration even at high currents and high operating frequencies
- High thermal conductivity to insure heat dissipation

The signal transmission delay time, τ=RC, is of critical importance for the multilayer devices that are connected to each other and to other devices via the metal interconnection lines. These multilayer devices consist of alternating layers of metal and dielectric. R and C stand, respectively, for the resistance of these interconnection lines, and the capacitance of the dielectric between them. A low RC value will result in a faster signal transmission speed of the device. At less than 1 micron feature sizes, the interconnect delay becomes very significant. In order to reduce the RC time constant, one may use lower resistivity metals and shorter metal conductor connections, as well as lower permittivity dielectrics (Murarka, S. P. et al., 1993). Low permittivity dielectric materials have a small amount of polar groups and their dissipation factors are small. Low dissipation factors are desirable for low power losses (Ku, C. C. and Liepins, R., 1987).

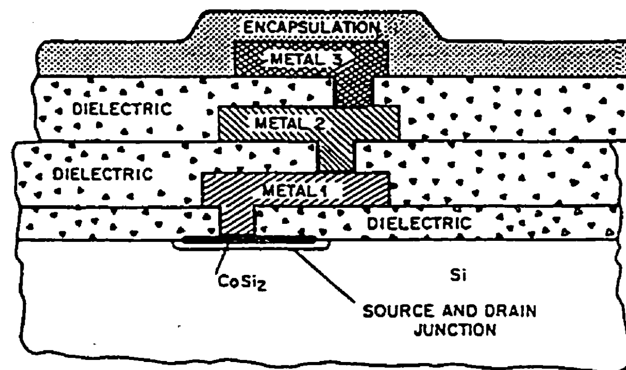

Fig. 1.1: Illustration of a multilevel interconnect scheme

Low resistance of the interconnections and contacts plays other important roles

as well: it generates less heat and has a lower electromigration-induced atomic flux. The importance of this is obvious if one considers that future current densities are expected to be at least an order of magnitude higher than today's.

There have been several candidates among the metals, as well as among the dielectrics which seem to satisfy most of the above requirements. However, to comply with all of them is not an easy task at all. Each possible candidate has its own advantages and disadvantages. Among the metal candidates are W, Al, Ag, Au, Ta, Ti, Mg, Be, Mo and Cu. The comparison in Table 1.1 clearly shows that Cu is one of the most promising materials.

Table 1.1: Possible candidates for low resistivity metal.

Metal	Resistivity ($\mu\Omega$-cm)	Thermal conductivity (W/cm)	Melting point at atmospheric pressure (°C)	Deposition
Cu	1.67	3.98	1085	Sputtering Evaporation
Ag	1.59	4.25	962	Sputtering Evaporation
Au	2.35	3.15	1064	Sputtering Evaporation
Al	2.66	2.38	660	Sputtering Evaporation
W	5.67	1.74	3387	Sputtering Evaporation

Cu has a lower resistivity than all other metals except Ag. If we take into consideration the higher melting point of Cu in comparison with Ag, an important factor responsible for low diffusivity of Cu at a given temperature compared to Ag, we can conclude that Cu is preferable. The high thermal conductivity of Cu is another positive property that helps lowering the effective temperature rise in copper interconnections.

Let us consider the possible low permittivity dielectric candidates. Among the materials of interest are the fluoropolymers, fluorinated polyimides, polyimide nanofoams, parylenes, porous silica, fluorinated SiO_2, aerogels, amorphous diamond-like carbon,....etc. Fluoropolymers have several superior properties compared to other dielectrics. Table 1.2 summarizes the characteristics of some low permittivity dielectric candidates. It is evident that only the aerogels and porous silica have a lower permittivity than the fluoropolymers. All the other dielectrics have substantially higher permittivities. Even though existing data on bulk aerogels confirm that they meet property requirements such as thermal stability, moisture absorption, and compatibility with conductors, they possess a diminished strength as compared to dense materials (Hrubesh L. W., 1995). Strength is important for film processing and subsequent device processing (metallization, etching, etc) (Smith D. M. et al., 1995). Parylenes, some having relatively low permittivities compared to other candidates, are prone to metal diffusion, and the diffusion coefficient is comparable to polyimides. In addition, parylenes do not adhere well to underlying surfaces, and the metals deposited on parylene have weak adhesion (Dabral S. et al., 1995).

Table 1.2: Candidates for low permittivity dielectric.

Material	Permittivity	Deposition technique	Thermal stability
Polyimide siloxane [1]	2.6-2.7	Spin-on	> 350 °C
Parylene-n [1]	2.6-2.8	Vapor phase	~400 °C
Parylene-f [1]	2.3-2.4	Vapor phase	> 450 °C
Vinyl ethers UV polymerized [1]	< 2.7	Spin on	< 450 °C
Polyimide-37B [1]	2.2-2.7	Spin-on	~250 °C
SiOF [2]	3.6-4.7	PECVD	> 400 °C
Porous silica [3]	1.6-2.0	Spin-coating	> 450 °C
Fluoropolymers [5]	< 2.0	Spin-on, PECVD, sputtering	< 400 °C
Aerogels [4]	1.2-1.8	Spin on	> 450 °C

References:

([1] Gutmann, R. J. et al., 1995)

([2] Sullivan, J. P.et al., 1996)

([3] Rosario, A. G., 1996)

([4] Ting, C. H. et al., 1995)

([5] This work)

The general objective of our work was to test copper and fluoropolymers as potential candidates for multilevel interconnects. Our specific objectives were to compare different fluoropolymers according to their fabrication process, dielectric properties over a large frequency range, thermal stability and their compatibility with the metallization process.

In the present work, we used several types of fabrication processes to obtain and compare different types of fluoropolymers. Fluoropolymer films were obtained using spin-coating, plasma polymerization and sputtering. Copper was either sputtered or evaporated. These are deposition techniques that can easily be incorporated in the manufacturing processes presently used.

The dielectric properties, which are the permittivity and the dissipation factor, were evaluated over large frequency (10^2 Hz-10^6 Hz) and temperature (25 °C-200 °C) ranges. The purpose of thermal cycling of the multilayer structures was to eliminate polar species incorporated in the films and thus to obtain reproducibly stable films. In addition to this, it gave us the opportunity to determine the temperature range over which these structures are stable. The stability of the copper-fluoropolymer interface is determined largely by the compatibility of the metallization process with the fluoropolymer films.

To understand the interface and bulk-related phenomena, as well as to interpret the possible problems, experiments were conducted to evaluate the adhesion, stress, diffusion, release of gases, as well as surface and bulk chemical properties, using

various methods such as PA FTIR, contact angle goniometry, XPS and mass spectrometry. In Chapter 5, we summarize our findings on the suitability of fluoropolymers and copper for multilevel interconnects.

CHAPTER II

CHARACTERISTICS OF FILM MATERIALS CONSIDERED FOR MULTILEVEL INTERCONNECTS

2.1. STRUCTURE AND DIELECTRIC PROPERTIES OF FLUOROPOLYMER FILMS

In this chapter, first the phenomena of relaxation and dielectric loss will be shortly described for polymers in general. Next, conventional and plasma-deposited fluoropolymers are described and a short comparison is made. The discussion involves the structures and the dielectric properties as they are described in the literature. The discussion on the part of the conventional fluoropolymers includes Teflon AF1600. Fundamental principles of plasma processes and the polymerization mechanism are given as part of the discussion on plasma-deposited fluoropolymers.

Polymers exhibit in general more than one region of dielectric loss (loss tangent) due to different motions of their segments (Ku C. C., Liepins R., 1987). Tangent of the dielectric loss angle is the ratio of the loss current to the charging current in a condenser, and it is expressed as:

$$\tan\delta = \frac{\text{loss current}}{\text{charging current}} = \frac{\varepsilon''}{\varepsilon'} \qquad (2.1)$$

Here, ε' is the real part of the dielectric constant (permittivity), and ε'' is the imaginary part of the dielectric constant.

For amorphous polymers at least two regions are observed, and for crystalline polymers loss regions may arise from four regions. The glass-rubber transition T_g, indicating a transition from the glassy state to a rubbery state, gives rise to a major dispersion for both amorphous and crystalline polymers. Short range motions such as side-group rotations or local mode motions lead to smaller dispersions (loss regions). These usually take place in the low-temperature range. Another source of dispersions is phase transformation.

One can label the various peaks using Greek letters: the highest temperature process is always α, with the remaining peaks being labelled in order of decreasing temperature. Therefore, analysis of dielectric spectra provides information about the structural characteristics of polymers.

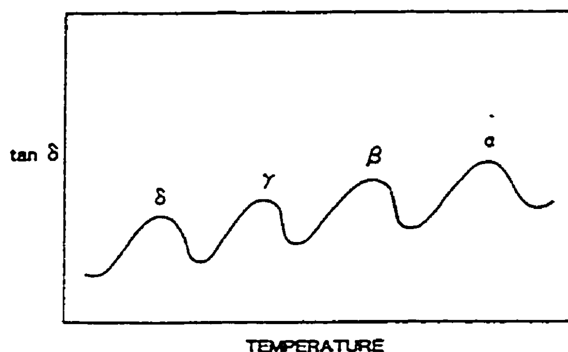

Figure 2.1: Relationship between tanδ and temperature at constant frequency. (from Ku C. C., Liepins R., 1987).

An important issue in our work is to achieve low values for the dielectric loss and the permittivity (ε' or κ). This involves both chemical and physical aspects. The chemical aspect is concerned with the synthesis of molecules that lead to short relaxation times and thus low tanδ values. The physical aspect of achieving low values

for the dielectric loss involves the effects of plasticization, molecular weight and morphology. For low-frequency (<1kHz) dielectric losses, the dc and ac conductivities are very sensitive to small amounts of moisture and impurities. This makes the dielectric properties very sensitive to local inhomogeneities and structural defects that introduce additional dipoles into the polymer. As a conclusion we can say that the elimination of impurities and structural heterogeneities is of utmost importance in order to achieve low $\tan\delta$. The requirements leading to low dielectric losses in polymers can be summarized as follows (Ku C. C., Liepins R., 1987):

(1) Prevention of short branch formation during the synthesis as well as during subsequent processing.

(2) Prevention of unsaturation to avoid oxidation.

(3) Prevention of oxidation during synthesis as well as during processing. Carbonyl groups can contribute significantly to the dielectric loss.

(4) One might choose plasticizers with polarities lower than that of the polymer itself.

(5) Elimination of impurities and structural irregularities by improving the synthesis and processing conditions.

In the following, we examine and compare conventional fluoropolymers and plasma polymerized fluorocarbons (PPFC) by referring to earlier published work.

2.1.1 CONVENTIONAL FLUOROPOLYMERS

In this section, conventional fluoropolymers will be discussed in general and

Teflon AF1600 will be dealt with in more detail.

Conventionally polymerized fluorocarbons, such as tetrafluoroethylene, are known to form a highly ordered structure. This could be explained to be due to the arrangement of oligomers (Nakano T. et al., 1988). The films are expected to have a more ordered structure when the substrate temperature during polymerization is high. Since the molecular motion occurs easily in the as-polymerized film, the degree of order of the film will increase if the film is heated after polymerization. On the contrary, plasma irradiation during deposition crosslinks the film.

"TEFLON AF" is a member of a family of amorphous copolymers based on 2,2-bistrifluoromethyl-4,5-difluoro-1,3-dioxole (PDD) with tetrafluoroethylene (Buck W. H., Resnick P. R., 1993). Copolymers of PDD with TFE are commercially available from Du Pont. Figure 2.2 shows the chemical structure of TFE and PDD copolymers, and Figure 2.3 shows the structure of Teflon AF1600.

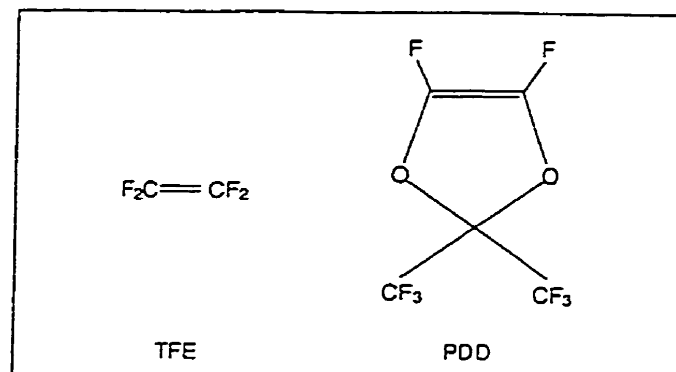

Figure 2.2: Teflon AF: A family of Amorphous

Fluoroplastics with Tg ranging from 80 °-300 °C.

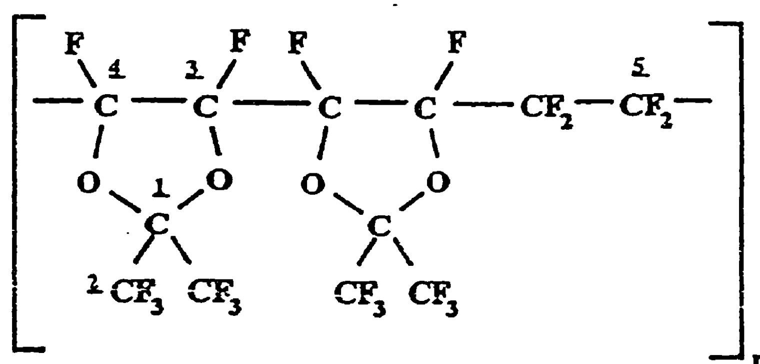

Figure 2.3: Chemical structure of Teflon AF 1600 repeat unit.

TEFLON AF polymers have the lowest dielectric constants (table 1.2 shows about 1.9 at room temperature) of any known solid polymer (Starkweather H. et al., 1991), extremely low refractive indices (Chow R. et al., 1994 and Lowry, J. H. et al., 1992), high gas permeability, and low thermal conductivities. These copolymers are soluble at room temperature in several fluorocarbon solvents. Properties may be varied by changing molecular weight and comonomer ratio. A summary of the properties given by the manufacturer is shown in table 2.1.

Table 2.1: Typical property data for Teflon AF (Grades 1600 and 2400).

Property	ASTM Method	Units	Grade 1600	Grade 2400
Electrical				1 MHz-10 GHz
Dielectric Constant	D150		1.93	1.90
Dissipation Factor	D150		0.0001–0.0002	0.0001–0.0003
Dielectric Strength	D149	kV/0.1 mm	2.1	1.9
Optical				
Optical Transmission	D1003	%	>95	>95
Refractive Index	D542		1.31	1.29
ABBE Number			92	113
Mechanical				
Yield Strength		MPa		
		23°C	27.4 ± 1.0	26.4 ± 1.9
		150°C	6.7 ± 5.9	
		220°C		8.7 ± 4.0
Tensile Strength	D638	MPa		
		23°C	26.9 ± 1.5	26.4 ± 1.9
		150°C	7.7 ± 6.1	
		220°C		4.2 ± 1.8
Elongation at Break	D638	%		
		23°C	17.1 ± 5.0	7.9 ± 2.3
		150°C	89.3 ± 13.1	
		220°C		8.4 ± 4.1
Tensile Modulus	D638	GPa	1.6	1.5
Flexural Modulus	D790	GPa		
		23°C	1.8 ± 0.1	1.6 ± 0.1
		200°C	1.0 ± 0.1	
		220°C		0.7 ± 0.1
Hardness				
Rockwell	D785	23°C	103	97.5
Durometer	D1706	Shore D		
		23°C	77	75
		150°C	70	
		220°C		65
Impact Strength	Notched Izod	N	—	—
Deflection Temp.	D648			
(66 psi)		°C	156	200
(264 psi)			154	174
Chemical				
Contact Angle with Water		Degrees	104	105
Critical Surface Energy		Dynes/cm	15.7	15.6
Taber Abrasion		cc/2000 cycles	0.107	0.2
Chemical Resistance				
• Water Absorption	D570	%	<0.01	<0.01
Gas Permeability				
• H_2O		Barrer	1142	4026
• O_2		Barrer	340	990
• N_2		Barrer	130	490
• CO_2		Barrer		2800
Other				
Tg	D3418	°C	160°C ± 5	240°C ± 10
Specific Gravity	D792		1.78	1.67
Melt Viscosity	D3835	Pa·s	2657 at 250°C, 100 s^{-1}	540 at 350°C, 100 s^{-1}
Volume Coefficient of Thermal Expansion	E831	ppm/°C	260	301

Figure 2.4 shows the variation of refractive index as a function of PDD/TFE copolymer composition.

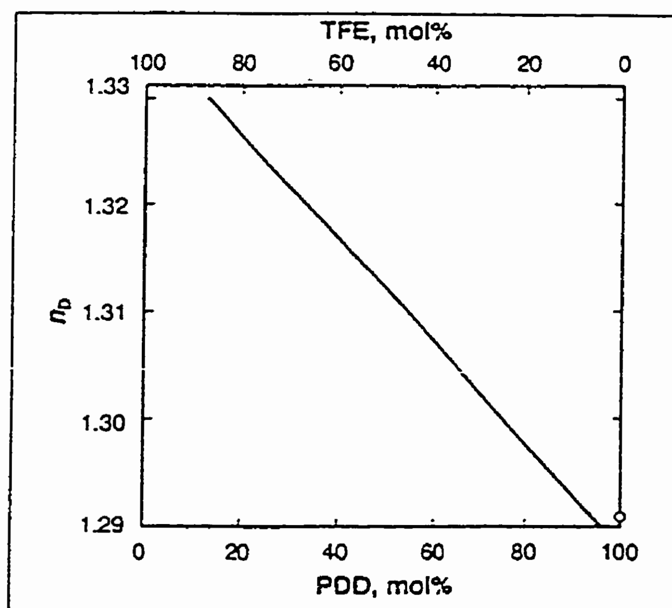

Figure 2.4: Refractive Index vs. Composition for PDD/TFE Copolymers (from Buck W. H., Resnick P. R., 1993).

There is a variety of solution processing methods due to the room temperature solubility of Teflon AF in perfluorocarbon solvents. In order to obtain thin to ultra-thin, uniform thickness coatings on flat substrates one can spin-deposit the dissolved TEFLON AF. From Figure 2.5 one can get an idea about the dependence of film thickness on spin speed and on the concentration of solution.

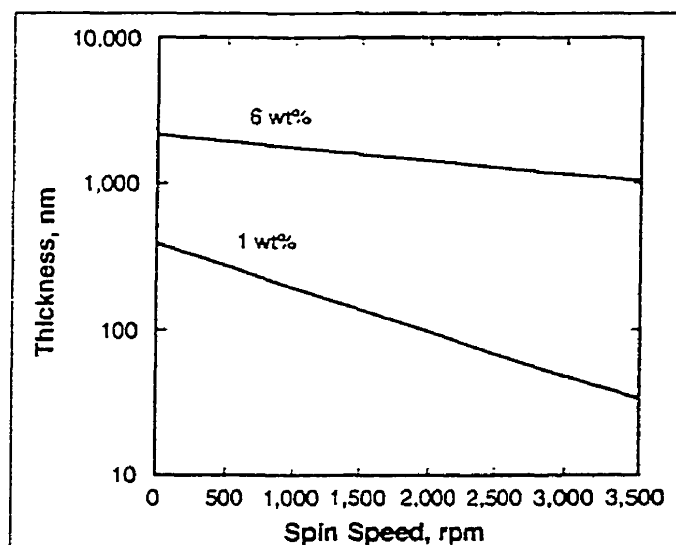

Figure 2.5: Film Thickness vs. Spin Speed for Teflon AF 1600 solutions diluted in Sigma Fluorinert FC-75 and spun onto glass.

Infrared spectra of a Teflon AF1600 film were compared to that of conventional PTFE (Polytetrafluoroethylene) (Nason T. C. et al., 1992). The most significant difference of Teflon AF from PTFE was the strong peak at ~980 cm^{-1}, indicative of CF_3 vibrations (more discussion will be provided in section 4.2.3). This peak is very weak for thin films of ordinary Teflon. The strong presence of CF_3 in Teflon AF films supports the contention that the dioxole monomer is not unduly discriminated against repolymerization of scission fragments. Also the peaks at 1100, 1245, 1270 and 1310cm^{-1} were present only in Teflon AF and can be attributed to the fluorinated dioxole component.

Teflon AF was proposed for several applications including high performance optical coatings such as anti-reflective (AR) and high reflector (HR) coatings (Chow R. et al., 1994). The bulk properties of this perfluorinated amorphous polymer show a high transmittance range from 200 nm to 2000 nm, and a low refractive index of about 1.29. It was shown that Teflon AF2400 can be thermally evaporated (Nason T. C. et al., 1992) as a corrosion barrier for extra-terrestial equipment (Grieser J. et al., 1990), and as an insulator for submicron electronic devices (Hiraoka H., Lazare S., 1990).

2.1.2 PLASMA-DEPOSITED FLUOROPOLYMERS

Before proceeding to our work, it would be appropriate to mention the basics of a plasma, in our case more appropriately the "cold" low-pressure plasma. A plasma can be defined as a partially ionized gas, with equal number densities of positive and negative charge carriers, in which the charged particles are "free" and possess collective behavior. A plasma thus consists of neutrals, ions, radicals, excited species, electrons and the accompanying UV radiation. In a low pressure, high frequency discharge, the heavy particles are essentially at ambient temperature (0.025 eV), while the electrons with higher kinetic energies (up to tens of eV) are capable of breaking bonds and causing further ionization. This is necessary to sustain the discharge. These reactive species can thus undergo either homogeneous (gas-phase) or heterogeneous reactions (with a solid surface in contact with the plasma). These take place near ambient temperature and, therefore, plasma processes are well suited for the deposition

of temperature sensitive polymer films and substrates that are coated with these. Plasma processes can be used for basically three types of applications: the deposition of thin films, etching and surface modification. Plasma polymerization can make flawless thin films particularly useful in the electronic device industry. Because of the fact that commercial applications of low pressure plasma processes for deposition and surface modification are relatively new in comparison to etching, the industry is changing its classical semiconductor processing schemes cautiously and gradually towards new alternatives. These thin films can be obtained either by the plasma-polymerization of a monomer gas or by the sputtering of a conventional polymer target. The second important effect is surface modification. The above-mentioned energetic particles and photons in the plasma interact with the polymer surface. In plasmas which do not lead to thin film deposition, four general effects can be observed: (i) surface cleaning, (ii) ablation or etching, (iii) crosslinking or branching and (iv) modification of surface chemical structure (Liston E. M. et al., 1993).

The discussion of this section includes fluoropolymer films obtained from plasma polymerization of a monomer, and fluoropolymer films that are sputtered from their conventional bulk target. In the case of fluorocarbons both methods result in qualitatively similar chemical and physical properties (Tibbitt J. M. et al., 1975).

Plasma polymerization is a good method to make nearly flawless thin films and therefore it has been considered promising in a variety of areas such as microelectronics, optoelectronics, optics, biomedical industry,...etc. Plasma polymerization can be used to deposit thin films from monomers which are very

difficult to polymerize by conventional methods (Nakano T. et al., 1988). The individual reactions involved in the process of polymer formation in a glow discharge are very complex.

Earlier studies involving X-ray photoelectron spectroscopy (XPS) (Rice D. W., O'Kane D. F., 1976; Clark D. T. et al., 1979) and nuclear magnetic resonance (NMR) (Dilks A., Kaplan S., 1982), have shown that plasma-polymerized fluorocarbons are highly cross-linked with some unsaturated carbon groups in contrast to their conventional counterparts. During plasma deposition, many electrons, ions and photons with enough energy bombard the film and freeze the structure in the disordered state. Therefore, the subsequent thermal treatment rarely increases the degree of order. IR absorption spectra of plasma-polymerized fluorocarbon films show the presence of C=O groups that appear upon exposure to air (Giegengack H., Hinze D., 1971; Alptekin A., et al., 1997). This is attributed to the reaction of free radicals (dangling bonds), created during the plasma-deposition process, with the atmospheric oxygen.

The structure and properties of plasma-polymerized films depend on feed composition and parameters of the plasma environment, such as power, pressure and monomer flow rate (Chen R. and Silverstein M. S., 1996). F/C ratios of 1.33, 1.55 and 1.71 were found for plasma-polymerized octafluorocyclobutane (PPOFCB) prepared under various fabrication conditions (Amyot N. et al., 1992). It was suggested that plasma-polymerized films with low F/C ratio are more highly crosslinked compared to films with high F/C ratios. Since crosslinking is known to contribute to enhanced electrical conductivity, this could help explain their observed high tanδ values (Amyot

N. et al., 1992).

The glow discharge polymerization of fluorine-containing compounds is very sensitive to the conditions of polymerization. In order to obtain polymers from fluorine-containing compounds, it is very important to use a relatively low discharge power in comparison to other polymers (Yasuda H., 1978). High discharge power leads to ablation by detaching the fluorine. Thus one can not easily produce polymer films with a high fluorine content by using high discharge powers. Etching in fluorocarbon plasmas makes the plasma polymerization a complex phenomenon (Yasuda H., 1985) (d'Agostino R. et al., 1990). Therefore it is helpful to employ techniques that suppress the etching effect of the detached fluorine, such as the addition of a small amount of H_2 (Winters H. F. et al., 1977) or hydrogen-producing compounds (Mogab C. J., 1977). It was observed for fluorocarbons with a high F/C ratio ($F/C>2.0$), the predominant process is etching, while for fluorocarbons with a low F/C ratio ($F/C<2.0$), polymerization is a dominant process (Kay E. et al., 1980).

To illustrate plasma polymerization mechanism more clearly, one may show some examples. Electron induced monomer fragmentation and ionization takes place when a fluorocarbon monomer is introduced into a plasma system. Fragmentation products produced depend on monomers being used (Kay E. and Dilks A., 1981). Various ions and radicals will also be formed. It was shown that in the case of saturated monomer injection, the rate of polymerization on a substrate is proportional to the rate of arrival of unsaturated species of the homologous series: $(CF_2)_n$ (Kay E. and Dilks A., 1981). The kinetic energy and number of ions bombarding the growing polymer surface

also influences the rate of polymerization and the structure of the polymer (Kay E. and Dilks A., 1981). The following surface reactions compete on all surfaces in contact with the fluorocarbon plasma (Kay E., 1986):

Ion enhanced polymerization:

$(CF_2)_{n(g)}$+Ions → $(CF_{2-x})_{n(s)}$↓ (a)

Chemical sputtering to form volatile species:

$(CF_{2-x})_{n(s)}$+F+Ions→$C_nF_{2n+2(g)}$↑ (b)

Physical sputtering of polymer:

$(CF_{2-x})_{n(s)}$+Ions→$C_xF_{y(g)}$↑ (c)

Physical sputtering of metal from reactor:

$M_{(s)}$+Ions→$M_{(g)}$↑ (d)

When an unsaturated monomer such as tetrafluoroethylene $(CF_2)_2$ is introduced into the plasma, then polymerization (reaction (a)) dominates because of the abundance of polymer precursors $(CF_2)_2$ and energetic ions. Physical sputtering (reaction (c)) will dominate the deposition process if ion energies are very high (E_i=10-5000 eV).

When a saturated monomer such as C_3F_8 is introduced into the plasma, electron-impact induced fragmentation results in CF_2, F and ions (primarily CF_3^+) (Kay E., 1986). Figure 2.6 shows that in a C_3F_8 plasma, the polymer deposition rate decreases with increasing ion energy. At high enough energies removal of electrode material (metal) takes over. This suggests that as the ion energy increases, reactions (b), (c) and

(d) become more dominant. At the grounded substrate electrode surface reaction (a) dominates.

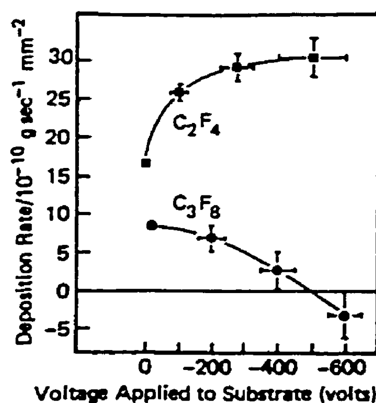

Figure 2.6: Polymer deposition rate in C_2F_4 and C_3F_8 discharge as a function of ion bombardment energy during film growth. (from Kay E., 1986)

Dilution of the plasma with inert gases such as Ar can lead to a less significant polymerization, but an enhanced physical sputtering of electrode material due to Ar^+. Therefore, one can control the ratio of metal sputtered atoms arriving at the substrate from the powered metal target electrode to the polymer precursor species CF_2 arriving at the grounded substrate (Kay E. and Hecq M. J., 1984).

Fluoropolymer films can also be sputtered from their conventional bulk target. Figure 2.7 illustrates a simplified cross section of a sputtering system and the sputtering process.

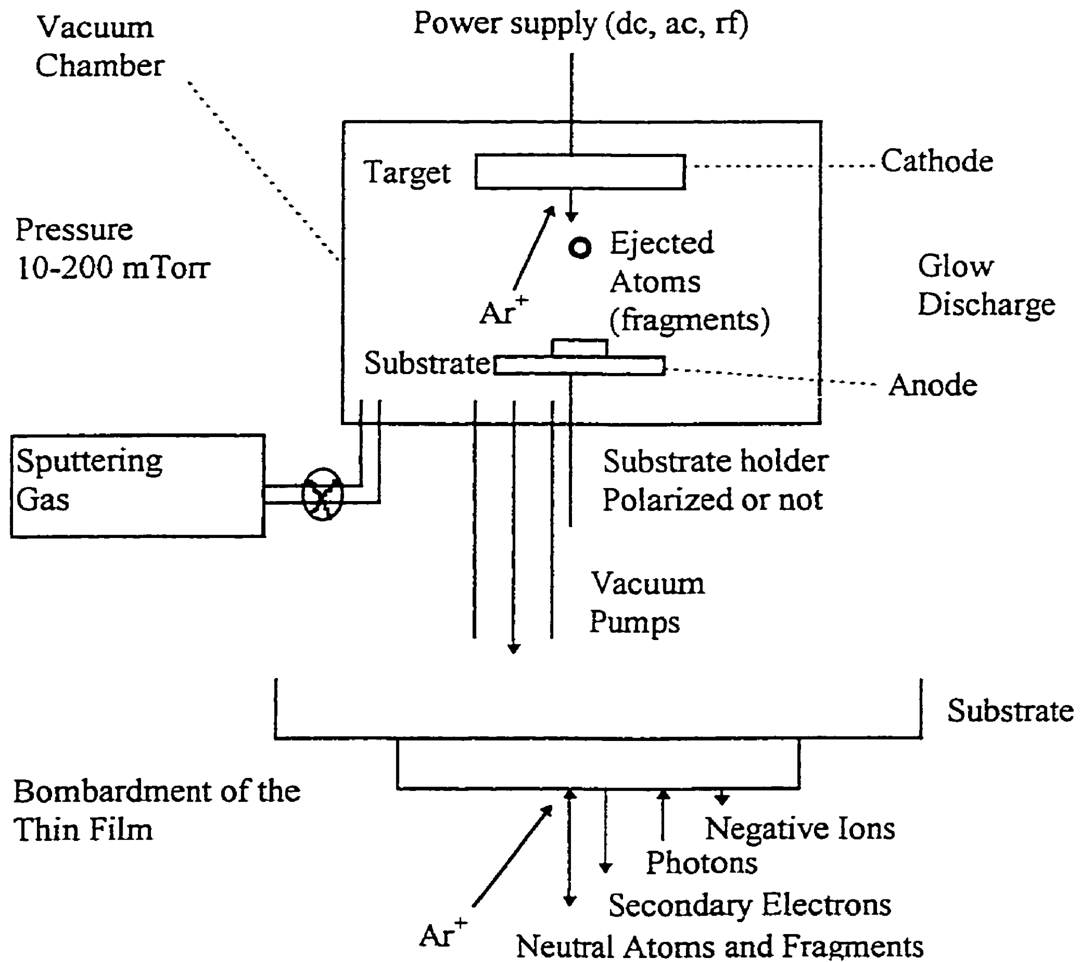

Figure 2.7: A simplified cross section of a sputtering system and the sputtering process.

Typically, the target (simply a plate of the material to be deposited) is connected to a negative voltage supply (dc or rf-induced), the substrates are attached to the substrate holder that faces the target. The holder may be grounded, floating, biased,

heated, cooled or some combination of these. A gas such as Ar is introduced into the evacuated chamber in order to provide a medium in which a glow discharge can be initiated and maintained. When the glow discharge is started, positive ions are accelerated by the electric field toward the target. These positive ions transfer their momentum to the mainly neutral target atoms and thus remove them. These atoms condense on the substrate into thin films. It should be noted that any material object immersed in a glow discharge acquires a negative potential with respect to its surroundings and, therefore, can be considered as a sputtering target. This depends on the plasma potential and the sputtering yield. Other particles such as secondary electrons, ions, desorbed gases, x-rays and photons are also produced at the target. The negative particles (electrons and negative ions) are accelerated towards the substrate platform and bombard the growing film (Vossen J. L., Kern W., 1978). All of these particles produced during the sputtering process influence the film growth.

The sputtering yield is defined as:

$$\text{Sputtering Yield} = \frac{\text{Number of Particles Ejected from Target}}{\text{Number of Incident Ions}} \qquad (2.2)$$

There is a threshold for sputtering approximately equal to the heat of sublimation. The energy range of ions used in sputtering processes is about 10-5000 eV. Generally speaking, the yield increases with incident ion energy and therefore mass of the incident ion (Vossen J. L., Kern W., 1978).

Fluorocarbon polymers deposited by plasma exhibit interesting dielectric properties. Typically, the permittivities are between 1.8-2.2, and the dissipation factors in the order of 0.001-0.0001 (Alptekin, A. et al., 1996). The amount of fluorine in the film depends on the deposition temperature among many other parameters. The F/C (fluorine to carbon) ratio falls and the permittivity increases with increasing deposition temperature (Mountsier T. W., Kumar D., 1996). The plasma assisted deposition of fluorocarbon films from hexafluoropropylene (C_3F_6) and hydrogen showed F/C ratios of 1.1-1.2 at 20 °C and 0.73-0.74 at 400 °C. Since the permittivity rises with increasing temperature due to thermal motions, a permittivity of 1.9 was observed at 20 °C, and this value increased to 2.4 at 400 °C (Mountsier T. W., Kumar D., 1996).

In order to show the importance of the deposition conditions during plasma polymerization and the thermal treatments on the dielectric properties of fluorocarbon films, it would be worth mentioning the results of some experiments performed with plasma-polymerized tetrafluoroethylene (PPTFE) (Nakano T. et al., 1988). Tetrafluoroethylene was polymerized in an RF 13.56 MHz system using Ar and H_2 as carrier gases. Figure 2.8 shows the effect of the thermal treatment on the temperature dependence of the dissipation factor for samples polymerized with a substrate temperature of 20 °C.

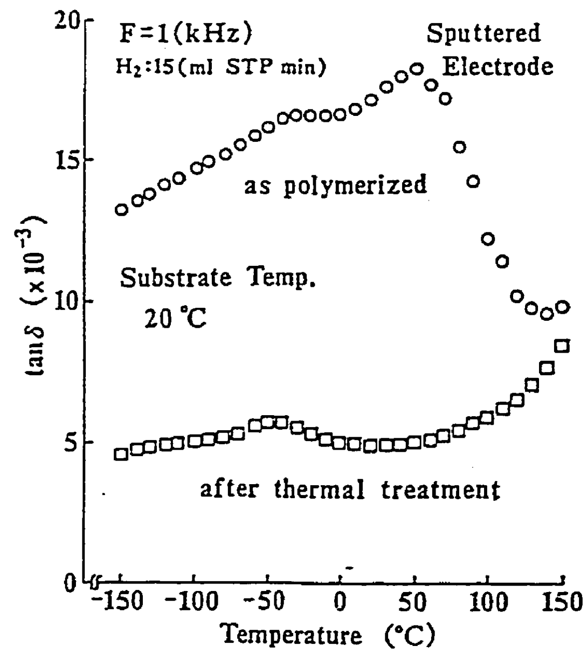

Figure 2.8: Temperature dependence of tanδ before and after thermal treatment in helium (from Nakano T. et al., 1988).

The dissipation factor is decreased by the thermal treatment, indicating the decrease in the number of free radicals in the film (Nakano T. et al., 1985) and the loss of low molecular weight species and water vapor. The as-polymerized film was unstable and the measured value fluctuated depending on how the sample was stored. It was also shown that the flow rate of the carrier gas, substrate temperature, measurement

frequency and the method of electrode deposition of the metal-insulator-metal (MIM) had important effects on the temperature dependence of the dissipation factor (Nakano T. et al., 1985).

An experiment performed with plasma-polymerized CF_3Cl (Martinu L. et al., 1986) showed that, after cooling the specimen in vacuum below -50°C and successive heating, a reproducible maximum in tanδ near 80 °C, similar to figure 2.8 was observed. In the second cycle this peak disappeared and tanδ decreased substantially, giving a reproducible curve. When the sample was exposed to the atmosphere and the measurement repeated, the original curve with the peak near 80 °C was obtained, an effect that can be attributed to the desorption of water vapor during heating.

In the following we examine and compare conventional fluoropolymers and plasma deposited fluoropolymers by referring to the earlier published work.

2.1.3 SHORT COMPARISON BETWEEN THE PLASMA DEPOSITED FLUOROPOLYMERS AND CONVENTIONAL FLUOROPOLYMERS

In order to illustrate typical dielectric behavior of plasma polymerized fluorocarbon films, the loss tangent versus temperature is shown in Figure 2.9 for a plasma-polymerized PTFE film.

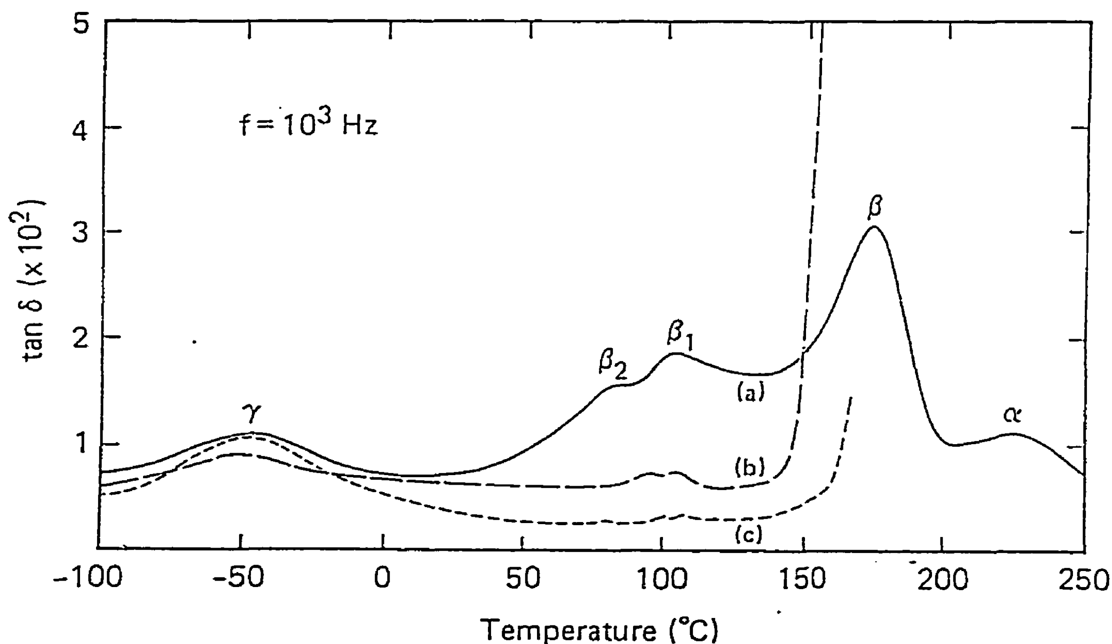

Figure 2.9: Dielectric loss versus temperature at 10^3 Hz for: (a) a fully oxidized, unannealed PPTFE film (full line); (b) a weakly oxidized, unannealed film (dashed line); (c) the fully oxidized film after annealing (dotted line) (Perrin J. et al., 1985).

In the latter scan, measurements are limited up to 170 °C where the conductivity effects appeared, due to short circuits at film fractures created by annealing during the first scan. In spite of several unsuccessful attempts this problem was not solved (from Perrin J. et al., 1985). As observed from the dielectric loss spectra, at least four relaxation peaks are present in the film and are denoted as α, β, β_1, β_2. As a general point we can state that the plasma-polymerized fluorocarbons are highly cross-linked with some unsaturated carbon groups, in contrast to their conventional counterparts. This makes them susceptible to oxidation upon exposure to air. The β_1 and β_2 relaxations observed

in figure 2.9 were attributed to the motion of tertiary carbon structures such as cross-link sites (Tibbitt J. M. et al., 1976). It was suggested that these relaxations are associated with irreversible structural, and possibly chemical, rearrangement of the polymer. The reversible relaxation taking place at around 70 ^{0}C disappears upon annealing. This is probably due to the curing effect consisting of physical and chemical rearrangements of the polymer segments which in turn result in a higher degree of cross-linking and a denser structure. It was hypothesized that the pairing (reaction) of neighboring unsaturated groups could lead to this cross-linking. The existence of such reversible relaxations is common for other plasma-polymerized materials as well (Morita S. et al., 1976). The γ relaxation is due to C=O groups introduced in the film upon oxidation (Hetzler U., Kay E., 1978). This type of relaxations were observed for other plasma polymerized monomers, such as C_2F_3Cl (Martinu L. et al.,1986). In the case of conventional fluoropolymers, these γ relaxations are due to the ordered structure. The ß relaxation in the 160-180 °C temperature region is ascribed to the glass-rubber transition of PTFE (Perrin J. et al., 1985).

An important difference between plasma polymerized fluoropolymers and conventional fluoropolymers is based on the stoichiometry of the deposited films. Films deposited using plasma polymerization possess some remaining impurity materials. Therefore, the deposited films are not stoichiometric. Laser ablation method using an UV laser beam was reported to produce stoichiometric films of PTFE (Blanchet G. B., Ismat S., 1993). Generally, films prepared by rf sputtering are found to be fluorine deficient. (Blanchet G. B., Ismat S., 1993). For a PTFE target used in magnetron rf

sputtering, an F/C ratio of 0.7 was found in the erosion track and a ratio of 1.3 in the center of the target (Biederman H. et al., 1997).

2.2. PROPERTIES OF COPPER FILMS

There has been a large effort over the past several years in the investigation of copper for use as an interconnection metal that would replace the currently used aluminum. The reason for this effort was mainly related to the lower resistivity (1.67 μΩ-cm vs. 2.7 μΩ-cm for Al) and higher electromigration resistance which is several orders of magnitude higher than Al. Besides these, copper has other positive aspects that support its use in silicon integrated circuits: For example corrosion resistance, ductility or formability and mechanical strength (Young's modulus=12.98×10^7 N/cm^2), relatively high melting point (1085 °C at atmospheric pressure) among usable electrical conductors and its high thermal (3.98 W/cm) and electrical conductivities (0.60 $\mu\Omega^{-1}cm^{-1}$). Copper is a near-noble metal and is chemically active mostly in the presence of oxidizing agents. We can say that copper is not altered by dry air (Murarka S. P., Hymes S., 1995). If one neglects the grain-boundary contribution to atomic diffusion, one can express the atomic flux due to electromigration in the single crystal or large-grained crystal as:

$$J_{atoms} = \frac{NDZ^{*}qj}{\sigma kT} \tag{2.3}$$

Here, N, D, Z*q, q, j, σ, k, and T are the atomic density, atomic diffusivity, effective charge on the moving atom, electronic charge, current density, electrical conductivity,

Boltzmann's constant, and temperature in K, respectively. Some of the most conductive metals are compared in Table 2.2 with respect to their electromigration parameters:

Table 2.2: Comparison of electromigration parameters for bulk materials (from Murarka S. P. and Hymes S., 1995).

			Diffusion parameters	
Metal	$-Z^*$	ρ ($\mu\Omega$-cm)	D(cm^2/s)at 100°C	$Z^*\rho D$($\mu\Omega$-cm^3/s) 100°C
Ag	9.4–23.4	1.59	1.1×10^{-26}	$2.84–7.07 \times 10^{-25}$
Al	6.5–16.4	2.65	2.1×10^{-20}	$3.62–9.12 \times 10^{-19}$
Au	5.9–7.4	2.35	2.2×10^{-27}	$3.05–3.83 \times 10^{-26}$
Cu	3.7–4.3	1.67	2.1×10^{-30}	$1.3–1.5 \times 10^{-29}$

Copper has acceptor levels in the middle of the silicon band gap, at 0.24, 0.37, and 0.52 eV with respect to the valence edge and, therefore, can act as a recombination-generation center for charge carriers. Thus it can diffuse in silicon and degrade the semiconductor devices. This was the reason it was avoided in silicon-based integrated circuits in the past. However, today the processing temperatures of copper have dropped from 1000-1300 °C to less than 900 °C and the postmetal processing temperatures from the 400-700 °C range down to less than 450 °C. These are todays reasons for considering copper interconnect technology for multilevel devices.

As mentioned earlier, the main purpose of this work is to achieve lower RC time

constants in order to increase the speed of integrated circuits. This RC delay time, τ, can be expressed as (Murarka S. P., Hymes S., 1995):

$$\tau = RC = \frac{\rho L^2 \varepsilon_{ILD}}{t_M t_{ILD}} \quad (2.4)$$

Here, ρ, t_M, L, ε_{ILD}, and t_{ILD} are the resistivity, thickness, length of the interconnection and interlayer dielectric (ILD) permittivity and thickness. For a given thickness of the metal and the ILD, the RC depends on ρ, L and ε_{ILD}. Table 2.3 shows the properties of possible interlayer metals:

Table 2.3: Properties of possible interlayer metals (from Murarka S. P. and Hymes S., 1995).

	Metal				
Property	**Cu**	**Ag**	**Au**	**Al**	**W**
Resistivity (μΩ-cm)	1.67	1.59	2.35	2.66	5.65
Young's modulus x 10^7 N/cm^2	12.98	8.27	7.85	7.06	41.1
TCR x 10^3/K	4.3	4.1	4	4.5	4.8
Thermal conductivity (W/cm)	3.98	4.25	3.15	2.38	1.74
CTE x 10^6/°C	17	19.1	14.2	23.5	4.5
M - Pt (°C)	1085	962	1064	660	3387
Specific heat capacity (J/kg K)	386	234	132	917	138
Corrosion in air	Poor	Poor	Excellent	Good	Good
Adhesion to SiO_2	Poor	Poor	Poor	Good	Poor
Deposition					
Sputtering	✓	✓	✓	✓	✓
Evaporation	✓	✓	✓	✓	✓
EVD	✓	?	?	✓ (?)	✓
Etching					
Dry	?	?	?	✓	✓
Wet	✓	✓	✓	✓	✓
Delay (ps/mm)	2.3	2.2	3.2	3.7	7.8
Thermal stress per degree for films on Si (10^2 N/cm^2-°C)	2.5	1.9	1.2	2.1	0.8

Note: Delay = RC = 34.5 R_s (ps/mm) for 1-mm-length conductor on 1-μm thick SiO_2.

Only Ag has a resistivity lower than Cu; unfortunately, it is prone to higher electromigration than Cu. The resistivity is not only important to decrease the RC delay but also to reduce the heat generation. The temperature rise in an adiabatic environment where no heat is absorbed or dissipated can be expressed as:

$$\Delta T = \frac{j^2 \rho}{gC} \tag{2.5}$$

Here, j is the current density, g the density, and C the specific heat capacity of the interconnection material. Table 2.4 compares the adiabatic temperature rise for different candidate metals:

Table 2.4: Relative adiabatic temperature rise due to Joule heating in various metals and their thermal conductivities (from Murarka S. P. and Hymes S., 1995).

Metal	ΔT	K (W/cm-°C)
Cu	1	3.98
Ag	1.29	4.27
Au	1.92	3.15
Al	1.93	2.37
Mo or W	4.40	1.4 or 1.78
Ta	10.19	0.54
Ti	32.66	0.2

In thin film applications, the thickness of the copper layer is also of critical importance. An increase in resistivity is observed due to surface and grain boundary scattering. The relative values of the electron mean free path in copper and the thickness or grain size

determine the contribution to the higher resistivity values that are sometimes observed. To avoid this kind of effect, one has to deposit films with thicknesses or grain sizes larger than the mean free path of the electrons in copper. Resistivity might be increased by crystal defects as well. This problem can be overcome by annealing, which leads to an increase in grain size and, therefore, a relative decrease in grain boundary area. This will lead to the elimination of defects. In the case of sputtering, the sputtering gas might be trapped, and its presence would cause a higher resistivity.

It is clear that the lowest temperature rise due to Joule heating is for copper which has also the second highest thermal conductivity only about 7% lower than that of Ag, which has the highest thermal conductivity among the metals. These make it clear that less heat will be generated if copper is used and thus the devices will work more efficiently. Furthermore, heat related problems will be of less concern by the proper use of copper.

Copper has superior mechanical properties compared to aluminum. Table 2.3 gives some of these properties. Young's modulus, yield strength, and ultimate tensile strength of copper at 300 K are 1.3×10^{7}, 6.9×10^{3}, and 2.21×10^{4} N/cm^{2}, respectively. These values are multiples of those for Al (Murarka S. P., Hymes S. W., 1995). Due to this high Young's modulus, stress effects might be of importance for copper films. Stress competes with adhesion strength and can cause adhesive failure of the metal from the dielectric substrate. The specific subject of stress will be discussed later.

2.3 ADHESION OF METALS TO FLUOROPOLYMERS

Adhesion is one of the most important reliability problems. The American Society for Testing and Materials (ASTM) defines adhesion as: "The state in which two surfaces are kept together by the forces at the interface which can be the valence forces or the interlocking forces or both" (Good, R. J., 1975.) When an adhesive failure occurs, the metal layers no longer adhere well to the dielectric substrate such as fluoropolymer. Therefore, one has to consider the issue of adhesion in materials selection and processing. In a multilevel device, due to the different thermal constraints such as different thermal expansion coefficients of the metal layers and the dielectric, stress effects might be cumulative and may very well lead to failure. Even though they limit the device performance to some extent and lead to higher cost of production, adhesion promoters may be effective. In an ideal case, the adhesion promoter can also act as a diffusion barrier between the metal layer and the dielectric. These adhesion promoters can be metals (for example Ti or Ta) as well as alloys (for example TiTa alloy) of some metals. Instead of depositing a thin layer of such a metal or metal alloy , one can pretreat the surface in order to promote adhesion. This treatment can be done using plasma, laser or simply thermally. These issues will be discussed below.

2.3.1 MECHANISMS OF ADHESION

It would be appropriate to look at the various forces of molecular attraction before mentioning the theories of adhesion. There are two main groups of forces of

molecular attraction: chemical and physical bonds. (Allen K. W., 1963.) A chemical bond is characterized by some kind of sharing of particles such as electrons which is the result of a chemical reaction whereas a physical bond is the result of an interaction of particles due to their electric and magnetic fields.

Chemical bonds can be categorized as:

(1) Ionic bonds due to Coulombic electrostatic forces between oppositely charged ions derived from elements of widely different electronegativities.

(2) Covalent electron pair bonds due to exchange forces between elements of similar electronegativities.

(3) Metallic bonding through the sharing of electrons in an electron gas which occurs for the least electronegative elements.

Physical bonds fall into the following categories:

(1) Keesom dipole-dipole forces (orientation effect) - molecules with permanent dipole moments will have a mutual attraction and will cause a mutual alignment.

(2) Debye dipole-molecule forces (induction effect) - a molecule with a permanent dipole moment will induce a dipole in a neighboring molecule by polarization.

(3) London molecule-molecule forces (dispersion effect) - general interaction between any two molecules or atoms in close proximity, irrespective of their permanent dipoles. If averaged over a period of time, molecules may have a zero dipole moment due to the symmetric electron distribution function. However, there will be instantaneous dipoles arising from the motion of the electrons, which will lead to induced dipoles in phase. At

larger distances, about 200 A, the London dispersion forces are reduced by the electromagnetic retardation. In addition, when molecules approach each other very closely a repulsion occurs between their electron clouds as they overlap.

To summarize, the total cohesion in any material will be the result of any primary chemical forces which are involved, Keesom orientation and Debye induction forces if there are any permanent dipoles, London dispersion forces in all cases, diminished by retardation at larger distances and repulsion forces important at short distances.

There are various theories of adhesion (Raevskii R.G., 1973) (Allen K. W., 1969.): chemical bonding theory, adsorption or wetting theory, electrostatic, diffusion, weak boundary layer, mechanical and rheological. According to Fowkes, the acid-base interactions at the film-substrate interface are also very important for the adhesion. Different models explaining adhesion are summarized in several reviews (Mittal K. L., 1976) (Sharpe L. H., 1993)

According to the chemical bonding theory, it is essential to have chemical reactions between the materials in order to achieve good bonding. This theory can be applied well to polymers. It postulates the existence of covalent bonding at the interface as was described above within the subject of molecular interactions. The efficiency of such bonding depends on the number of interfacial bonds and the chain lengths, in the case of polymers.

Wetting has been proven to be a necessary but not sufficient condition for good adhesion. It was observed that some adhesives showed good spreadability (i.e. makes

contact angles close to zero) but did not adhere well (Iyengar Y. and Erickson D. E., 1967).

Electrostatic theory resembles the film-substrate system to a planar capacitor with plates carrying opposite charges (Deryagin, B. V. and Krotova, N. A., 1948).

According to the diffusion theory of adhesion developed mainly by Voyutskii (Voyutskii, S. S., 1963) adhesion arises through the interdiffusion of the adherent and the adhesive. It has been principally applied to joints involving polymeric materials. Sometimes it is a one-way diffusion of adhesive molecules and sometimes a two-way diffusion of both the adhesive and adherend molecules (interfacial mixing). In either case there is no more a clear-cut boundary, but rather an interfacial layer ("interphase") representing a gradual transition from polymer to its substrate.

According to the mechanical interlocking theory, the adhesive has to enter into the pores and irregularities of the materials. The microgeometry of the interface explains adhesion.

The rheological theory relates adhesion to mechanical properties and stress distribution at the film-substrate interface.

2.3.2 EVALUATION OF ADHESION

There are several techniques utilized for estimating the strength of adhesion of thin films deposited on substrates. None of these techniques can be accepted as perfect. All of them have some kind of problem related to the performance of the test and interpretation of the results. This is the reason why one usually tries to evaluate

adhesion by using more than one technique at a time. Thus one can compare the results of the different techniques and come to more meaningful conclusions. There are two fundamental difficulties that limit the measurement of adhesion: 1) the surface irregularities that can be at atomic dimensions do not permit an ideal contact between the two solid surfaces, 2) there are no easy ways to directly measure interfacial atomic bond strengths (Ohring M., 1992). There exist mainly three types of tests to evaluate adhesion: (i) tensile-type test, (ii) shear-type test, and (iii) scratch test. A review of various testing methods can be found in literature (Valli J., 1986) (Steinmann P. A. and Hintermann H. E., 1989) (Martinu L., 1998).

(i) The direct pull-off test is in the most straightforward way related to the adhesion force, F_A, which is equal to the force applied perpendicularly to the contact area. Tested specimen has to be glued or soldered to the tested coating. If contamination of the interface has to be avoided, contact-less methods such as the acceleration test or the pulsed laser test have to be used. The acceleration test consists of a cylinder, onto which the sample is mounted and which is rotated at a very high speed in order to delaminate the coating with the effect of the centrifugal force. In the case of pulsed laser test, a shock wave due to a laser pulse from the back of the substrate causes the coating delamination.

(ii) The simplest shear-type test is the adhesive tape peel test. This test usually provides just a qualitative measure of adhesion. If the percentage of the peeled film is evaluated, a semiquantitative analysis can be made. An estimation of the adhesion force can be obtained by measuring the peel force as a function of angle and extrapolating the

plot to zero angle. The units of peel force are N/m, i.e. the force applied to a given width of the tape, and it does not have the same dimensions as N/m^2 of F_A.

(iii) The scratch test provides qualitative and quantitative information about adhesion. The principle is to drive a stylus of known radius, R_S, over a film under increasing vertical load (see Figure 2.11). During scratching, stresses induced due to indentation and friction combine, and contribute to the total compressive and tensile stresses in front of the stylus and at its trailing edge, as shown in Figure 2.10. As a consequence, the film starts to delaminate.

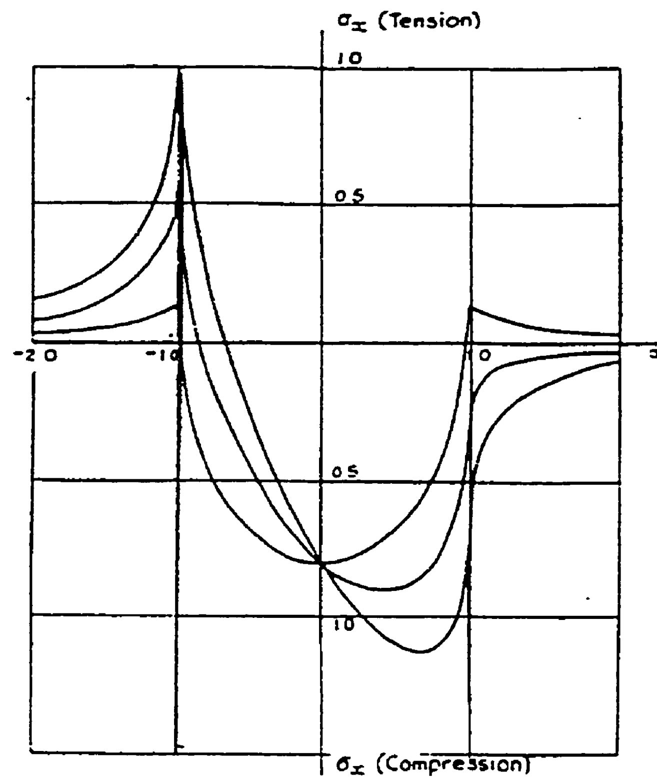

Figure 2.10: Calculated stress distribution during the scratching procedure (from Hamilton G. M. and Goodman L. E., 1966).

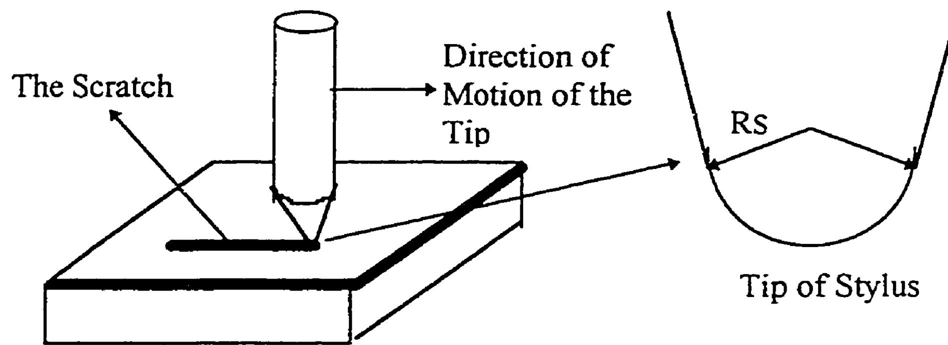

Figure 2.11: Illustration of the scratch test.

The critical load L_C [N] is determined as a load when the film starts to delaminate from the interface. Once the scratching is completed, one can analyze the film adhesion by the following methods (MST Micro-Scratch-Tester, User's Manual, Version: 1.0):

- Acoustic emission detection
- Frictional force measurement
- Penetration depth measurement
- Optical observation (through the attached microscope)

According to the type of film and substrate and their thicknesses as well as the experimental parameters one or several of these methods are more informative in comparison to the others.

The L_C is a semiquantitative measure of adhesion, which can be theoretically correlated with the adhesion force (M. Ohring, 1992):

$$F_A = KH_V L_C / \pi R_S^2 \qquad (2.6)$$

where the magnitude of coefficient K depends on the model details (K can range from 0.2 to 1), H_V is the Vickers hardness of the film, and R_S is the radius of the stylus tip.

According to the model of Bull and Rickerby (Bull S. J. and Rickerby D. S., 1990), three contributions to the stress responsible for the coating delamination are related to the work of adhesion, W_A. These three contributions are: elastic-plastic indentation stress, internal stress and tangential friction stress. The work of adhesion is then expressed as:

$$W_A = \frac{d}{2E}(8L_C / \pi w^2)^2 \qquad (2.7)$$

Here, d is the coating thickness, E the elastic modulus of the coating, and w is the scratch width at L_C.

The ease of application and low cost make the adhesive tape peel test very popular. However, to make a more comparative analysis and determine the modes of failure, one can use the scratch test. The peel test is widely regarded as qualitative. This is not completely true. To make a comparative study, the peel test and the scratch test can both be used and the results can be compared. Semiquantitative information can be obtained from peel test by using differently graded adhesives or by evaluating the percentage of the area of the peeled film, such as in the cross-hatch pattern shown in figure 2.12.

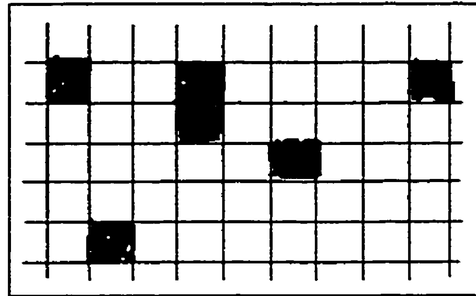

Figure 2.12: Cross-hatch peel test

A consistent procedure has to be adopted in applying the peel test. The type of tape, the weight of roller to be rolled over the tape, the speed and angle at which the tape is peeled and the temperature are some of the factors that have influence on the outcome. Peel test can be applied in several ways, as is shown in Figure 2.13 (Hardy A., 1963).

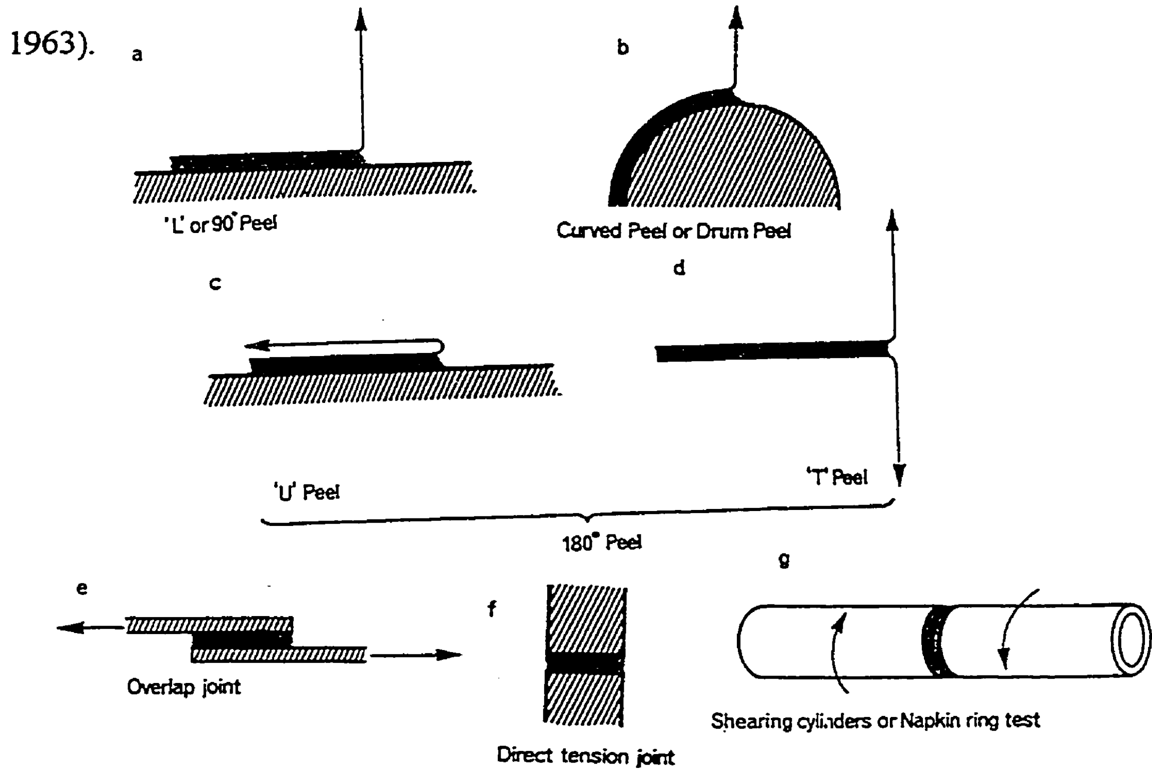

Figure 2.13: Various simple peel tests (from Hardy A., 1963).

2.3.3 METAL-FLUOROPOLYMER INTERFACES

An interface is a region where there is a steep gradient in the local properties of the system. This gradient might be in properties such as chemical composition, as when two immiscible phases are in molecular or atomic contact; or it might be a gradient in structure, such as the interface between two phases which have the same chemical composition, but are different in density or arrangement of atoms or molecules. The gradient across the interface is in properties such as elastic modulus, Poisson's ratio, refractive index,...etc (Good, R. J., 1975.).

Here, we are concerned with the copper-fluoropolymer interface. Fluoropolymer surfaces are inert, possess very low surface energy and contain constituents of weak boundary layers, such as C_xH_y-containing groups on the surface (Shi M. K. et al., 1995). Therefore, films deposited onto fluoropolymers do not sufficiently wet or react chemically with the surface. These can partly explain the reason behind the weak adhesion of copper to fluoropolymers.

The notion of a structured interfacial region is important to illustrate the profile of a film substrate system such as that of copper and fluoropolymer. Figure 2.14 shows the interface structure between the adhering layer and polymer substrate.

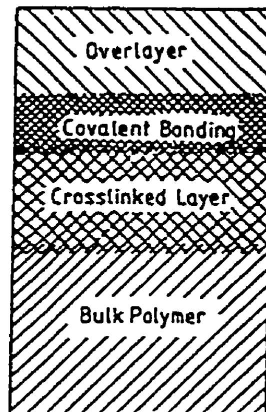

Figure 2.14: Illustration of a structured interface region (Liston E. M. et al., 1993).

Interfaces may control the overall mechanical behavior of coating/substrate systems and therefore should be taken into account in evaluating and improving its properties (Sharpe L. H., 1993). The modification of polymer surfaces for enhanced adhesion by an atmospheric corona discharge or by low pressure plasma treatment, has many advantages in comparison to other, conventional methods such as wet-chemical treatments. Plasma changes the composition and structure of molecular layers up to about 1000 nm depth at or near the surface of the material being treated. The surface interacts with electrons, ions, energetic neutrals, free radicals and photons. Depending on their concentrations, fluxes and energies, we have different effects. Plasmas which do not give rise to thin film deposition, lead to four major effects on polymer surfaces (Liston E. M. et al., 1993):

(i) Surface cleaning with the removal of organic contamination from the surfaces;

(ii) Ablation, or etching of material such as weak boundary layer from surfaces and

increasing the surface area.

(iii) crosslinking or branching of near-surface molecules to cohesively strengthen the surface layer.

(iv) modification of surface-chemical structure during plasma treatment and after re-exposure of the materials to air. This results in the reaction of free radicals with atmospheric oxygen or water vapor.

An XPS experiment performed to study the interaction of Cu with untreated and N_2-plasma-treated surface of Teflon AF shows the importance of covalent bonds on the adhesion of Cu to fluoropolymers (Shi M. K. et al., 1995). As can be seen from Fig 2.15, after Cu evaporation, new features at around 285 and 531 eV in the C(1s) and O(1s) spectra of the XPS analysis may be identified. (Shi M. K. et al., 1994). The feature around 285 eV in the C(1s) peak may contain components from the formation of C-C and Cu-O-C bonds, and the feature around 531 eV in the O(1s) peak may be due to Cu-N-C- structures (Shi M. K. et al., 1994).

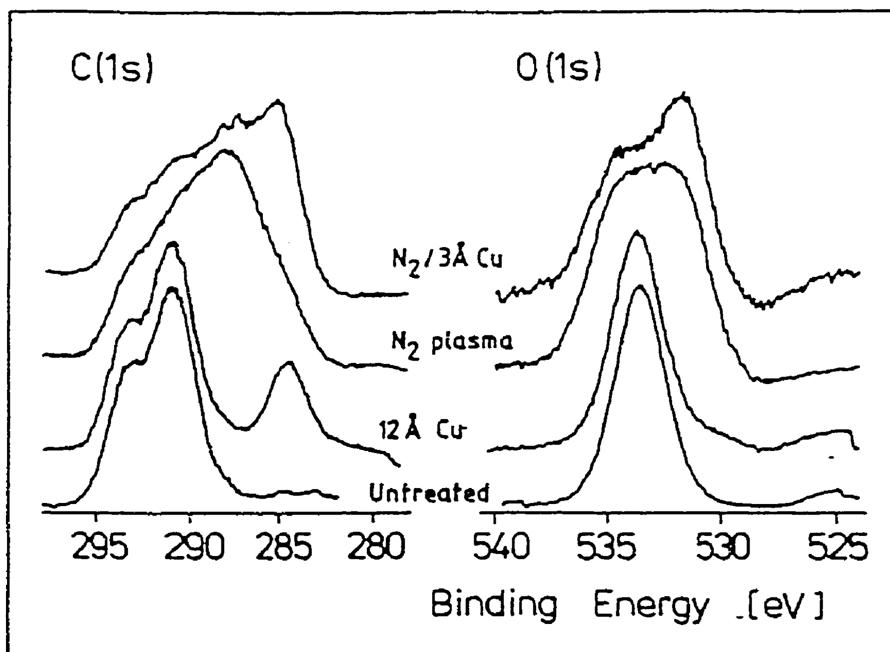

Figure 2.15: XPS C(1s) and O(1s) spectra of Teflon AF (from Shi M. K. et al., 1995).

Another XPS analysis was performed for the plasma-polymerized trifluoroethylene (C_2F_3H) (Shi M. K. et al., 1995) (Figure 2.16). The C(1s) envelope shows the presence of C-C (C-H), CF, CF_2 and CF_3 groups (D'Àgostino R., 1990). After Cu evaporation, the peak at 286 shifted to a lower binding energy at around 285.5 eV, which may indicate Cu-O-C bond formation (Shi M. K. et al., 1995), and the F(1s) spectrum was changed by an additional peak at around 682.5 eV, due to -F.

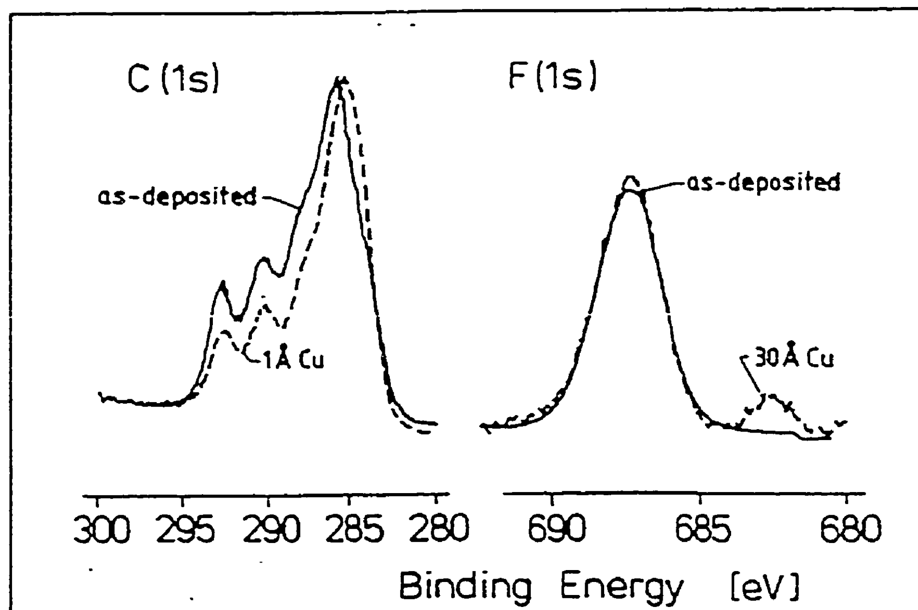

Figure 2.16: XPS C(1s) and F(1s) spectra of PPFC before and after Cu deposition (from Shi M. K. et al., 1995).

These observations from the XPS experiments suggest that Cu-O-C and Cu-N-C bonds may be responsible for superior copper adhesion to N_2-plasma-treated fluoropolymers. As mentioned earlier, the highest energies of interaction are associated with covalent bonding (200-800 kJ/mole). Plasma surface treatments involving other gases such as O_2, H_2, O_2+H_2 and N_2+H_2 also improve the adhesion of copper to fluoropolymers (Shi M. K. et al., 1995; Liston E. M. et al., 1993).

Literature involving plasma surface treatments gives insight into the contribution of various factors to the copper-fluoropolymer adhesion (Liston E. M. et

al., 1993). Plasma treatments and surface analysis have shown very important reactions going on in the near-surface region. As an example, it has been observed that the chemical composition of the plasma treated surfaces may be modified by the reactions with atmospheric oxygen and water vapor. No oxidation was detected by in-situ XPS analysis following N_2 plasma-treatment for polyethylene surface. This explains the post-oxidation process that leads to oxygen incorporation on PFA surfaces treated with gases such as He, N_2, H_2 and N_2+H_2 (M. K. Shi et al., 1995).

An important point that should be noted is that despite the reaction of Cu with both oxygen and nitrogen to form Cu-O and Cu-N bonds, there has not been an observation of a reaction of Cu with carbon and fluorine (M. K. Shi et al., 1994)

As mentioned earlier, adhesion is related to both physical and chemical effects. In a study using scanning electron microscopy, there were no observed changes in the surface topography of PFA surface after treatment in O_2 plasma at 50 sccm and 200 mTorr for 1 minute (Shi M. K. et al., 1994). This was thought to suggest that physical effects are not as important as chemical effects in the case of Cu/PFA adhesion. However, a more recent AFM study showed that, indeed, there is a similar trend of microroughness and adhesion strength as a function of different treatment gases used in the plasma (Klemberg-Sapieha J.E., 1997). The measured RMS values for plasma-treated Teflon PFA surfaces are shown in Fig 2.17, together with the critical load values obtained with the Microscratch Tester for copper evaporated onto Teflon PFA. This result can be used to explain the effect of microroughening on the adhesion improvement by two effects: (i) enhanced mechanical interlocking, and (ii) making

more surface area available for chemical bonding. It is believed that these two mechanisms, together with surface mechanical stabilization by crosslinking, contribute to enhanced film adhesion found for plasma-treated polymer surfaces.

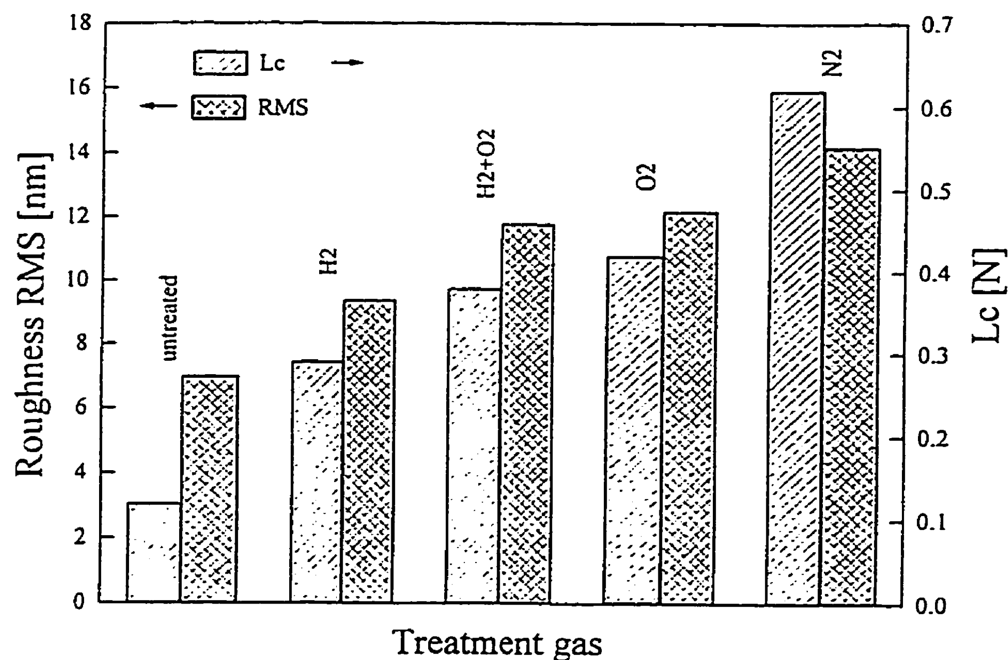

Figure 2.17: Effect of treatment gas in microwave plasma on the critical load, Lc, of 200 nm thick evaporated copper films, and on the mean surface roughness (RMS) of as-treated Teflon PFA surfaces (from Klemberg-Sapieha J.E., 1997).

CHAPTER III

EXPERIMENTAL METHODOLOGY

3.1 FABRICATION OF FLUOROPOLYMER FILMS

The fluoropolymer samples we evaluated in this study include plasma-polymerized (PP) C_2F_4 and C_2F_3H, sputtered (SP) Teflon PTFE, and spin-deposited (SD) Teflon AF1600. We chose these fluoropolymers due to their availability or the compatibility of their deposition methods with the presently used technologies.

3.1.1 PLASMA DEPOSITION

The plasma system used in our laboratory is shown in Figure 3.1. Both the sputtering and the plasma polymerization of fluorocarbon were performed in an RF plasma system operating at 13.56 MHz and at a pressure of 20-40 mTorr, as measured by an MKS Baratron pressure gauge. The chamber was evacuated using turbomolecular or diffusion pumps. The distance between the RF and the grounded electrodes was 2.2 cm and the electrodes were 8.4 cm in diameter. In the case of SP films, a disc of 3 mm thick conventional PTFE was placed on the RF electrode, and glass or silicon substrates were placed on the grounded electrode; Ar and CF_4 gases were used at a flow rate of 10 sccm measured by MKS flowmeters, and the RF power was about 250 W, as indicated by the power source. For PP films, C_2F_3H or C_2F_4 monomers were used at the same flow as for sputtering but with an RF power of about 20 W. The Si or glass substrates

were placed on the grounded substrate holder. All fluoropolymer films in this study were about 1 μm in thickness (see section 3.3.5 for the measurement of film thickness) unless otherwise mentioned. This was so for all samples prepared for various characterization techniques. The shapes of substrates however were different, as will be specifically described as part of the analysis technique that was used.

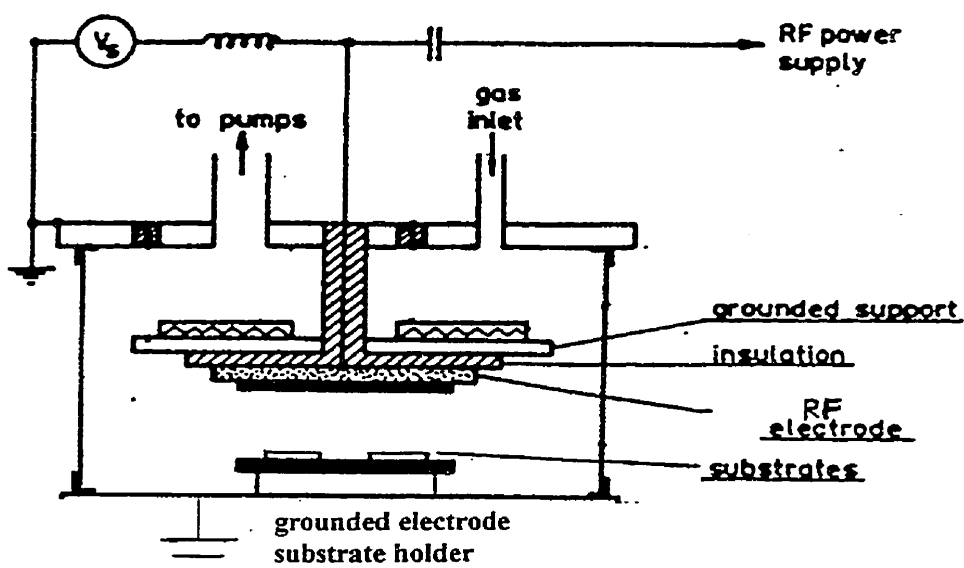

Figure 3.1: Plasma system used in our laboratory.

3.1.2 SPIN COATING

For our experiments, TEFLON AF1600 solution was diluted in Fluorinert Sigma FC-77, to obtain a 6% solution, and spin-deposited. First, a 2 inch wafer was placed firmly onto the Teflon holder of the instrument using a pump. Before applying the

liquid polymer solution, the wafer was rotated at the highest speeds for some time to be well centered. A large pipette was filled with 1.2 ml of the solution and this was poured manually onto the center of the wafer. Immediately thereafter the spin coater was turned on at a speed of 6200 rpm for 20 seconds. The fluoropolymer films were about 1 μm thick. The standard curing procedure consisted of two steps. The first step was to anneal the coated substrates at 170 °C for 15 minutes, and the second step was an annealing at 330 °C for 15 minutes. This procedure however did not assure uniform film thickness in some cases; in those cases the Teflon AF1600 was washed from the wafer and the deposition process was repeated. Three small scratches were made on the films, one at the center of the wafer, and the other two on the sides. Using a DEKTAK profilometer as described in section 3.3.5, the thickness was evaluated at these points and statistical averages were taken.

3.2. FABRICATION OF COPPER FILMS

Copper was deposited using either evaporation or sputtering. Copper thickness was about 200 nm in both cases as measured by placing a clean microscope slide among the experimental samples and using profilometry as described above. Since the sticking coefficients are different for glass and fluoropolymer, the copper thicknesses were also evaluated using the differences in thickness of metallized and unmetallized fluoropolymer films. The results were close to those obtained from bare microscope slides for a copper thickness of 200 nm. The principles of profilometry are described in

section 3.3.5.

For our experiments, high-purity copper (99.999 %) was thermally evaporated from a filament at a pressure of around 10^{-5} Torr measured by a Penning gauge, the filament to substrate distance being 30 cm. The chamber was evacuated primarily by a mechanical pump, after which pumping was switched to a diffusion pump. In our experiments we chose a resistive coil type of filament in order to avoid overheating of fluoropolymer substrates. The coil was aligned horizontally and pieces of copper were clamped on it. We placed the samples in close proximity to each other in order to achieve similar thicknesses for the films.

In our experiments, we used a planar disc shaped cathode (which served as the sputtering source) parallel to an anode surface (grounded, served as the substrate holder).

Copper was sputtered, using a DC planar magnetron at a pressure of 10 mTorr of Ar as measured by an MKS Baratron gauge, a flow rate of 6 sccm as measured by an MKS flowmeter, a current of 0.5 A and a negative target bias of 355 V. The chamber was evacuated using a turbomolecular pump. The parallel disc-shaped cathode was 8 cm in diameter and the distance between the cathode and the anode was about 7 cm.

To avoid possible problems that might have occurred due to the high power dissipation, the cathode was cooled with a high flow of water.

3.3 CHARACTERIZATION OF FILM MATERIALS

3.3.1 DIELECTRIC MEASUREMENTS

For the dielectric measurements, copper electrodes (about 200 nm thick) were evaporated on both sides of the fluoropolymer (1μm thick) to form metal-insulator-metal (MIM) structures (see Fig. 3.2). The effective areas of the electrodes were squares of 3×3 mm dimensions achieved by using a mask. The multilayer structure was fabricated on standard microscope glass slides of 2×2 cm dimensions. The 200 nm thickness of copper is larger than the mean free path of electrons, thus surface effects should not be of concern and conductivity is sufficiently high ($\rho \sim 1.67$ μΩ-cm). The samples were placed and firmly clamped on a copper plate of 5x5 cm dimensions that was attached on top of a square-shaped ceramic heater. Thermal cycling was performed inside a grounded metal chamber kept at 10^{-2} Torr. The dielectric behavior was stabilized by annealing at 200°C for 30 minutes. The heating rate was approximately 2°C/min and was controlled manually using an adjustable power source. The temperature was measured using a very thin thermocouple installed on the substrate holder, its tip touching the sample surface in order to measure the temperature with higher precision. We found that there exists a temperature gradient between the interior of the heater and the sample surface ($\Delta T \approx 70$ °C when $T \cong 200$ °C on the sample surface). The annealing removed low molecular weight fragments and caused the free radicals to react in the case of PP and SP polymers and removed residual solvent in the case of

(SD) Teflon AF1600. In addition to these, water was desorbed. These results will be discussed later in this work. Atmospheric contaminants were removed in all cases. The thermal cycling was found necessary to obtain reproducibly stable dielectric properties.

Dielectric measurements were performed using an HP 4274A multi-frequency LCR meter, at frequencies ranging from 100 Hz to 100 kHz. Experiments have shown that direct mechanical contact of the sample electrodes and the LCR multifrequency meter gives the best results with almost no noise at elevated temperatures. Previous attempts with a conductive paste (silver paste) caused noise at temperatures above the room temperature. In order to reduce the additional, unwanted capacitive effects, a pair of BNC coaxial cables were used to connect the sample chamber to the measuring apparatus.

The permittivity at high frequency in the visible range ($\sim 10^{15}$ Hz) was evaluated from the refractive index, obtained using a Perkin Elmer UV/VIS/NIR Lambda 19 spectrometer which measured the optical transmission and reflection. By changing thickness and refractive index iteratively, a minimum error function (difference between simulated and measured transmission and reflection) was found. Using different dispersion curves describing the continuity of the optical constants over a certain wavelength range, the refractive index was found at the wavelengths of 450 and 750 nm. The dielectric constant was obtained by squaring the refractive index. The Sellmeier formula (Tatian B., 1984) was used in our calculations:

$$n(\lambda)^2 = 1 + \sum_{j=1}^{k} \frac{A_j \lambda^2}{\lambda^2 - B_j^2} \tag{3.1}$$

Here n(λ) is the refractive index at wavelength λ, A_j and B_j are constants determined by the fitting process.

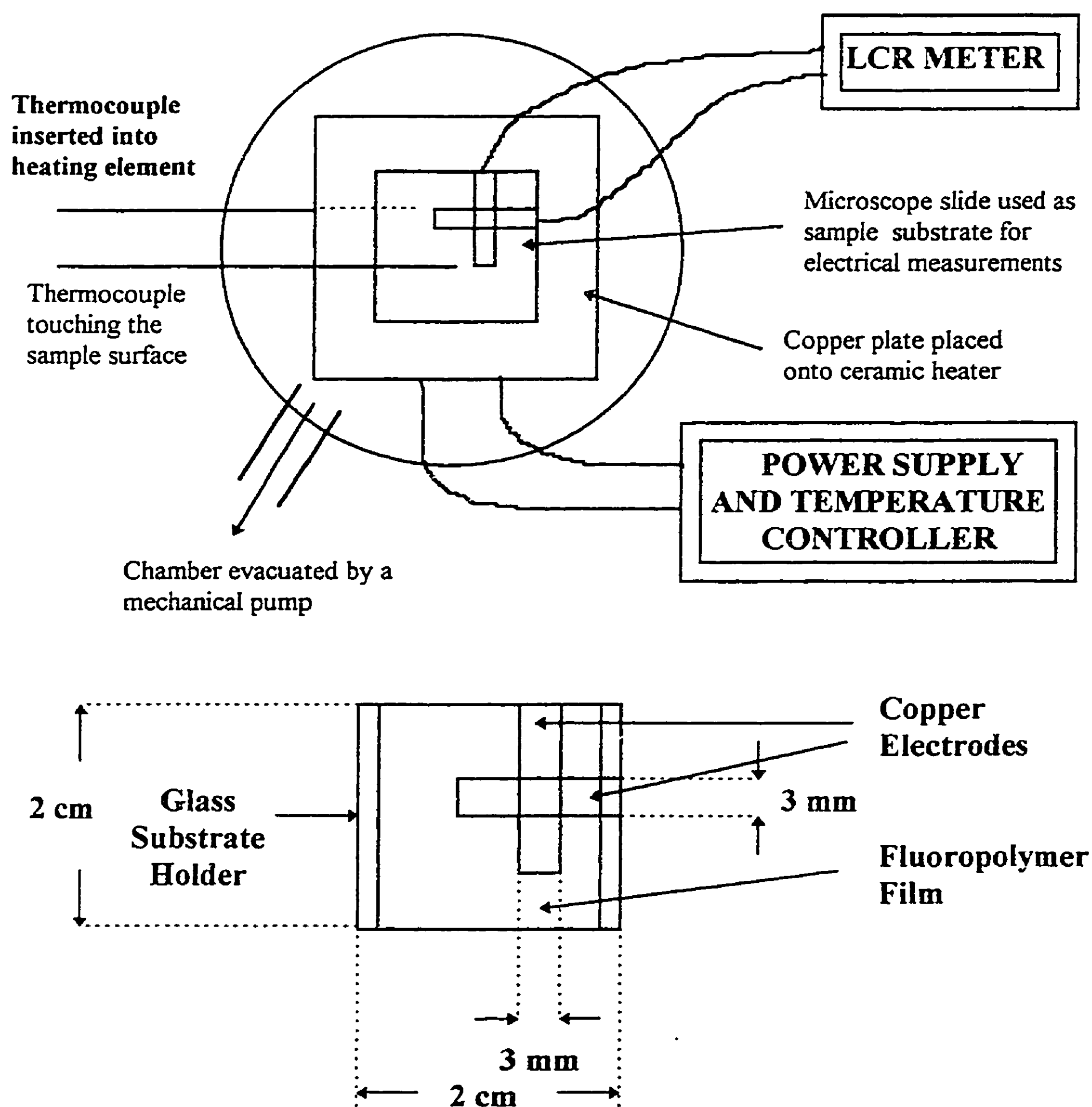

Figure 3.2: The experimental set-up and metal-insulator-metal (MIM) sample structure used in our experiments.

3.3.2 ADHESION MEASUREMENTS

The microscratch tester (MST CSEM Switzerland) and type 600 3M Scotch Tape peel test were used to measure adhesion. The main reason for choosing these techniques was their ease of use in evaluating various types of samples. In addition to these, the possibility of making quantitative, semiquantitative and qualitative analyses with the microscratch tester made it an attractive instrument to be used in order to make a comparative analysis of differently treated fluoropolymer samples.

When using the MST, a linearly increasing force, over the range of 0-3 N, was applied to a 0.8 mm hemispherical diamond tip moving across the surface at a speed of 5 mm/min at a loading rate of 1 N/min. The scratches were analyzed, using both optical microscopy and SEM, to determine the critical load necessary to delaminate copper from the polymer substrate. In our case, where a 2000 Å copper film is deposited on a 1μm fluoropolymer, it is easier to evaluate adhesion by optical observation. The reason for this is the fact that the slope of friction force versus normal force does not change significantly when copper starts delaminating. The acoustic emission was not sensitive enough at the point of first copper delamination. In all measurements the critical load was usually obtained from 5 scratches on each sample.

Several samples were analyzed for each different treatment condition. The films to be analyzed with the microscratch tester were deposited on 2×2 cm glass slides. It was observed that small irregularities (such as dust particles originating from the air)

entering between the stylus tip and the film surface along the path of the scratch could mislead the experimenter by delaminating the film. Therefore critical load values largely deviating from the average were omitted. Generally, small scale plastic deformations or delaminations gradually turn to more extensive, large scale delaminations as the normal force increases. The possible failure modes are summarized in Figure 3.3. However, one should keep in mind that these modes are just simplifications of the observed results. The actual observations are more complex and, sometimes, a combination of several of these modes occurs at the same time. Therefore, it is up to the experimenter to define a reasonable critical load. Figure 3.4, obtained with SEM, shows the point at which L_c was typically measured.

An important problem to be solved is to distinguish the delamination of Cu films at the Cu/fluoropolymer interface from the delamination of fluoropolymer films at the fluoropolymer/substrate interface. Generally, the former occurs first and the latter is observed at higher load values. To clarify this problem, we observed the scratches under optical microscopes operating in reflection and transmission modes. The microscope operating in the transmission mode of polarized light makes it possible to see whether a fluoropolymer film remains on the glass substrate, which would imply that copper delaminates from the fluoropolymer. In case the fluoropolymer film remains adhering but copper is removed the color is light green. If the polymer is delaminated, the color will turn to light blue, indicative of the presence of bare glass substrate.

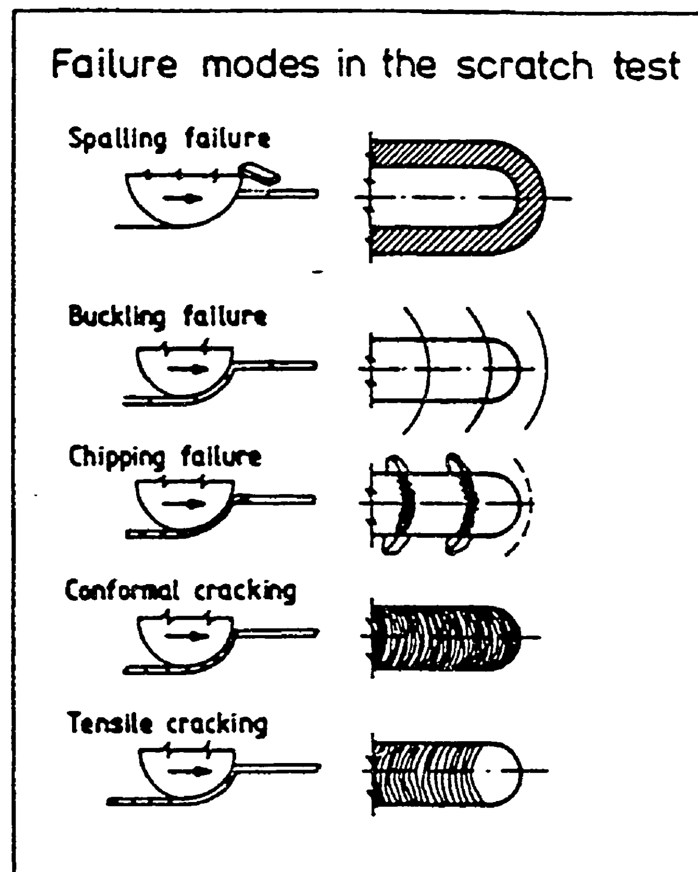

Figure 3.3: A summary of possible failure modes observed after the scratching (from Burnett P. J. and Rickerby D. S., 1987)

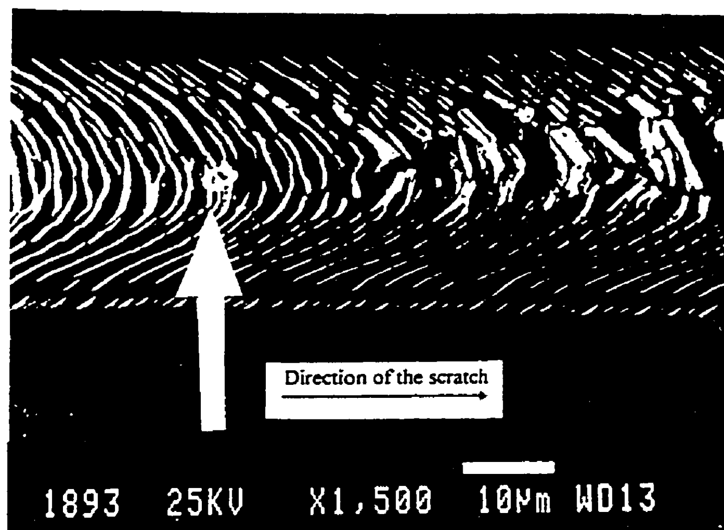

Figure 3.4: SEM picture showing the point at which L_c is typically measured.

Type 600 3M Scotch Tape was used to perform the peel test, to provide additional information about adhesion. Samples were prepared by depositing a fluoropolymer film (~1µm thick) on 2×2 and 2×4 glass microscope slides, followed by copper deposition

(~200nm thick). The tape was placed gently over the sample and a 2 kg roller was rolled twice over it. Immediately thereafter, the tape was peeled from the surface perpendicularly and the percentage of remaining copper was estimated by dividing the area into segments and counting the number of segments retaining the copper.

3.3.3. STRESS MEASUREMENTS

Film stress was measured as a function of temperature for both bare and

metallized fluoropolymers, using the Tencor flx-301 Flexus system under N_2 atmosphere. The possibility of measuring film stresses as a function of temperature in a N_2 atmosphere made this instrument particularly attractive for our copper-metallized samples, since copper oxidation had to be avoided. The films were deposited on 2 inch Si (100) wafers, the thickness of polymer and copper being about 1 μm and 200 nm, respectively. The principle is based on the evaluation of changes in the radius of curvature of the substrate resulting from film deposition. By measuring this deformation one can find the strain and thereby the stress using the Stoney equation:

$$\sigma_f = \frac{ED^2}{6(1-\nu)Rt} \tag{3.2}$$

Here, E and ν are Young's modulus and Poisson's ratio of the substrate, respectively. D and t are the thickness of the substrate and film. The substrate radius before, R_1, and after, R_2, film deposition will give the effective radius defined as:

$$R=(R_1-R_2)/R_1R_2 \tag{3.3}$$

It should be noted that we considered only the elastic constants of the substrate and therefore this equation is valid only when $t \ll D$. There exist several different methods to measure the radii. Our Flexus system uses a scanning beam technique: A movable assembly of solid state lasers, mirrors, and a position-sensitive detector. The angle of reflection, θ, is measured as a function of distance x travelled along the substrate. The derivative of the angle θ with respect to the distance will give the radius. In other words:

$$R=d\theta/dx \quad (3.4)$$

The schematics of the Flexus apparatus utilized is shown in Fig 3.5.

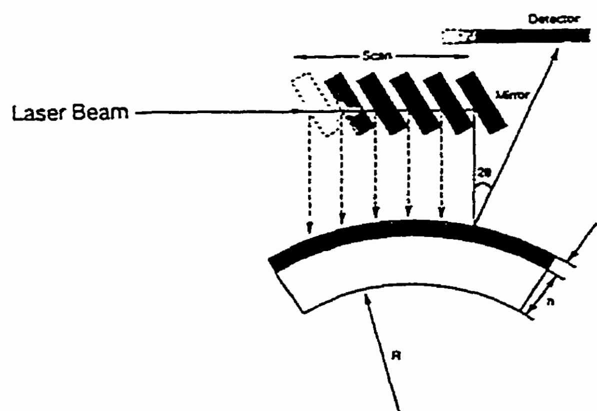

Figure 3.5: Schematics of the flexus laser scanning mechanism (Flexus Corp., Sunnyvale, CA).

The Flexus system can be employed to analyze the stress-temperature behaviour. Resistive coils heat the sample uniformly in a N_2 atmosphere. However, it should be noted that in these in-situ stress versus temperature measurements, the Young's modulus and other elastic constants of the Si substrate are assumed to be temperature-independent because they show only a very small temperature dependence: elastic constants decreasing with increasing temperature (Flexus Corp., Sunnyvale, CA).

3.3.4. CHEMICAL CHARACTERIZATION OF THE SURFACES AND INTERFACES

a) FTIR: The chemical structure of the films and interfaces was also evaluated: FTIR spectra were obtained in transmission (volume) and photoacoustically (surface) on a MATTSON RS-1 FTIR spectrometer using an MTEC model 300 photoacoustic sample attachment. Fluoropolymer samples were prepared using glass and Si substrates. Photoacoustic spectroscopy (PAS) works on the principle that modulated IR radiation striking the surface of the sample is absorbed in the first thermal diffusion length, converted to heat, which changes the pressure of the coupling gas in the photoacoustic cell. A standing sound wave develops and is detected by a microphone. Only those frequencies that are absorbed will lead to the development of sound waves. In other words, in PAS sound waves are being used to detect infrared absorption frequencies. Due to its suitability for the nondestructive characterization of fluoropolymers, we used this technique. PAS can be applied to analyze the near surface region, down to several hundred angstroms (DiRenzo M. et al., 1995). The surface regions of fluoropolymers were analyzed with PAS in order to determine differences in surface chemical structure.

The question that also had to be answered was which chemical groups may contribute to the adhesion of copper to fluoropolymers. Using transmission, one can obtain information about the interior of the material. Figure 3.6 shows a photoacoustic cell:

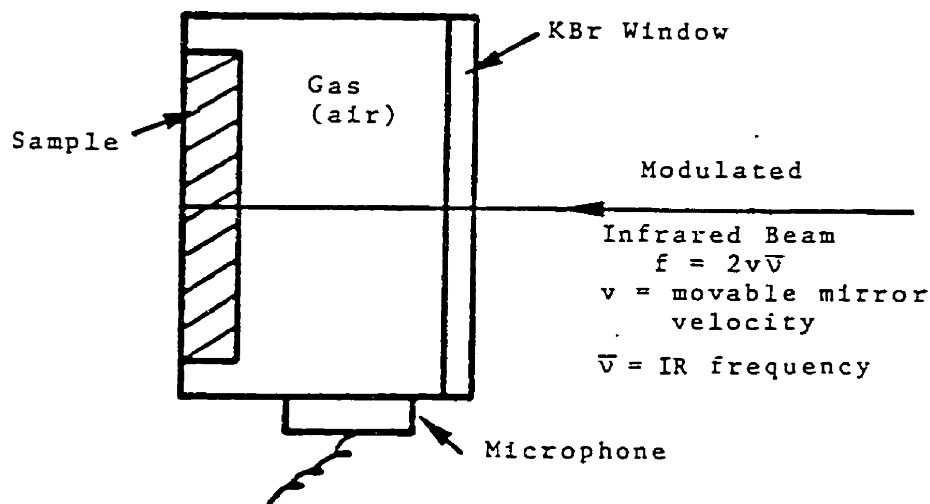

Figure 3.6: Schematic diagram of photoacoustic cell (from Graf R. T. et al., 1987).

b) XPS: XPS spectra were obtained using a VG ESCALAB MKII instrument with Mg K_{α} radiation (1253.6 eV), operated at 12 kV and 20 mA. These conditions were used to minimize the degradation of the fluoropolymers due to the X-rays which affected the entire surfaces of the samples. The following procedure was used for this experiment: newly deposited fluoropolymer samples were carried inside a dessicator and introduced into the preparation chamber of the XPS system. They were covered with a few monolayers of evaporated copper. Since no quartz crystal microbalance was used, the copper thicknesses were different for different fluoropolymer samples. Immediately thereafter the samples were transferred to the analysis chamber for the first

evaluation before heating. Survey spectra of metallized fluoropolymers, as a function of heat treatment, gave details on Cu diffusion. This was accomplished by successively heating the metallized samples inside the preparation chamber and then transferring them back to the analysis chamber for survey scans. Photoelectrons were collected at take-off angles of 35^0, 70^0 and 90^0 with respect to the sample plane. Since these photoelectrons originate from a depth approximately a distance of $3\lambda\sin\theta$, where λ and θ are mean free path and take-off angle, respectively, varying depths up to 3λ could be probed. The analyzed surface area was 2×3 mm^2. Peak areas were evaluated; by taking into consideration the elemental sensitivity factors, quantitative analysis gave us the concentration profiles of various elements, including copper. Thus, it was possible to obtain depth profiles of the elements after different annealing temperatures. In our case, following the evaporation of copper, the heat treatments were performed in-situ at 25, 100, 150, 200 and 250 ^{0}C for 10 min intervals.

c) Contact angle goniometry: Surface tension, for atmosphere-annealed bare fluoropolymer films on glass, was obtained using contact angle goniometry and applying small drops of 6 different liquids. Kaelble's method (Kaelble D. H. et al., 1974) gives the dispersive (γ^d) and polar (γ^p) components of the surface tension. Small drops of predetermined liquids were applied to the polymer surface and the changing contact angle was recorded every 20 second over a period of about two minutes. The values of undisturbed contact angle θ were evaluated from an extrapolation of all data to zero time. The cos θ and the work of adhesion (W_a) were calculated. Using the value

of W_a, a least squares fit was made and the dispersive and polar components of surface tension were determined.

3.3.5. THICKNESS MEASUREMENTS

Thicknesses of fluoropolymer and metal films were evaluated using profilometry (DEKTAK). This was accomplished by making several scratches on different locations of the films using a razor blade. Thereafter the stylus was moved perpendicularly to the scratches and the thickness was evaluated from the step profile. Statistical averages were obtained from several positions. The accuracy of this test instrument is within 10%.

In order to evaluate the changes in thickness after annealing, we used profilometry and thermomechanical analysis (TMA) in some cases. The principle of TMA is based on the measurement of the relative change in film thickness with respect to its original value during annealing in N_2 atmosphere. A free-standing piece of film was placed in between the flat, cylinder-shaped tips of a few mm diameter and a very low load (1 mg) was applied on the tips to press the film. Free-standing Teflon AF1600 was obtained by dipping a piece of Teflon AF1600-coated Si wafer into water and peeling off a small piece of the film. Free-standing plasma deposited films were obtained by peeling pieces from the rf powered electrode. The films were then heated at a rate of 2 °C/min to the required temperatures (usually 200 °C), and the changes in thicknesses were recorded.

CHAPTER IV

RESULTS AND DISCUSSION

4.1 DIELECTRIC PROPERTIES OF FLUOROPOLYMER FILMS

In this chapter, the experimental results obtained for MIM (metal-insulator-metal) structures will be presented. These results include both permittivity and dissipation factor as a function of temperature and frequency. With the exception of PP(C_2F_3H), which short-circuited above room temperature, all other fluoropolymers showed permittivity values below 1.9 and dissipation factors in the order of 10^{-3}-10^{-4} at room temperature and at frequencies 1-100 kHz, subsequent to vacuum annealing. It will be shown below that the deposition parameters for PP(C_2F_3H) led to gas phase reactions which, in turn, resulted in non-uniform films with cauliflower-like surfaces, very prone to copper diffusion and short-circuiting. It should also be mentioned that a decrease in fluoropolymer thickness of about 20 % was measured after 30 minutes of annealing. This was taken into consideration in the calculations.

4.1.1 THERMAL HISTORY

The dielectric properties of polymers depend to a large extent on their thermal history. For this reason the sandwich structures were thermally cycled and the dielectric spectra observed. Another reason for thermal cycling was to evaluate thermal stability of these Cu/fluoropolymer multilevel structures. It was seen that the values of

permittivity and dissipation factor were significantly greater prior to annealing, and they reached lower values with increasing numbers of thermal cycles, before reaching their stable values. The noise observed during the first heating disappeared once the samples were sufficiently heated and stabilized: Very stable properties were measured for films after annealing at 200 °C for 30 minutes in vacuum (see Figures 4.1 and 4.2). Annealing led to the desorption of water vapor, low molecular weight species and a reduction of free radicals. Mass spectroscopic analyses further indicated that the annealing process at higher temperatures was accompanied by the loss of low molecular weight species in the case of the SP and PP fluoropolymers, and by the loss of solvent retained in the Teflon AF1600 films (G. Czeremuszkin et al., 1997). When stabilized samples were exposed to air, the permittivity values increased slightly but they returned to their former values upon evacuation.

The dielectric behavior of the fluoropolymer films is further documented with the effect of temperature on dielectric constant (κ) and dissipation factor (tan δ) (see Figure 4.1 and Figure 4.2). After annealing, the dependence curves were found to be featureless in the given temperature range. The κ values were found to decrease with rising temperature. The dissipation factors, on the other hand, experienced a sharp increase starting at around 100 °C and suggested the presence of a relaxation peak above 200 °C (see Figure 4.2). This peak shifted to higher temperature values as the frequency increased. The spectra were similar for different samples of the same kind of fluoropolymer. Furthermore, there were only minor differences from one kind of

fluoropolymer to another, evaluated in this work. These observations are consistent with earlier publications indicating that the dissipation factor varies as a function of temperature in a similar way for different plasma-deposited fluoropolymers (Martinu et al., 1986). The dielectric behaviour of fluoropolymer films was explained in section 2.1.3. Figures 4.3 to 4.8 summarize the plots of dielectric constant and dissipation factor as a function of temperature for the fluoropolymers we investigated.

The dielectric behavior of Teflon AF1600 (see Figure 4.3 and Figure 4.4) is similar to results obtained earlier. Here too, the κ values were found to decrease with rising temperature. It was expected that the permittivity would increase with increasing temperature, as is found for many other polymers. We corrected the κ(T) curve, considering thermal expansion of the capacitor area and of the thickness, using a linear thermal expansion coefficient of 74 ppm/°C (Starkweather H. et al., 1991). This approach, however, did not change the temperature dependence significantly. The κ(T) curve agrees well with the Clausius-Mossotti equation.

The reproducibility of the spectra gave us an understanding of thermal stability. Up to about 200°C, stability is maintained, but beyond 200 °C the spectra showed features such as large deviations from the general trend. These deviations can be explained as due to the diffusion of copper into the polymers and, eventually, shortcircuiting (diffusion of copper into fluoropolymers will be discussed) and an increased DC conductivity. These deviations were manifested as substantial increases in dissipation factors by orders of magnitude, observed for all samples. Once such

deviations were observed, it was no longer possible to obtain the former dielectric constant and dissipation factor values from these samples.

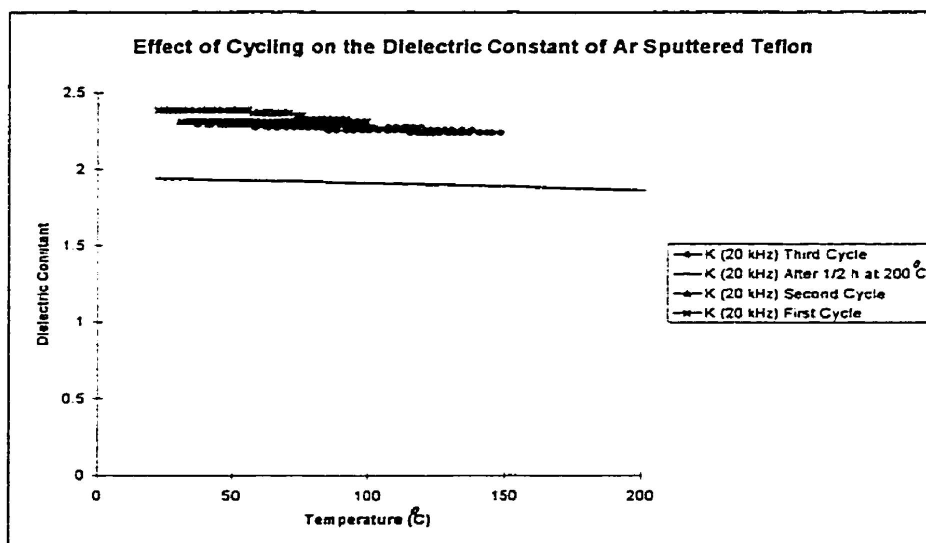

Figure 4.1: Effect of cycling on the dielectric constant of Ar-sputtered Teflon.

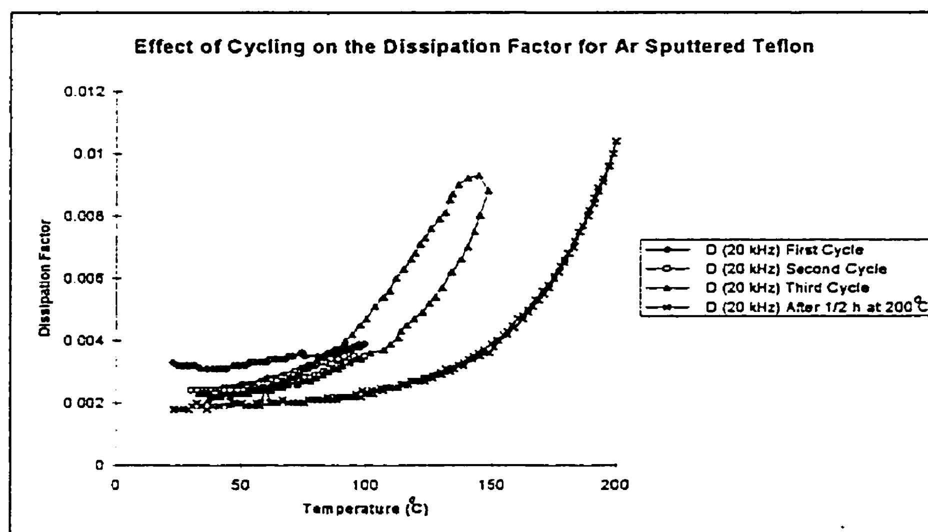

Figure 4.2: Effect of cycling on the dissipation factor of Ar-sputtered Teflon.

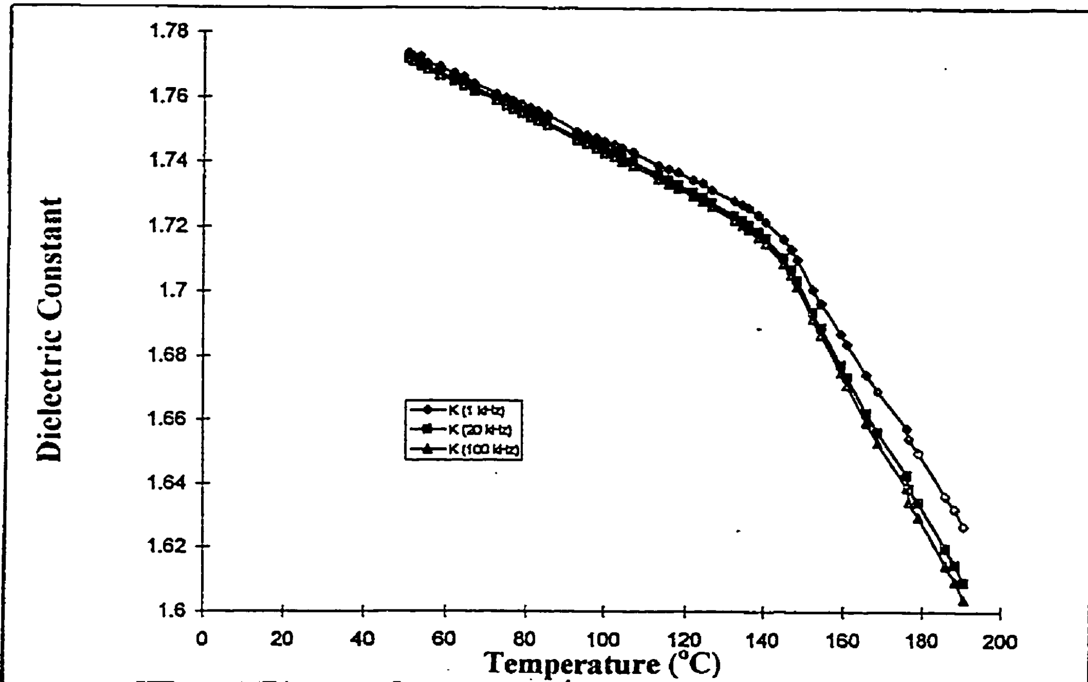

Figure 4.3: Dielectric constant vs temperature for a vacuum annealed Teflon AF1600.

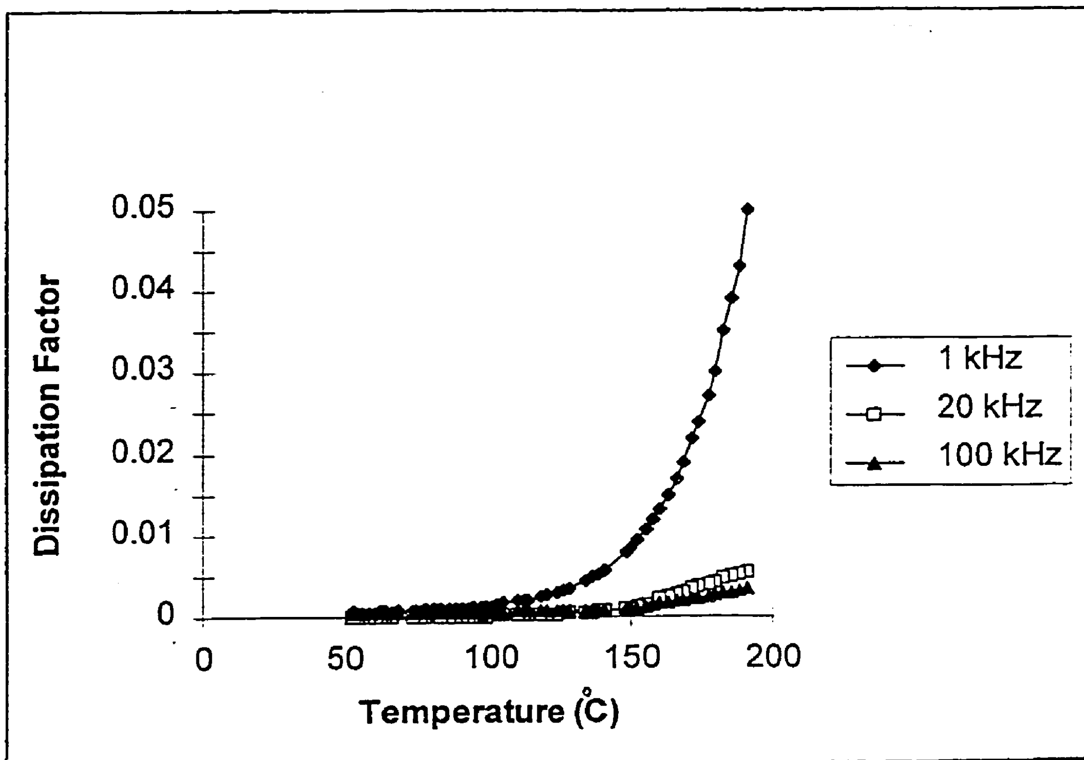

Figure 4.4: Dissipation factor vs temperature for a vacuum annealed Teflon AF1600.

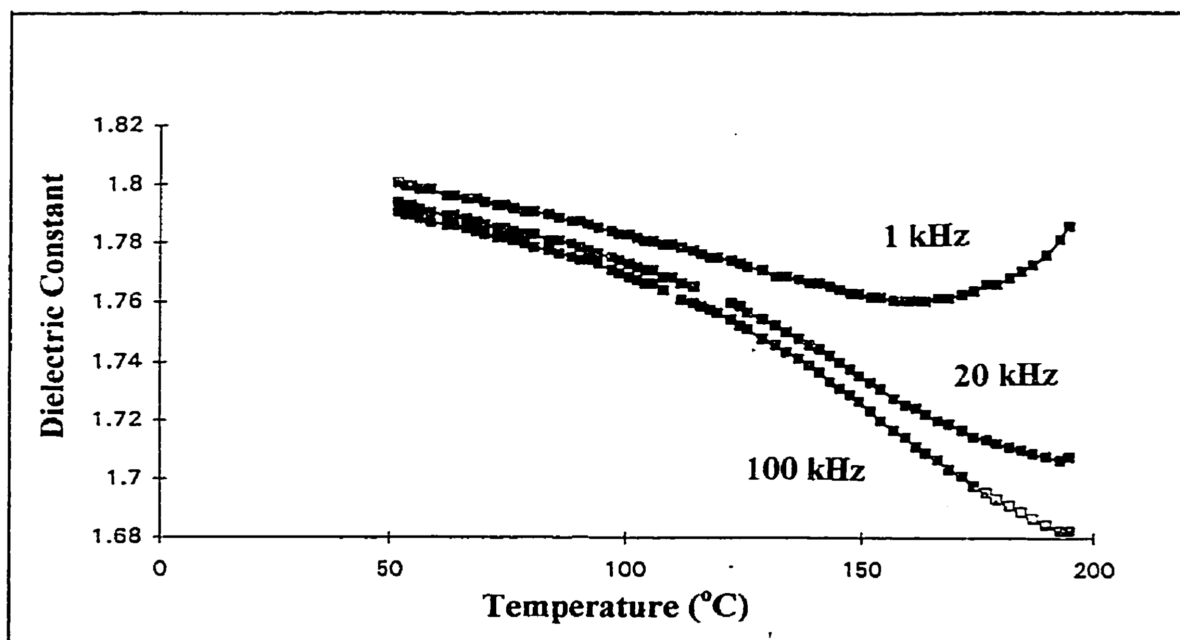

Figure 4.5: Dielectric constant vs temperature for a vacuum annealed $PP(C_2F_4)$.

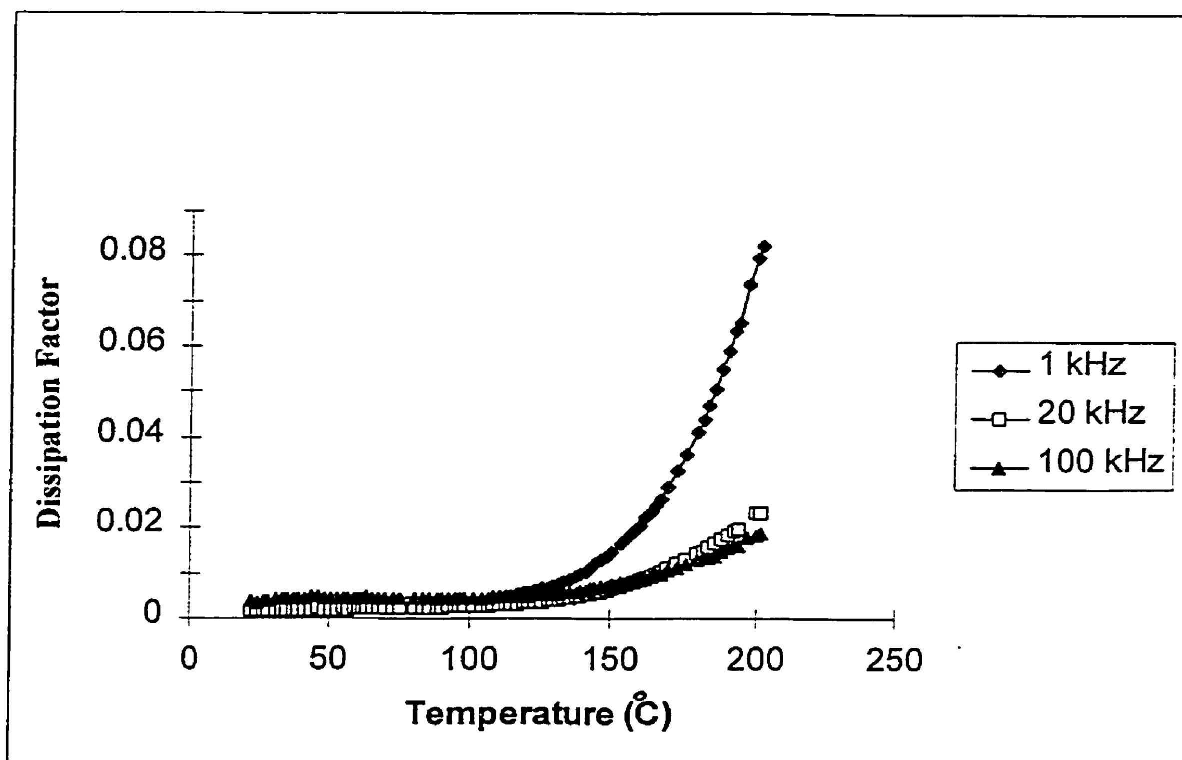

Figure 4.6: Dissipation factor vs temperature for a vacuum annealed $PP(C_2F_4)$.

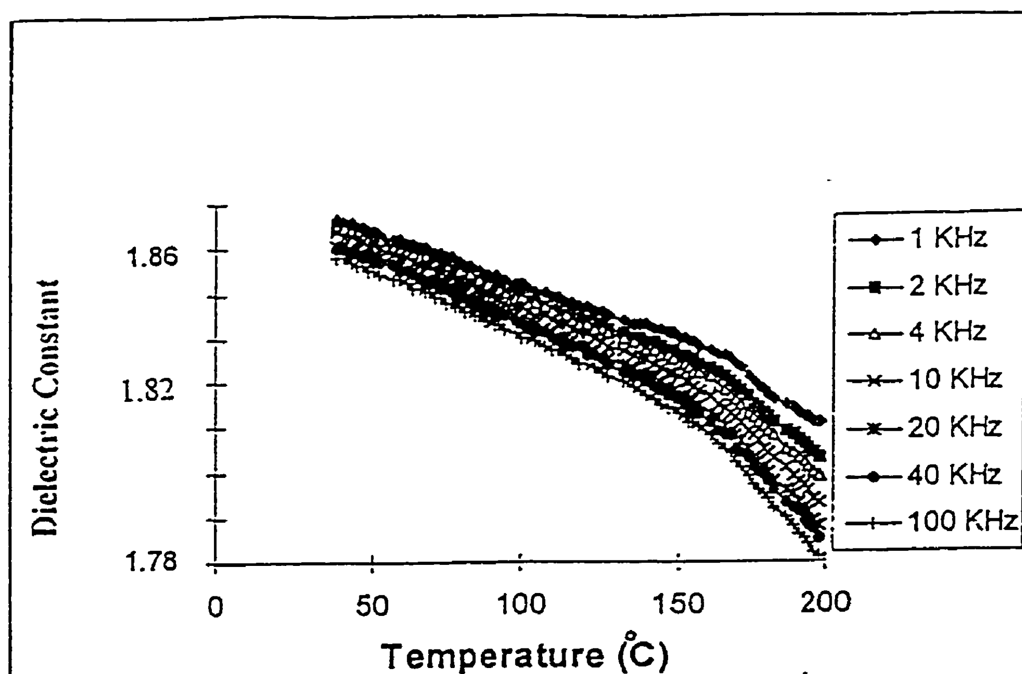

Figure 4.7: Dielectric constant vs temperature for a vacuum annealed CF_4 sputtered Teflon.

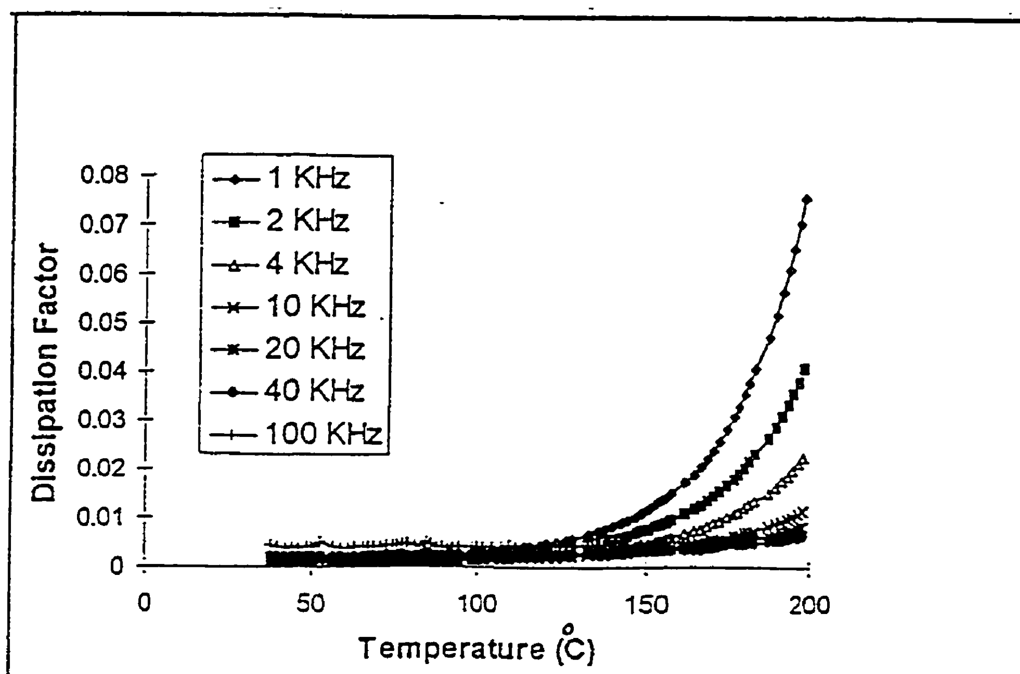

Figure 4.8: Dissipation factor vs temperature for a vacuum annealed CF_4 sputtered Teflon.

4.1.2 FREQUENCY DEPENDENCE OF THE DIELECTRIC PROPERTIES

When the room temperature dielectric constants are plotted as a function of frequency (see Figure 4.9) we see a slight decrease with increasing frequency. It is possible that this effect is due to a loss peak present between 10^5 and 10^{15} Hz values. This can be explained in terms of dipole relaxation (e.g. C=O). The dissipation factor, on the other hand, exhibits a sharp increase in the lower frequency region of the spectrum, and then a decrease towards the higher frequency part (visible range) of the spectrum (see Figure 4.10). We do not know however how the curves exactly behave in the intermediate region, and more experiments would be necessary.

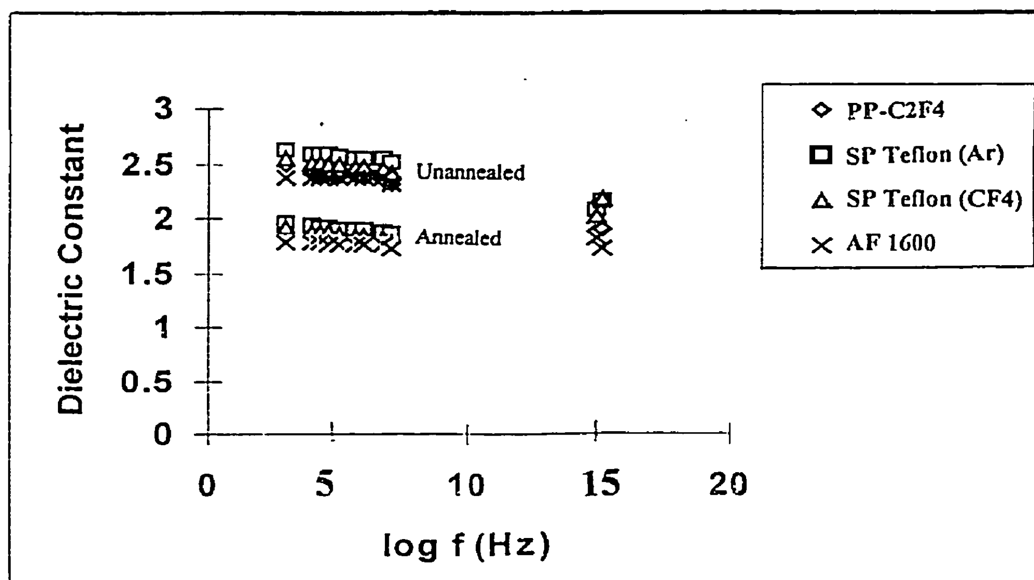

Figure 4.9: Dielectric constant as a function of frequency at room temperature for unannealed and annealed fluoropolymers in vacuum.

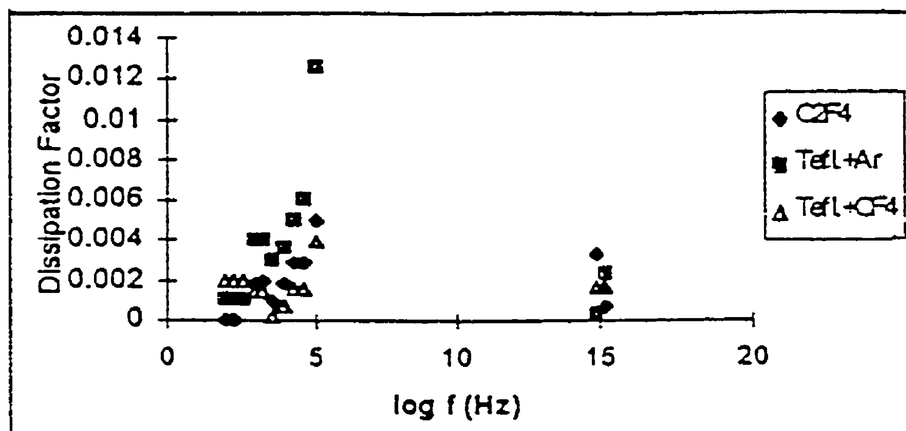

Figure 4.10: Dissipation factor as a function of frequency at room temperature for annealed fluoropolymers in vacuum (It must be emphasized that near 10^{15} Hz there are two different log f (Hz) values: 14.6 and 15.8 obtained for two frequencies corresponding to a wavelength of 450 and 650 nm).

4.2 ADHESION OF COPPER TO FLUOROPOLYMERS

4.2.1 MICROSCRATCH AND PEEL TEST ANALYSIS

Figure 4.11 shows the microscratch and peel test results for samples exposed to various heat treatments. The abbreviations 'atm' and 'vac' indicate, respectively, annealing under the atmosphere or in vacuum. All these treatments were performed at 200 °C for 30 min. The results show that preannealing in atmosphere significantly increases adhesion for the PP and SP fluoropolymer samples. It is believed that free radicals produced during the plasma deposition are thermally activated during pretreatment to react with air to produce chemical groups (C=O) capable of reaction with copper. As was confirmed earlier using XPS analysis on plasma treated

fluoropolymers, chemical bonds (possibly Cu-O-C and Cu-N-C) at the metal/fluoropolymer interface can be used to explain the higher adhesion for PP and SP fluoropolymers (Shi M. K. et al., 1995). In the case of Teflon AF1600, no such radicals are available. This leads to lower adhesion and further preannealing in atmosphere does not improve the adhesion.

The chemical species at the fluoropolymer surfaces responsible for stronger bonds with copper were analyzed using FTIR, and the results are presented in section 4.2.3.

The results show that postannealing also makes a significant contribution to adhesion, due, probably, to the diffusion of copper into the fluoropolymers (see section 4.2.2). The upper plot in Figure 4.11 shows clearly that sputtered copper adheres better than evaporated copper, as indicated by higher L_c values. This is reasonable because the sputtering process is associated with much higher energies (typically 5-100 eV in our case) of depositing particles which in turn leads to different and more extensive reactions compared to evaporation. In addition, the first layers of sputtered metal can easily penetrate deep into the soft polymer and lead to a larger mixed interface compared to the more abrupt interface in the case of evaporation. This is suggested by the results of an XPS analysis carried out in order to assess the interaction of vapor deposited and sputtered copper with Teflon AF1600 (Popovici D. et al., 1997). For evaporation, half of a fixed amount of the depositing copper reacted at the interface. The higher energies of the incident atoms on sputtering led to the total reaction of copper, even at thickness equivalents in excess of 10 monolayers. Reacted copper did

not remain accumulated at the Teflon surface but, rather, was uniformly distributed throughout the observation depth (Popovici D. et al., 1997).

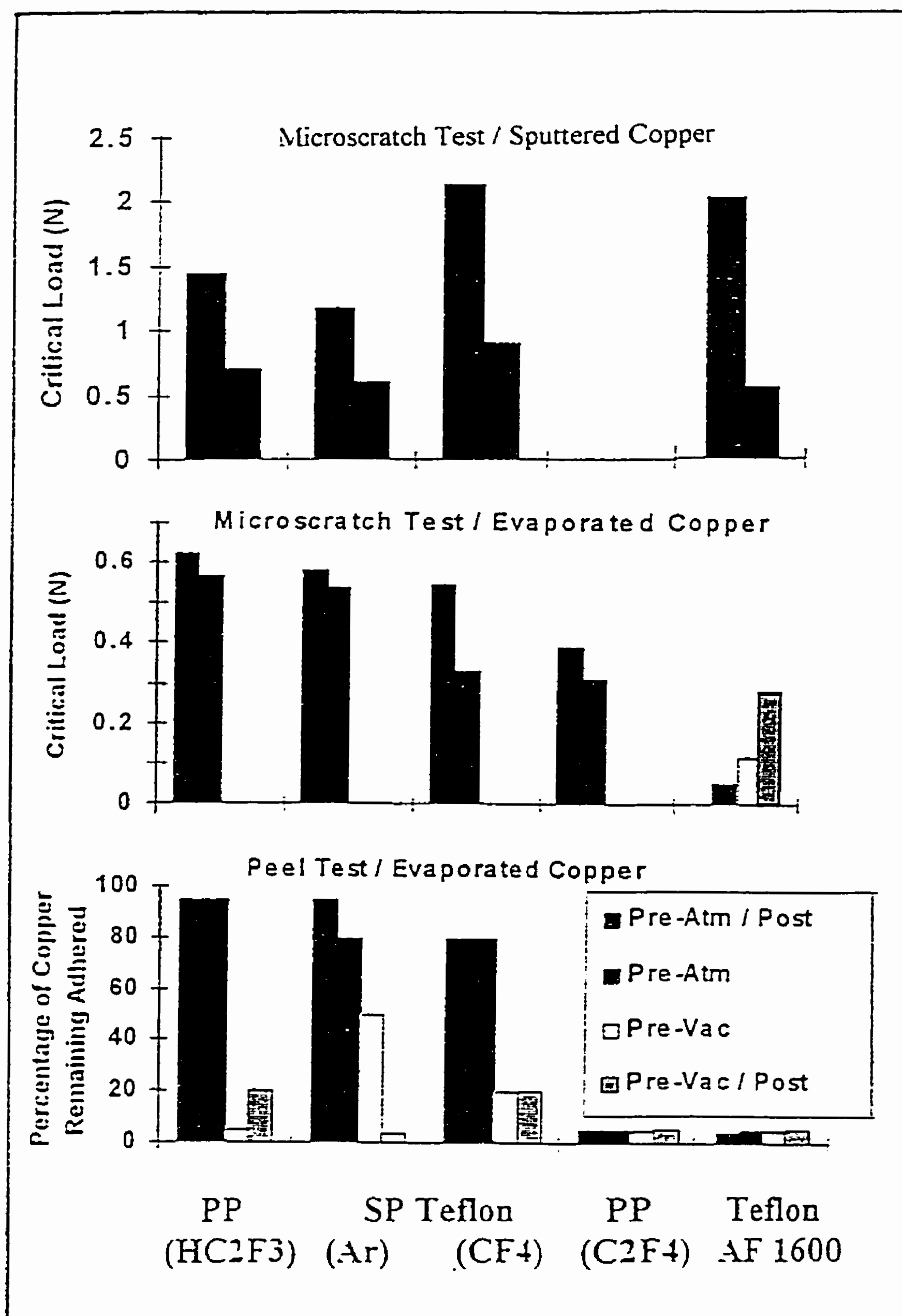

Figure 4.11: MST and peel test results for copper deposited on fluoropolymers.

The experiments performed to determine the effect of plasma surface treatment on the adhesion of evaporated copper onto Teflon AF1600 showed that N_2, Ar and air plasma treatments show only minute increases in critical force values for the set of parameters used in this work. The critical forces obtained were around 0.15 N for the non plasma-treated reference sample and close to 0.2 N for the plasma-treated samples, as is shown in Figure 4.12:

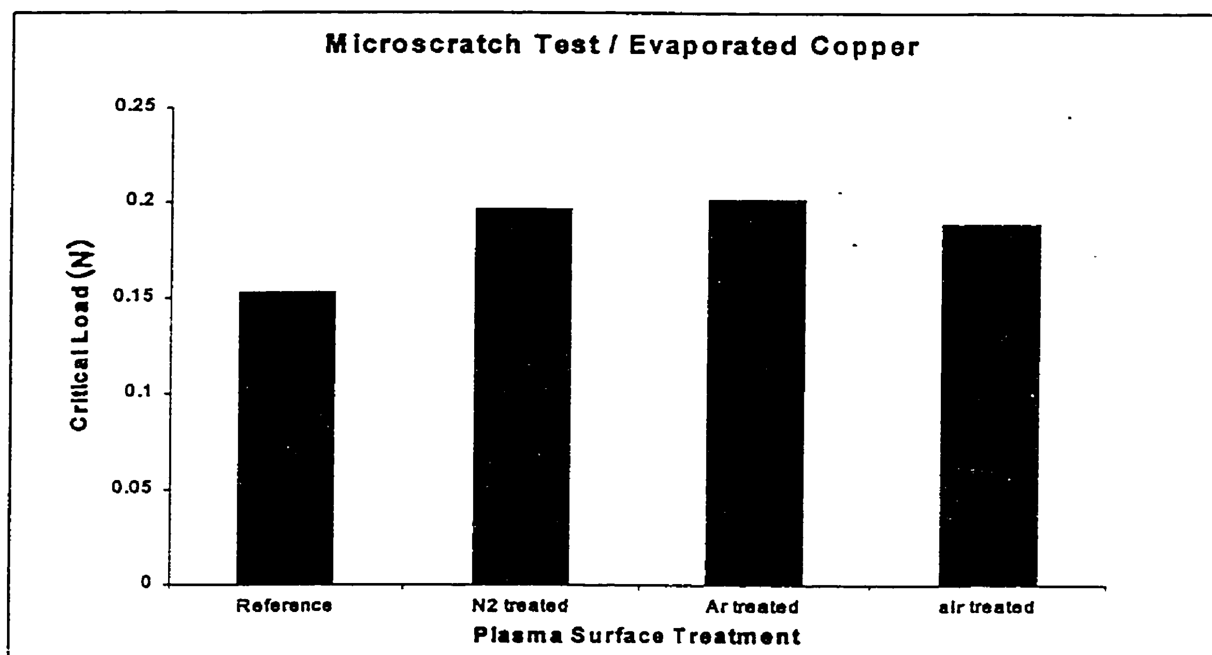

Figure 4.12: The effect of plasma surface treatment on the adhesion of evaporated copper onto Teflon AF1600.

These experiments do not represent a thorough study of plasma pretreatment on the Teflon AF1600/Cu system, but rather a preliminary attempt.

The copper delaminations starting at a very low critical force value can be observed in Figure 4.13 seen by SEM. Here, the copper film cracks in front of the stylus under the effect of mainly compressive stresses. On the sides of the scratch we can identify the chipping off of the copper film from the Teflon AF1600 surface.

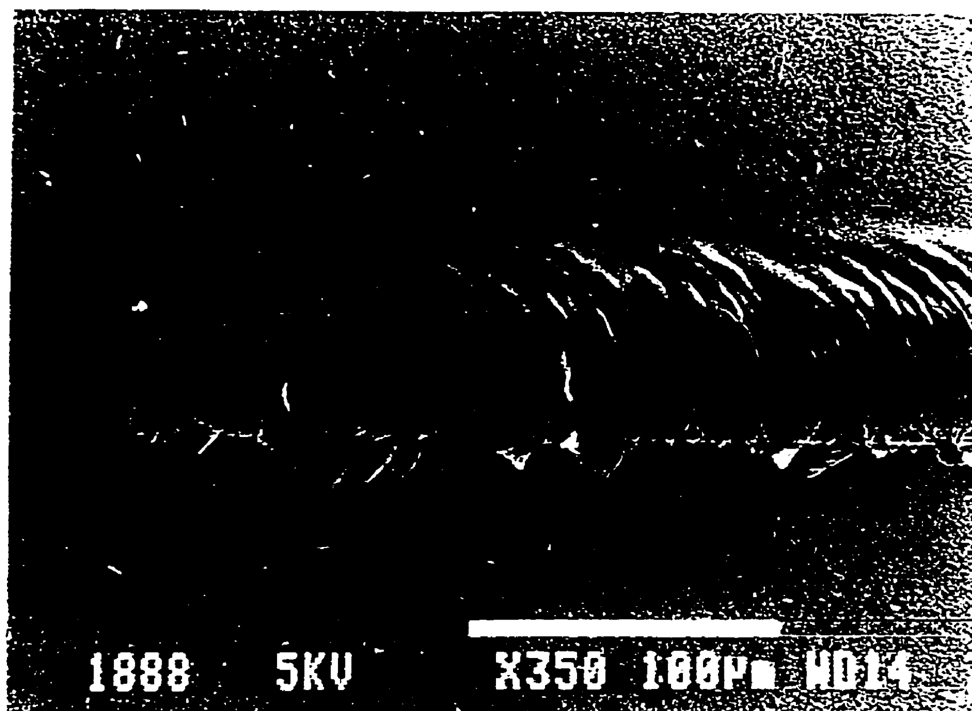

Figure 4.13: Delaminations of evaporated Cu from the atmosphere-preannealed Teflon AF1600. The critical load was around 0.05 N.

Figure 4.14 shows the scratch patterns with a higher magnification. It is possible to distinguish the copper delaminations from the fluoropolymer and the fluoropolymer delaminations from the glass or Si substrate. The latter occurs at much higher forces compared to the former. In the upper right corner of the picture, we can identify, by its irregular surface and gray color, the Teflon AF1600 that lost its copper coating during

the scratching procedure. Between isolated areas of copper we can distinguish the cracks in the polymer, appearing as dark holes.

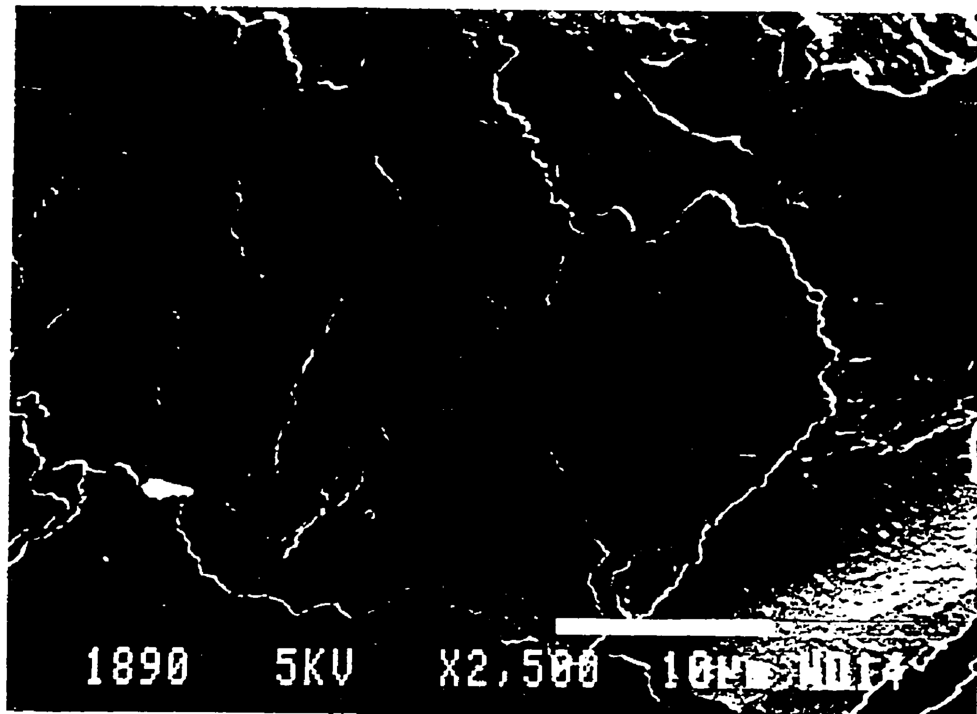

Figure 4.14: Delaminations of evaporated copper from Teflon AF1600 observed with more detail.

To confirm this, we analyzed unmetallized fluoropolymer films deposited on glass slides using the microscratch test (MST). It was observed that no complete delaminations of the fluoropolymer from the glass occurred and the only failure modes showing cracks and partial delaminations occurred at higher load values. Even at the end of the scratch we see cracks and an irregular surface which identifies the presence

of the fluoropolymer on the glass substrate. Figure 4.15 is a scratch with pictures showing a sequentially increasing load.

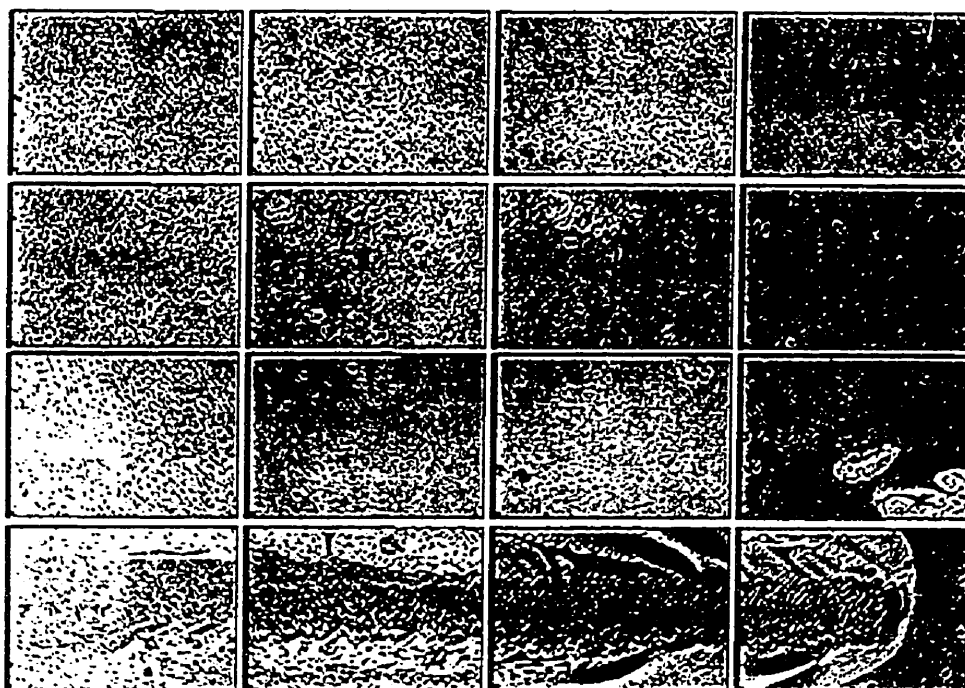

Figure 4.15: Sequence of pictures seen with the reflection mode of an optical microscope. Bare PP(C_2F_3H) on glass annealed in the atmosphere and analyzed using the scratch tester (Magnification: 550×, tip size:0.8 mm, range of load: 0-3 N, loading rate: 1 N/min, speed of tip: 5 mm/min).

The sequence of pictures seen in Figure 4.16 illustrates the gradual development of failures observed under the transmission mode of an optical microscope. It should be noted that the light green color seen on the substrate after the first delaminations indicates the presence of the fluoropolymer whereas, at later stages, the color turns to light blue and matches that of an uncoated glass slide.

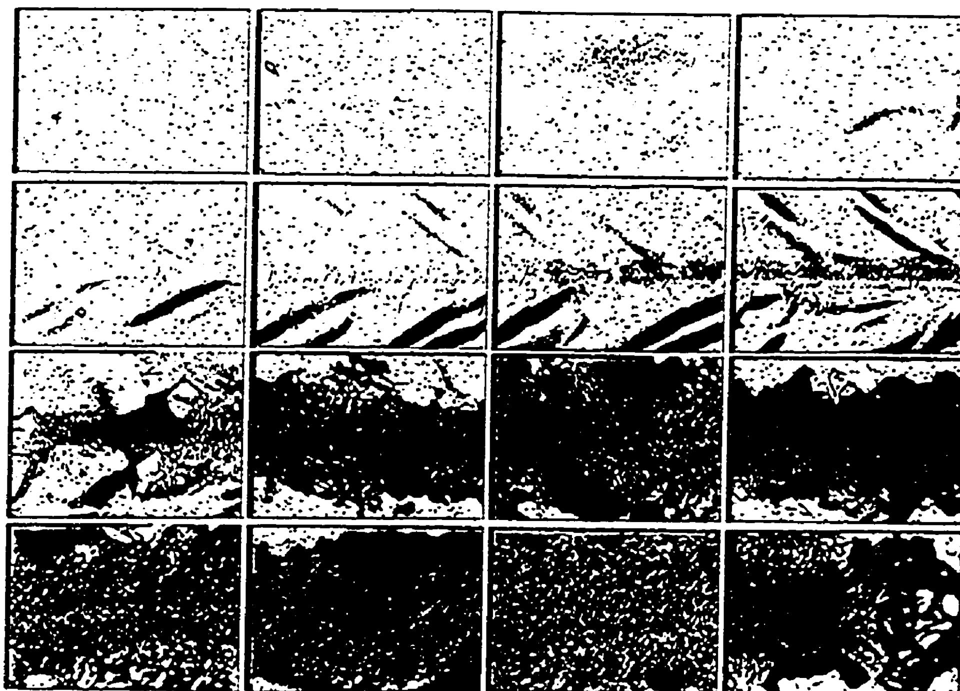

Figure 4.16: Sequence of pictures seen with the transmission mode of an optical microscope. PP(C_2F_3H) film sputtered with Cu. The sample was not postannealed. (Magnification : 550×, tip size: 0.8 mm, range of load: 0-3 N, loading rate: 1N/min, speed of tip: 5 mm/min).

We showed that the adhesion of copper onto fluoropolymers can be enhanced using thermal annealing techniques. Annealing can improve adhesion and, at the same time, stabilize the dielectric properties of these films. Therefore, it would be worth considering thermal cycling of these films at some stage of their manufacturing process.

4.2.2 XPS PROFILE ANALYSIS

When postannealed, the samples showed an improvement in adhesion strength. Our interpretation of this result was based on an XPS profile analysis we conducted in order to observe possible diffusion phenomena taking place as metallized samples were postannealed. In other words, the diffusion of the first layers of depositing copper into the polymer can lead to a stronger interface and result in better adhesion due to "mechanical interlocking".

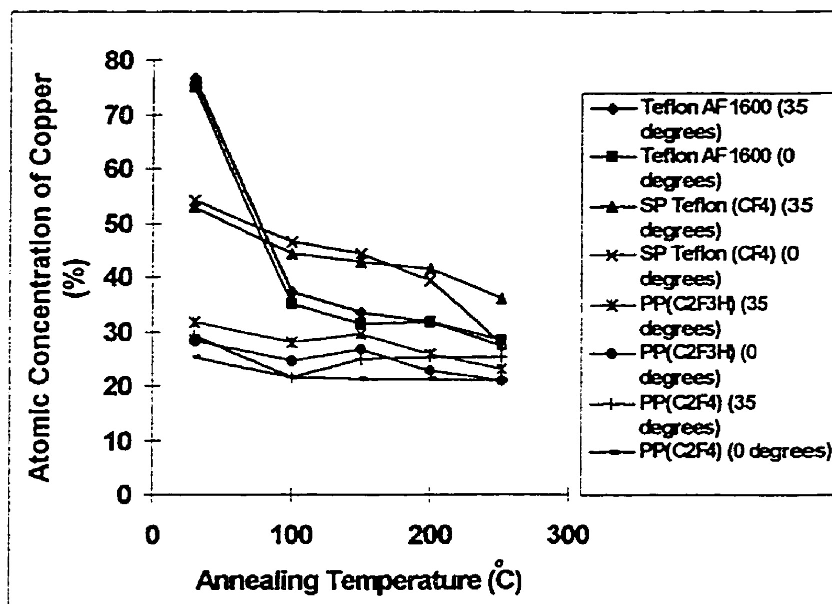

Figure 4.17: Atomic concentration of copper as a function of annealing temperature at 0° and 35° take-off angles from normal obtained by XPS.

Figure 4.17 shows the plot of this experiment. Atomic profiles of copper indicate that, with increasing temperatures, the diffusion of copper towards the interior regions of the film is enhanced. Therefore, we observe a decrease of copper concentration at 0° and 35° take-off angles in the near surface regions as the sample is annealed at higher temperatures. This decrease in copper concentration is higher for the Teflon AF1600 compared to the plasma-deposited samples. This difference may be explained to be due to the noncrosslinked structure of Teflon AF1600 in contrast to the denser, crosslinked plasma deposited polymers. In this figure we do not include the 70° take-off angle data because, they do not necessarily follow the general trend. This observation may be due

to the very shallow depth probed at this take-off angle, which may be affected by the irradiation damage caused by x-rays. In an earlier study, F and O losses were observed even at low doses of x-ray irradiation (D. Popovici et al., 1997).

4.2.3 FTIR ANALYSIS

Photoacoustic spectra originating from near-surface region are shown in Figure 4.18.

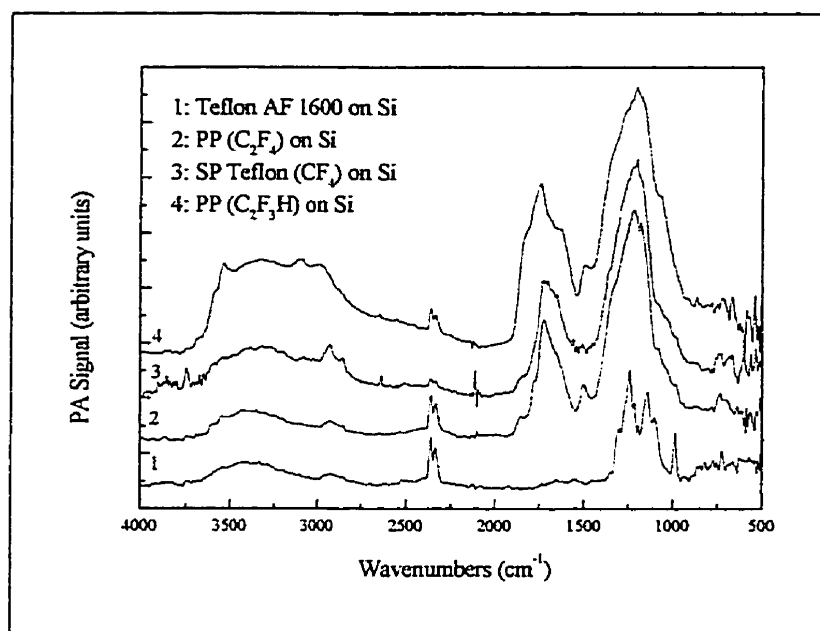

Figure 4.18: PA signal for fluoropolymers.

The PP and SP films reveal a broad peak around 1200 cm^{-1}, which is mostly due to the stretching of CF_n groups (Shi M. K. et al., 1994) (Giegengack H. and Hinze D., 1971) (Martinu L., 1986). The peak around 1700 cm^{-1} may be the confirmation of the presence of carbonyl (C=O) groups, as a result of the reaction of the film free radicals

with the atmospheric oxygen upon exposure to the ambient (Shi M. K. et al., 1994) (Sacher E., 1994) (Martinu L., 1986). As a result, active sites containing oxygen are available for reaction with copper (Alptekin A. et al., 1997). We explain the higher adhesion observed for PP and SP fluoropolymers to be due to the formation of chemical bonds at the metal-polymer interface (Shi M. K. et al., 1995). The weak absorption around 3400 cm^{-1} is due to -OH groups, present either because of the reaction of free radicals with water, or the bonding of water to the ether linkages in Teflon AF1600. In the case of Teflon AF1600, the characteristic peaks observed are due to CF_2 stretching (1250 cm^{-1}), the C-O-C stretching of the fluorinated dioxole component (1150 cm^{-1}), and CF_3 vibrations (980 cm^{-1}) (Nason T. C. et al., 1992). In all cases, there remained some residual CO_2 in the measuring compartment which gives rise to a peak around 2400 cm^{-1}, unrelated to the film structure.

We also observed that, in the case of Teflon AF1600, the CH_n contamination peak can be significantly reduced in size upon evacuation whereas in the case of plasma-deposited fluoropolymers, this cannot be achieved. It is this inert nature of Teflon AF1600 that suggests the need for an enhancement of adhesion. Figure 4.19 shows the photoacoustic spectra of two Teflon AF1600 samples, one of which was kept in a dessicator under vacuum and, within a few seconds, inserted into the FTIR spectrometer, whereas the other was kept in the laboratory atmosphere for some time before analysis. Evidently, the latter sample exhibitted a more pronounced CH_n and OH peak. It is known that CH_n generally leads to poor adhesion because the C-H bonds are not attacked by adsorbed metal (Chen T. C. S., Mukhopadhyay S. M., 1995).

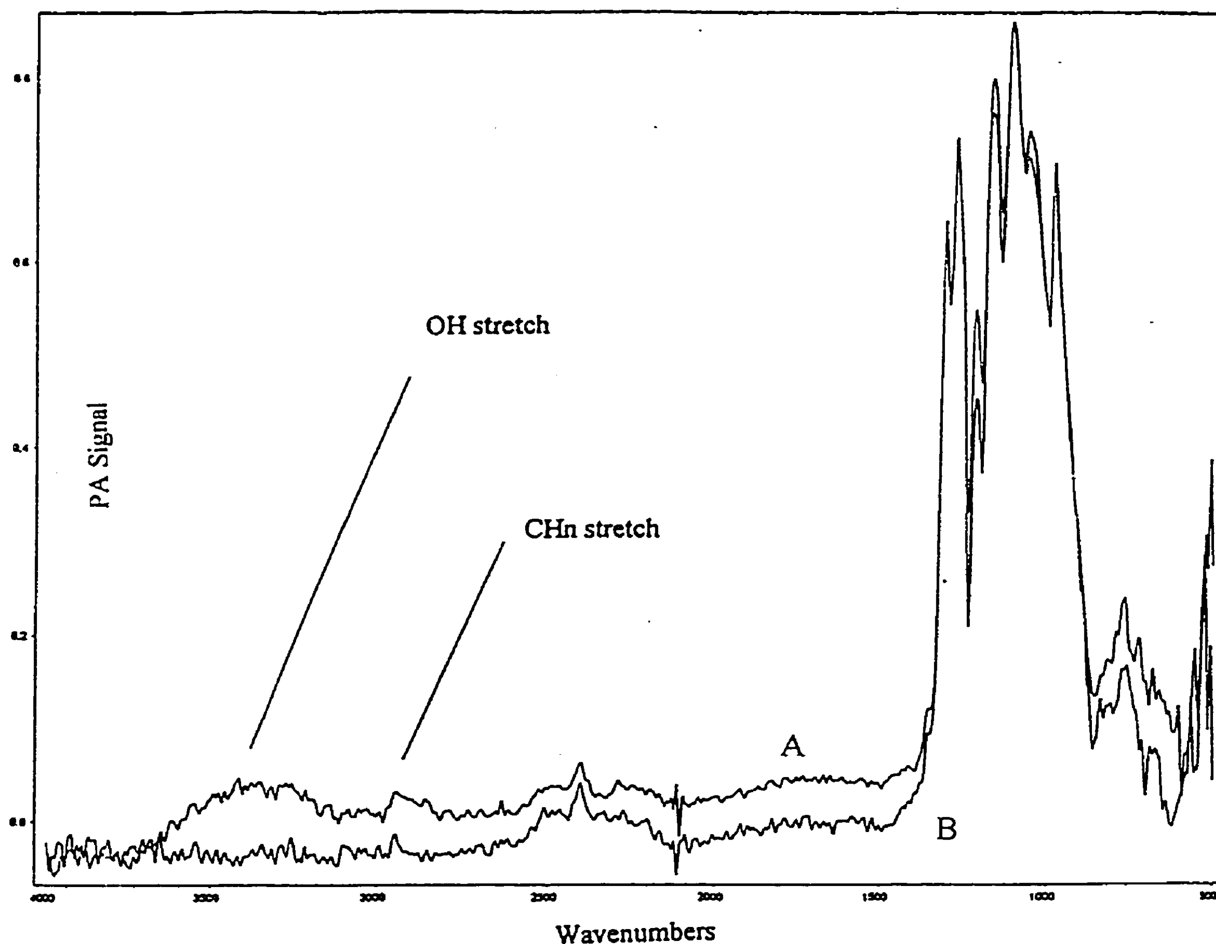

Figure 4.19: Contamination peaks (CH_n) of two Teflon AF1600 samples. Sample A was kept in laboratory atmosphere for some time whereas sample B (kept in a dessicator) was inserted within seconds into the FTIR spectrometer.

4.2.4 SURFACE TENSION MEASUREMENTS

The dispersive and polar components of the surface tension, as well as their sum, are plotted in figure 4.20 as a function of critical load, obtained for different fluoropolymers. It is evident that both components of surface tension increase with

increasing critical load. This suggests the contribution of both polar and dispersive forces to the adhesion of copper onto fluoropolymers. Mittal has discussed several examples in his review (Mittal K. L., 1975), noting that the adhesion strength is maximized when the surface tensions of the two components have similar magnitudes. This may be due to a minimization of the interfacial tension, which is inversely proportional to adhesion strength (Sell P. J. and Neumann A. W., 1966). Adhesion is governed by different mechanisms in different cases however, and therefore no definitive statements should be made.

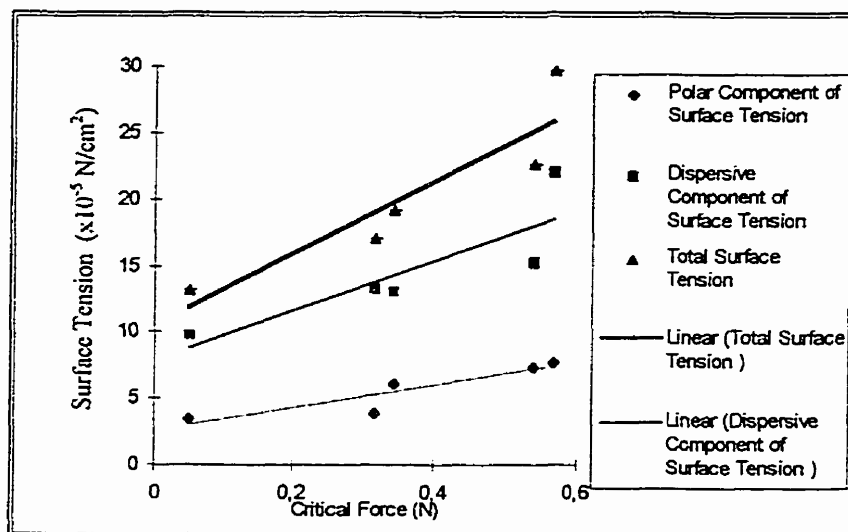

Figure 4.20: Surface Tension as a function of critical load for atmosphere-annealed fluoropolymers (in the order of increasing critical load: Teflon AF1600, PP(C_2F_4), SP Teflon (CF_4), SP Teflon (Ar), PP(C_2F_3H)).

4.2.5 OBSERVATION OF THE FLUOROPOLYMER SURFACES BY SEM AND AFM

Figures 4.21 to 4.23 show the surfaces of PP(C_2F_3H) and PP(C_2F_4) observed under SEM and AFM. It appears that the deposition parameters lead to a gas phase reaction in the case of PP(C_2F_3H) which, in turn, results in a cauliflower-like surface structure. When "smooth-appearing" regions of the cauliflower-like surface were observed with higher magnification, it became evident that those regions were not smooth. In the case of PP(C_2F_4), as the picture shows, the surfaces were smooth. We have intentionally focused on a dust particle to make the observed features evident. Obviously Figure 4.21 shows a rougher surface compared to Figure 4.23. Rougher surface indicates more porosity, more tendency to "short-circuit", which explains the problems associated with the dielectric measurements mentioned in section 4.1.

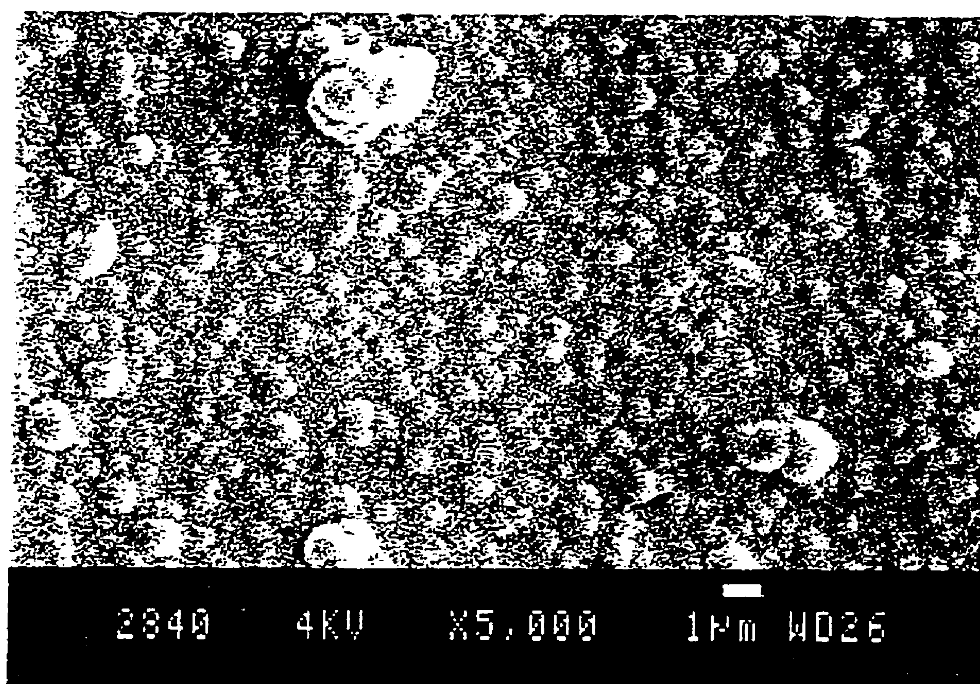

Figure 4.21: Cauliflower-like surface structure of PP(C_2F_3H) observed under SEM.

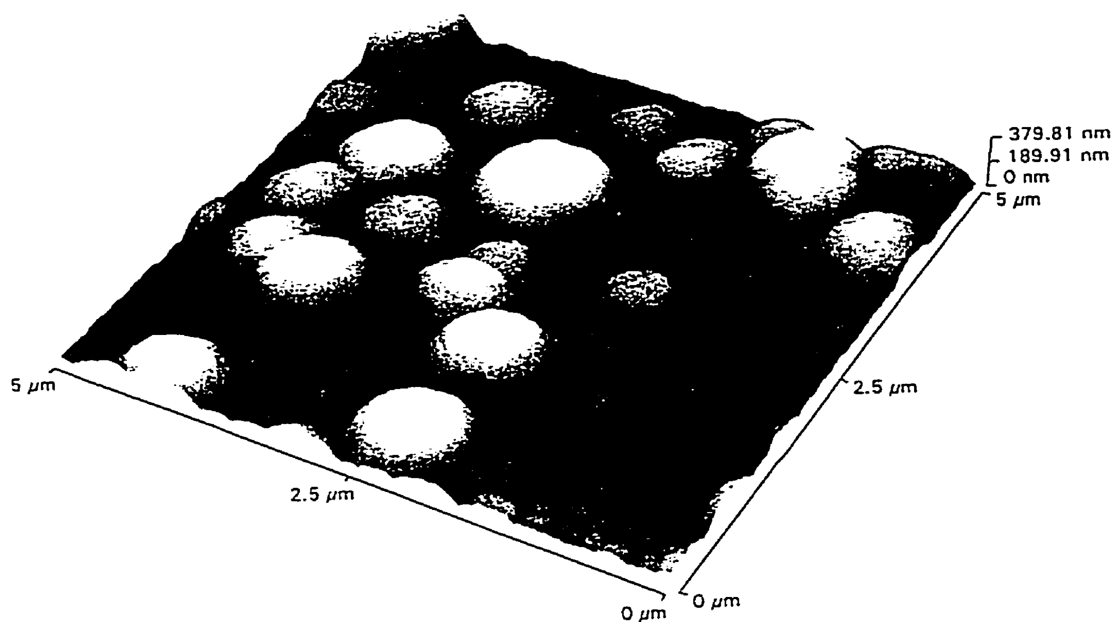

Figure 4.22: Cauliflower-like surface structure of PP(C_2F_3H) observed under AFM.

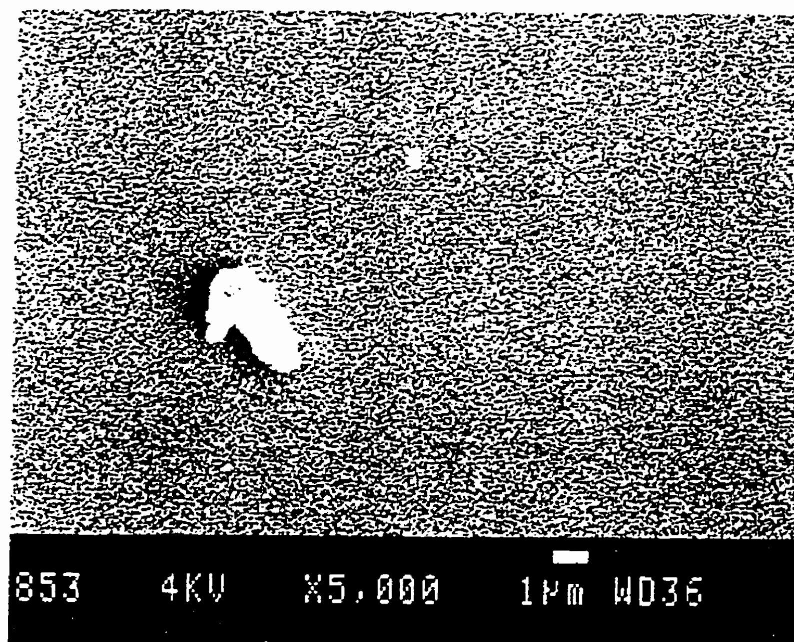

Figure 4.23: The smooth surfaces of $PP(C_2F_4)$ under SEM. We have intentionally focused on a dust particle to make the observed features evident.

4.2.5 MEASUREMENT OF STRESS

The evolution of film stress as a function of temperature is shown in Figures 4.24 and 4.25 for bare and metallized fluoropolymer films. The starting point of the experiments are indicated with little arrows showing the increase of temperature, and the end points of the experiments are indicated with little cross signs. It should also be noted that at the maximum point of each temperature cycle the samples were kept at a constant temperature for 30 minutes. During the first heating cycles, irreversible changes in the stress of bare PP and SP fluoropolymer films were observed. In the case

of SP Teflon (Ar) and $PP(C_2F_4)$ the stress is initially very low (~0 MPa). When the temperature is increased, the stress values become tensile above 100 °C for $PP(C_2F_4)$ and reproducibly stable in subsequent thermal cycles. A loss or desorption of low molecular weight species can be the cause of this observed behavior. The SP Teflon (Ar) develops a compressive stress when heated, suggesting film densification, and it, too, reaches reproducibly stable values in the following cycles. These reproducibly stable stresses for bare SP Teflon (Ar) can be seen between -100 MPa and -150 MPa values. The two lines in this region were obtained for successive thermal cycles, with the more compressive values corresponding to the latter cycle.

We analyzed two Teflon AF1600 samples. Sample 1 was put into the chamber immediately after deposition without any annealing prior to the experiment (i.e. no curing at 170 °C and 330 °C). Sample 2, however, was annealed in vacuum at 170 °C for 15 minutes and at 330 °C for another 15 minutes and then analyzed as recommended in the procedure. Teflon AF1600 shows a compressive stress which appears to be quite stable up to 200 °C, but it becomes more compressive when heated to 350 °C. At this high temperature, both samples (samples 1 and 2) of the Teflon AF1600 are probably releasing their solvent Fluorinert 77, degrading and therefore losing weight (Czeremuszkin G. et al., 1997). It should be noted from figure 4.24 that the Teflon AF1600 was cyled to 200 °C several times and no such significant changes in stress were observed.

When the samples were metallized after thermal cycling, a tensile contribution to the overall stress was observed in all cases. Metallization contributed about 30 MPa

of stress in the case of PP(C_2F_4), PP(C_2F_3H), SP Teflon (Ar), and about 200 MPa in the case of Teflon AF1600. Except in the case of Teflon AF1600, the stress did not appreciably change upon further thermal cycling. These small changes can be explained in terms of the stress relaxations at the copper/fluoropolymer interface. The high temperature annealing (350 °C) of Teflon AF1600 probably continues to degrade the polymer and, at the same time, enhances diffusion.

The general conclusion about stress measurements would be that stress effects do not seem to be very high in copper/fluoropolymer film structures. We believe that these values observed would not lead to a stress-related failure in two layer films such as ours, involving copper and fluoropolymers. The reason for our belief is mainly due to the observation that no failure such as cracking was observed for the copper evaporated fluoropolymer samples when they were removed from the stress testing flexus system. Only sputtered copper samples showed cracks when they were annealed. However, we did not analyze their stresses. In addition, stress values can be reproducibly stabilized after sufficient thermal cycling, another indication of a film that is appearently free of stress-related failure.

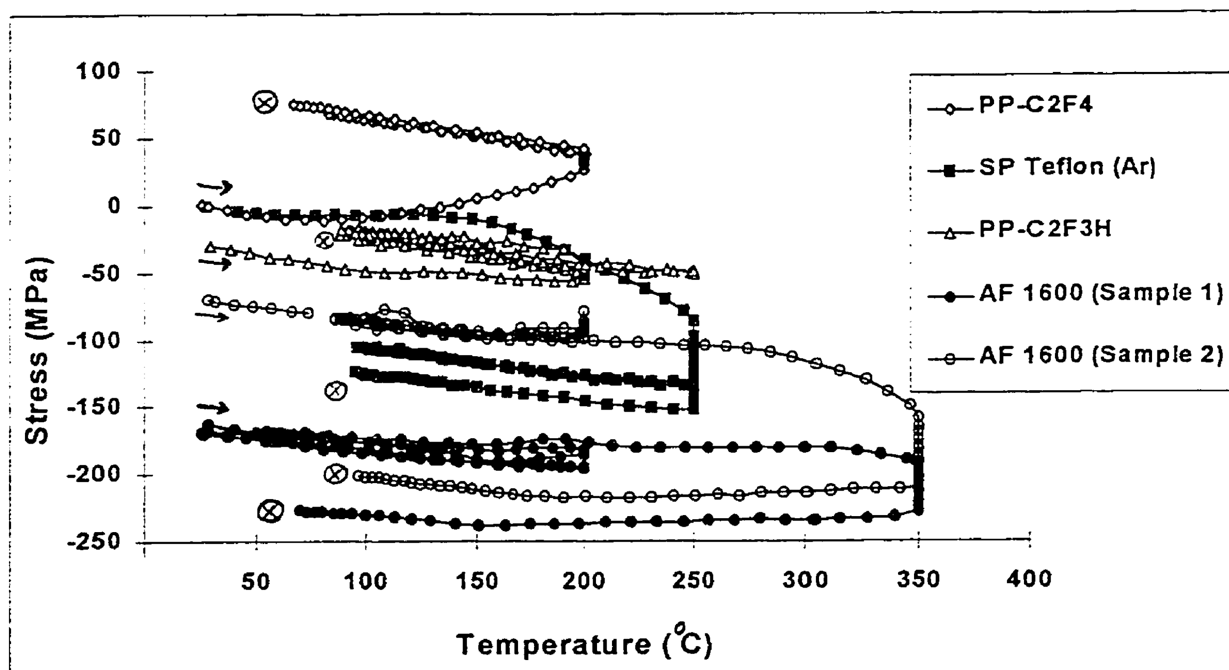

Figure 4.24: Stress as a function of temperature for bare fluoropolymer films.

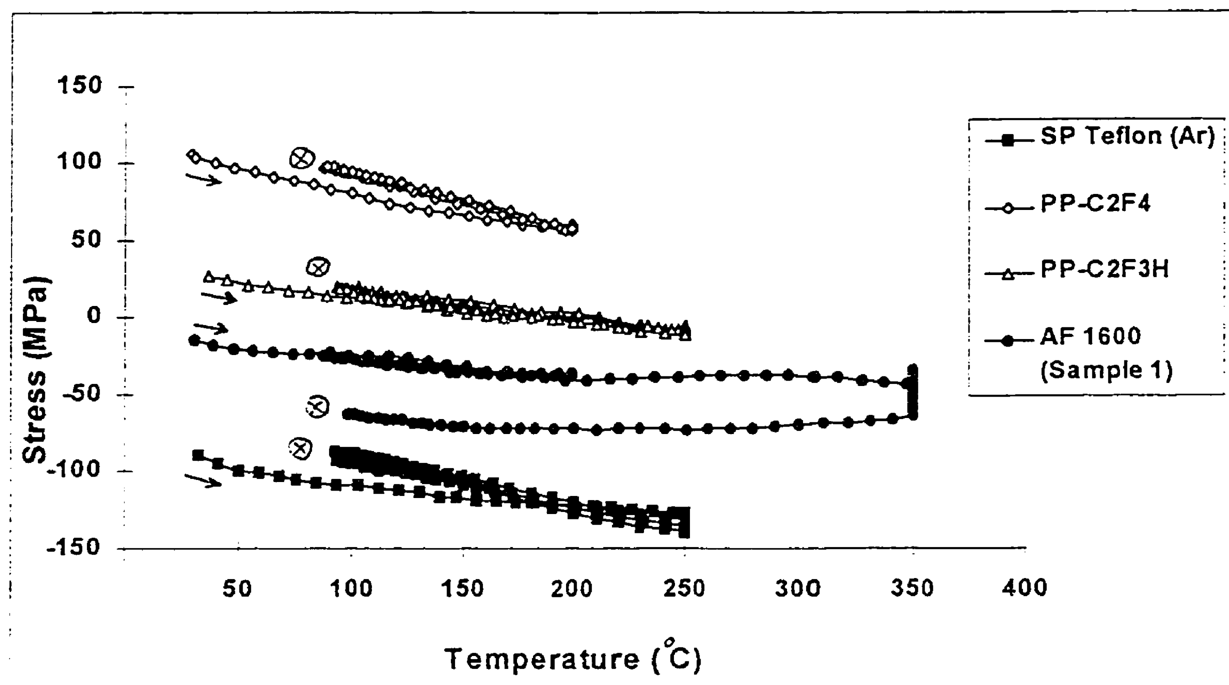

Figure 4.25: Stress as a function of temperature for copper evaporated fluoropolymer films.

This analysis of stress involved two layers only. In order to obtain more comprehensive information about stresses and to better know whether copper and fluoropolymer are reliable as possible multilevel interconnect materials, one should extend the study of stress to multilayer structures.

CHAPTER V:

SUMMARY AND CONCLUSIONS

The general objective of this work was to evaluate copper and fluoropolymers as potential candidates for multilevel interconnects. This objective was, in general, met to a large extent: It was shown that multilevel structures of the form metal-insulator-metal (MIM) exhibit promising dielectric and mechanical properties at temperatures and frequencies close to those they could be used at in the future. The specific objectives of this project were, in general, met by comparing different fluoropolymers according to their fabrication process, dielectric properties, thermal stability and compatibility with the metallization process.

We studied the dielectric properties, i.e. dielectric constant and dissipation factor, of metal-insulator-metal (MIM) sandwich structures over the temperature range from 25 °C to 200 °C, and frequency range from 100 Hz to 100 kHz, as well as at 10^{15} Hz. With the exception of plasma-polymerized C_2F_3H, which frequently showed behavior indicating short-circuiting, the fluoropolymers we studied show dielectric constants of less than 1.9 and dissipation factors around 10^{-3}-10^{-4} in the temperature range in which they would be used. The deposition parameters for plasma-polymerized C_2F_3H led to gas phase reactions which, in turn, resulted in non-uniform films with cauliflower-like surfaces prone to copper diffusion and short-circuiting. The

fluoropolymers studied show stable behavior after thermal cycling when isolated from the open atmosphere. These effects of vacuum heating were related to the reaction of free radicals, removal of low molecular weight species in the case of PP and SP polymers, and to the removal of residual solvent in the case of Teflon AF1600. In addition, unbound atmospheric contaminants were removed in all cases.

The dielectric constant shows a decrease with increasing temperature. A volume correction of the dielectric constant for Teflon AF1600, considering thermal expansion, does not make a significant change to its dielectric properties. The dissipation factor starts to increase sharply beyond 100 °C, a temperature above which these materials will be used, suggesting a loss and dc conduction to be present above 200 °C. The dielectric constant at room temperature shows a very slow decrease with increasing frequency. Plots for the dissipation factor show a sharp increase in the lower frequency region and a decrease for high frequencies in the optical range near 10^{15} Hz. The region in between may possess a maximum, the overall shape of the plot suggesting a dipolar loss. This can be explained in terms of dipole relaxation (e.g. C=O).

The samples of temperature cycling showed reproducibly stable dielectric properties to a maximum temperature of about 200 °C. The problem however remains that today's technology requires, during manufacturing, stability up to about 400 °C. Thermal stability issues thus seem to be the limiting factor for the immediate application of Cu/fluoropolymer combinations. However, this problem will eventually be solved as processing temperatures are expected to decrease in the future (Gutmann R. J. et al., 1995).

The problems associated with thermal stability can be grouped into two main classes. The first class includes the intrinsic properties of the materials, i.e. the temperatures which the polymer itself can withstand without continuously losing weight and/or degrading. The second class is associated with the interactions of the polymers with Cu, such as copper diffusion into fluoropolymers. The first class of problems definitely necessitates the use of suitable temperatures and there is not much to be done except to explore methods aimed at decreasing the processing temperatures. However, the second class of problems can be more readily solved by preventing migration of copper atoms deep into the polymer, by using possible diffusion barriers such as TiN, Ti, Ta. With minimum copper interconnect feature sizes of 0.25 μm or lower, only thin, high resistivity materials such as these can be considered as diffusion barriers, in order to keep the total interconnect resistance low (Gutmann R. J. et al., 1995).

Throughout our study we analyzed the effects of two types of annealing procedures. The first type was preannealing and it was performed in open atmosphere or in vacuum prior to metallization of the fluoropolymers. The second type, postannealing, was performed in vacuum after the fluoropolymers were metallized with copper. All these were done at 200 °C for 30 minutes. It was observed that evaporated copper adhered poorly to plasma deposited polymers unless the samples were preannealed in the open atmosphere and postannealed in vacuum. The adhesion of copper was worst in the case of Teflon AF1600 and did not show a significant improvement after preannealing the fluoropolymer. Plasma surface treatments in N_2, Ar and air improved the adhesion of copper to Teflon AF1600 from a critical load value of

0.15 to 0.20 N, an observed increase of about 33 %. A more significant improvement for this polymer was achieved upon postannealing at 200 °C for 30 minutes which increased the critical load to about 0.3 N. Sputtered copper however adhered better, giving critical loads between 0.5-1 N without postannealing, and values above 1.0 N after postannealing. These values are higher than those obtained for evaporated copper which were less than 0.7 N even after postannealing for all polymers investigated in this work.

Infrared spectroscopy was used in an effort to understand the observed adhesion properties. The surface sensitive photoacoustic spectra revealed significantly larger C=O and -OH peaks at 1750 cm^{-1} and 3400 cm^{-1}, respectively, for the plasma-deposited fluoropolymers compared to Teflon AF1600, as a result of the reaction of free radicals, produced on plasma deposition, with air. As a result, active sites containing oxygen are available for reaction with copper. We interpret the higher adhesion found for PP and SP fluoropolymers by the formation of chemical bonds (probably Cu-O-C and Cu-N-C) at the metal-polymer interface observed in an earlier work in this laboratory.

Results showed that stress values associated with metallized polymer films do not indicate an important problem for adhesion and reliability. We qualify the stress values obtained as moderate. There were irreversible changes in stress during first heating cycles. More stable stress values were obtained after temperature cycling the samples. It was observed in the case of Teflon AF1600 that, when annealed, the major changes in stress towards more compressive values took place at high temperatures, similar to the behavior of SP Teflon. The sputtered Teflon became compressive after

heating. This was explained to be due to film densification. The plasma polymerized C_2F_4 showed stress values which, on annealing, became more tensile. The plasma polymerized C_2F_3H showed a similar trend, i.e. a small increase towards more tensile stress. These observations were related to the loss of low molecular weight species.

Surface energy values obtained for atmosphere preannealed fluoropolymer films were found between $12x10^{-5}$ and $27x10^{-5}$ N/cm^2. When these values were plotted as a function of critical load, measured for the same fluoropolymers after the same thermal treatments, it was observed that both the dispersive and polar components of surface tension increased linearly with increasing critical load. This may suggest that both of these components contribute to the adhesion of copper to fluoropolymers .

In summary, our work contributed the following:

1. This work once more confirmed the reproducibility of results for similar types of fluoropolymers. There is an agreement of our results with those obtained earlier for plasma-deposited polytetrafluoroethylene (PTFE), plasma-polymerized fluorocarbons and Teflon AF1600. This is important because even though the deposition systems and conditions are somewhat different from one laboratory to the other, similar fluoropolymer films with low permittivity and dissipation factor can be obtained.

2. This study involved various techniques in order to analyse copper/fluoropolymer film systems, providing thus a complementary and consistent assessment of the film characteristics.

3. This work is original and it was not previously performed with the materials investigated. The heat treatments of fluoropolymers before and after metallization, and

the comparison of adhesion constitute an example of originality.

In conclusion, fluoropolymer films showing low dielectric constants and dissipation factors can be obtained by various deposition techniques. It is possible to enhance the adhesion of copper onto fluoropolymers. There remain, however, problems to be solved. One of them is copper diffusion into fluoropolymers which may cause short-circuiting which leads to lower reliability especially at higher temperatures. Some ways to accomplish this could be to use an appropriate diffusion barrier between metal and fluoropolymer or to investigate the effect of surface treatments of fluoropolymers on copper diffusion. Another open question is how the fluoropolymer adheres to copper. This must definitely be investigated, because, in our work, we only looked at the adhesion of copper onto fluoropolymers. We used metal-insulator-metal (MIM) film structures which consisted of three films only. In order to have a better understanding of the reliabilities of these materials, this study should be extended to multilayers. This would be closer to the real situation of multilayer structures used in microelectronics.

REFERENCES

ALLEN, K. W., in Aspects of Adhesion, Vol. 5, ALNER D. J., Ed., CRC Press, Cleveland, Ohio, 1969.

ALLEN, K. W., Proceedings of the conference held at Northampton College of Advanced Technology, EC1 on 21 and 22 March, 1963.

ALPTEKIN, A., SACHER, E., CZEREMUSZKIN, G., MARTINU, L., Presented at the Electrochemical Soc. Meeting, Montréal, May 1997.

AMYOT, N., KLEMBERG-SAPIEHA, J. E., WERTHEIMER, M. R., IEEE Transactions on Electrical Insulation, 27, (1992) 1101-1107.

BERNETT, M. K., ZISMAN, W. A., J. Coll. Interface Sci., 28, (1968) 243.

BIEDERMAN, H., BILKOVA, P., JEZEK, J., HLIDEK, P., SLAVINSKA, D., Journal of Non-Crystalline Solids, 218, (1997) 44-49.

BLANCHET, G. B. and ISMAT S., Appl. Phys. Lett., 62, (1993) 1026.

BUCK, W. H. and RESNICK, P. R., Paper Presented at the 183rd Meeting of the Electrochemical Society, Honolulu, HI, May 17, 1993.

BULL, S. J. and RICKERBY D. S., Surface and Coating Technol., 42, (1990) 149.

BURNETT, P. J. and RICKERBY, D. S., Thin Solid Films, 154, (1987) 403.

CHAUG, Y.S. and ADAMS, R., J. Vac. Sci. Technol., 11, (1993) 2269.

CHEN, R. and SILVERSTEIN, M. S., Journal of Polymer Science: Part A : Polymer Chemistry, 34, 207-216 (1996).

CHEN, T. C. S. and MUKHOPADHYAY, S. M., J. Appl. Phys., 78, (1995) 5422-5426.

CHOW, R., LOOMIS, G. E., SPRAGGE, M. K., LINDSEY, E. F., RAINER, F., WARD, R. L., KOZLOWSKI, M. R., SPIE vol. 2253, (1994), 512-520.

CLARK, D. T., DILKS, A. and SHUTTLEWORTH, D., Polymer Surfaces, D. T. CLARK and W. J. FEAST, eds. (Wiley, London, 1979).

CZEREMUSZKIN, G., MARTINU, L., ALPTEKIN, A., POPOVICI, D., and SACHER, E., Electrochemical Society Meeting Abstract Vol. 97(1), 1997.

DABRAL, S., ZHANG, X., WANG, B., YANG, G. R., LU, T. M., MCDONALD, J. F., Proceedings of the MRS 1995 Fall Meeting, Volume 381, 205-215.

D`AGOSTINO, R., ed., Plasma Deposition, Treatment and Etching of Polymers, Academic Press, New York, 1990.

D`AGOSTINO, R., CRAMAROSSA, F., FRACASSI, F., and ILLUZZI, F., in Plasma Deposition, Treatment, and Etching of Polymers, D`AGOSTINO R., Ed., Academic, New York, 1990, p. 95.

DERYAGIN, B. V., et KROTOVA, N. A., Doklady Akad. Nauk S.S.S.R., 61, (1948) 843-849.

DILKS, A. and KAPLAN, S., Proc. Electrochem. Soc. 82-6 (1982), Proc. 3rd Symposium Plasma Process, Denver, Colorado, 1981.

DIRENZO, M., ELLIS, T. H., SACHER, E. and STANGEL, I., Prog. Surf. Sci., 50, (1995) 407.

GERENSER, L. J., J. Vac. Sci. Technol. A, 6, (1988) 2897.

GIEGENGACK, H. and HINZE, D., Phys. Status Solid, A8, 513 (1971).

GOOD, R. J., Polym. Sci. Technol. A, 9, (1975) 107-127.

GRAF, R. T., KOENIG, J. L. and ISHIDA, H., Fourier Transform Infrared Characterization of Polymers, ISHIDA H., Polymer Science and Technology, vol.36 (1987).

GRIESER, J., SWISHER, R., PHIPPS, J., PELLEYMOUNTER, D., HILDRETH, E., "Next generation thermal control coatings," in Optical Surfaces Resistant to Severe Environments, ed. S. MUSIKANT, SPIE vol. 1330, (1990) 111-118.

GUTMANN, R. J., CHOW, T.P., LAKSHMINARAYANAN, S., PRICE, D. T., STEIGERWALD, J.M., YOU, L., MURARKA, S.P., Thin Solid Films, 270, (1995) 472-479.

HIRAOKA, H. and LAZARE, S., Appl. Surface Science, 46, (1990) 342.

HRUBESH, L. W., Proceedings of the MRS 1995 Fall Meeting, Volume 381, 267-272.

HRUBESH, L. W. and RESNICK, P. R., paper presented at the 183rd Meeting of the Electrochemical Society, Honolulu, HI, May 17, 1993.

HARDY, A., Proceedings of the conference held at Northampton College of Advanced Technology, ECI on 21 and 22 March, 1963.

HETZLER, U. and KAY, E., J. Appl. Phys. 49, (1978) 5617.

IYENGAR, Y. and ERICKSON, D. E., J. Appl. Polymer Sci., 11, (1967) 2311.

KAY, E., Z. Phys. D - Atoms, Molecules and Clusters, 3, (1986) 251-262.

KAY, E., COBURN, J., DILKS, A., in 94 Topics in Current Chemistry, edited by VEPREK, S. and VENUGOPALAN, M., 1980 Springer-Verlag.

KAY, E., DILKS, A., J. Vac. Sci. Technol., 18, (1981) 1.

KAY, E., DILKS, A., Thin Solid Films, 78, (1981) 309.

KAY, E., HECQ, M., J. Appl. Phys., 55, (1984) 370.

KAELBLE, D. H., DYNES, P. J., and CIRLIN, E. H., J. Adhesion, 6, (1974) 23.

KLEMBERG-SAPIEHA, J. E., In Plasma Treatments and Deposition of Polymers, D'AGOSTINO R., Ed., Kluwer Academic Publishers, Dordrecht, The Nederlands, 1997.

KU, C. C. and LIEPINS, R., Electrical Properties of Polymers (Macmillan, New York, 1987).

LISTON, E. M., MARTINU, L. and WERTHEIMER, M. R., J. Adhesion Sci. Technol., 7, (1993) 1091.

LOWRY, J. H., MENDLOWITZ, J. S., and SUBRAMANIAN, N. S., In "Optical characteristics of Teflon AF fluoroplastic materials", Optical Engineering., 31, (1992) 1982.

MARTINU, L., Thin Solid Films, 140, (1986) 307.

MARTINU, L., BIEDERMAN, H. and NEDBAL, J., Thin Solid Films, 136, (1986) 11-19.

MARTINU, L., In "Plasma Treatments and Deposition of Polymers", R. D'AGOSTINO, Ed., Kluwer Academic Publishers, Dordrecht, The Nederlands 1997.

MITTAL, K. L., J. Vac. Sci. Technol., 13, (1976) 19.

MITTAL, K. L., J. Adhesion Sci. Technol., 9, (1975) 129.

MOGAB, C. J., J. Electrochem. Soc., 124, 1262 (1977).

MORITA, S., SAUER, G., IEDA, M., in "Plasma Chemistry of Polymers" (M. DEKKER, New York, 1976) p.133.

MOUNTSIER, T. W., KUMAR, D. Proceedings of the MRS 1996 Fall Meeting, Symposium H, December 2-6 Boston.

MST Micro-Scratch-Tester, User's Manual, Version: 1.0.

MURARKA, S. P., GUTMANN R. J., KALOYEROS, A. E., LANFORD, W. A., Thin Solid Films, 236, (1993), 257.

MURARKA, S. P. and HYMES, S. W., Crit. Rev. Solid St. Mater. Sci., 20, (1995) 87-124.

NAKANO, T., FUKUYAMA, M., and OHKI, Y., Japanese Journal of Applied Physics, Vol. 27, No.6, June, 1988, pp. 1042-1046.

NAKANO, T., KASAMA, Y., OHKI, Y. and YAHAGI, K.: Jpn. J. Appl. Phys., 24, (1985) 83.

NASON, T. C., MOORE, J. A. and LU, T. M., Appl. Phys. Lett., 60, (1992) 1866.

OHRING, M., Chapter 9 in The Materials Science of Thin Films, Academic Press, New York 1992.

PERRIN, J., SIEMENS, R. L., KAY, E., Solid State Phys., 4792, (1985) 50801.

POPOVICI, D., KLEMBERG-SAPIEHA, J. E., CZEREMUSZKIN, G., ALPTEKIN, A., MARTINU, L., MEUNIER, M., SACHER, E., Metallized Plastics V., MITTAL K., Ed., 1997.

POPOVICI, D., KLEMBERG-SAPIEHA, J. E., SACHER, E., MEUNIER, M., MARTINU, L., J. Vac. Sci. Technol., submitted.

RAEVSKII, R. G., J. Adhesion, 5, (1973) 203.

RICE, D. W. and O'KANE, D. F., J. Electroochem. Soc. 123, 1308 (1976).

ROSARIO, A. G., Proceedings of the MRS 1996 Fall Meeting, Symposium H.

SACHER, E., Prog. Surf. Sci., 47, (1994) 273.

SHARPE, L. H., Chapter 1, pp.1-20 in Interfacial Interactions in Polymeric Composites, AKOVALI G, Ed., NATO-ASI Series E: Applied Sciences 230, Kluwer, Dordrecht, 1993.

SHI, M. K., SELMANI, A., MARTINU, L., SACHER, E., WERTHEIMER, M.R. and YELON, A., J. Adhesion Sci. Technol., 8, (1994) 1129.

SHI, M. K., MARTINU, L., SACHER, E., SELMANI, A., WERTHEIMER, M. R. and YELON, A., Surface and Interface Analysis, 23, (1995) 99-104.

SHI, M. K., KLEMBERG-SAPIEHA, J. E., CZEREMUSZKIN, G., MARTINU, L. and SACHER, E., Proc. Int. Symp. on Plasma Chemistry ISPC 12, Minneapolis, MN, August 1995, p.51.

SMITH, D. M., ANDERSON, J., CHO, C. C., JOHNSTON, G. P., JENG, S. P., Proceedings of the MRS 1995 Fall Meeting, Volume 381, 261-266.

STARKWEATHER, H., AVAKIAN, P., MATHESON, R., FONTANELLA, J. and WINTERSGILL, M., Macromolecules, 24, (1991) 3853.

STEINMANN, P. A. and HINTERMANN, H. E., J. Vac. Sci. Technol. A7, (1989) 2267.

SULLIVAN, J. P., DENISON, D. R., SEAGER, C. H., NEWCOMER, P. P., APBELT, C. A., ALBERT G. B., Proceedings of the MRS 1996 Fall Meeting, Symposium H.

TATIAN, B., Applied Optics, 23, (1984) 4477-4485.

TIBBITT, J. M., SHEN, M. and BELL, A. T., Thin Solid Films 29, L43 (1975).

TIBBITT, J. M., BELL, A. T. and SHEN, M., Plasma Chemistry of Polymers (DEKKER, M., New York, 1976).

TING, C. H., SEIDEL, T. E., Proceedings of the MRS 1995 Fall Meeting, Volume 381.

VALLI, J., J. Vac. Sci. Technol., A4, (1986) 3007.

VOSSEN, J. L., KERN, W. (1978), Thin Film Processes, Academic Press, San Diego, CA, USA.

VOYUTSKII, S. S., Autohesion and Adhesion of High Polymers, p. 138, inter-science, 1963.

WAITS, R. K. (1978), Thin Film Processes, Academic Press, San Diego, CA, USA.

WINTERS, H. F., COBURN, J. W., and KAY, E., Electrochem. Soc. Extend. Abstr. No. 77-2, (1977) 393.

YASUDA, H. and HSU, T., Surf. Sci., 76, 232 (1978).

YASUDA, H. in Thin Film Processes, edited by JOHN L. VOSSEN and WERNER KERN, 1978 Academic Press Inc.

YASUDA, H., Plasma polymerization, Academic, New York, 1985.

IMAGE EVALUATION TEST TARGET (QA-3)

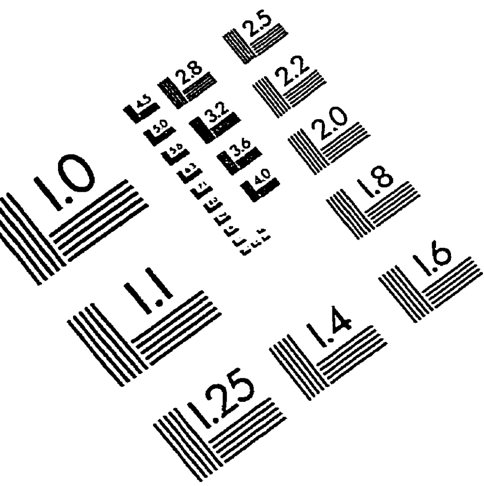
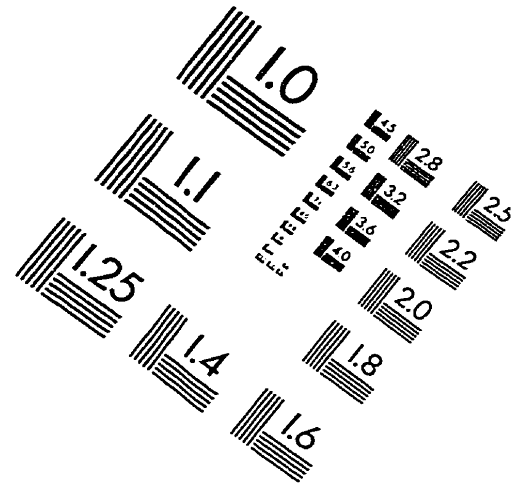
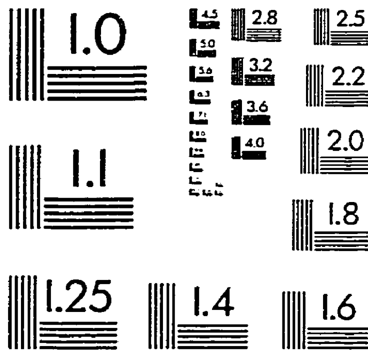
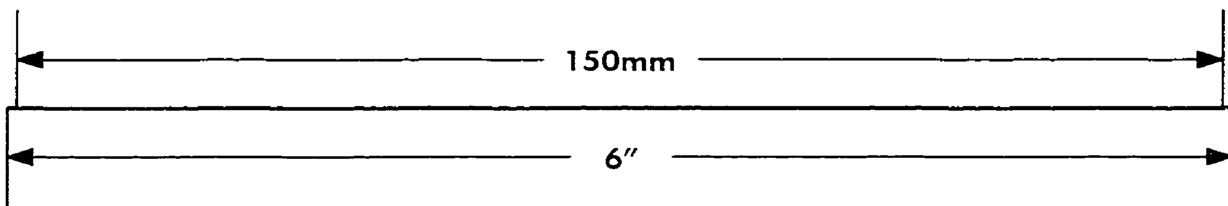

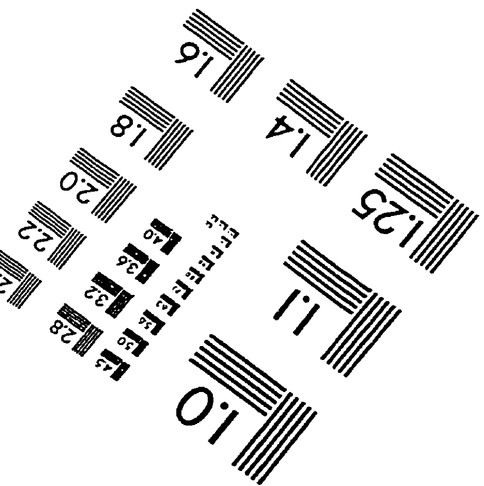

APPLIED IMAGE . Inc
1653 East Main Street
Rochester, NY 14609 USA
Phone: 716/482-0300
Fax: 716/288-5989

© 1993, Applied Image, Inc., All Rights Reserved